Layer-by-Layer Nanoparticles for Cytokine Delivery to Treat Cancer

By

Antonio Eric Barberio

BSE Chemical and Biomolecular Engineering, University of Pennsylvania (2015)

SUBMITTED TO THE DEPARTMENT OF CHEMICAL ENGINEERING IN PARTIAL FULFILLMENT OF THE REQUIREMENTS FOR THE DEGREE OF

DOCTOR OF PHILOSOPHY IN CHEMICAL ENGINEERING

AT THE MASSACHUSETSS INSTITUTE OF TECHNOLOGY

SEPTEMBER 2020

Signature of Author:……
Antonio E. Barberio
Department of Chemical Engineering
July 16, 2020

Certified by:……...
Paula T. Hammond
David H. Koch Professor of Chemical Engineering
Thesis Supervisor

Accepted by:……..
Patrick S. Doyle
Robert T. Haslam Professor of Chemical Engineering
Graduate Officer

Layer-by-Layer Nanoparticles for Cytokine Delivery to Treat Cancer

By

Antonio Eric Barberio

Submitted to the Department of Chemical Engineering

on July 16, 2020 in Partial Fulfillment of the Requirements for the Degree of

Doctor of Philosophy in Chemical Engineering

Abstract

Since the initial approval of checkpoint inhibition in 2011, immunotherapy has become an ever more present therapeutic strategy in the clinic and an increasingly large focal point in preclinical cancer research. Much of the success of immunotherapy in the clinic has focused on expanding indications of checkpoint inhibitors which "take the brakes off" the immune response to cancer. However, this strategy has seen limited success in many solid tumors, with only a small fraction of patients responding. One explanation for this phenomenon is a "cold" or poorly immune infiltrated tumor environment. An alternative strategy to utilize the immune system to fight the tumor in these cases is to deliver a proinflammatory agent such as a cytokine to drive immune infiltration and activity within the tumor environment, or "hitting the gas" on the cancer immunity cycle. Unfortunately, many proinflammatory cytokines, such as interleukin -12 (IL-12), that have been translated to the clinic have shown high, schedule dependent toxicity at relevant doses, making translation infeasible. One strategy to potentiate administration of therapies that are too toxic for systemic delivery is to use a nanoparticle delivery vehicle to concentrate the therapy within tumors and avoid off-target exposure. However, proinflammatory cytokines such as IL-12 pose unique design challenges for optimal delivery from a nanoparticle, including efficient encapsulation, subcellular targeting to cell surfaces to maintain activity on external receptors, and targeting to tumor cells to concentrate IL-12 in tumors and avoid systemic exposure. In this thesis we utilize the layer-by-layer (LbL) nanoparticle technique to adjust the material properties of a nanoparticle delivery vehicle to meet these design criteria. We demonstrate extensive *in vitro* and *in vivo* characterization of the designed LbL nanoparticles. We demonstrate reduced toxicity and enhanced efficacy of systemic IL-12 therapy from optimized LbL nanoparticles not only compared to carrier-free IL-12 but also compared to a simpler nanoparticle design that does not incorporate targeting polymer layers. Importantly, we demonstrate this effect in an orthotopic ovarian tumor model, a malignancy that has been particularly refractory to immunotherapies currently available in the clinic.

Thesis Supervisor: Paula T. Hammond
Title: David H. Koch Professor and Department Head of Chemical Engineering

Thesis Supervisor
Paula T. Hammond
David H. Koch Professor and Department Head of Chemical Engineering
Massachusetts Institute of Technology

Thesis Committee
Darrell J. Irvine
Professor of Materials Science and Engineering and Biological Engineering

Robert S. Langer
Professor of Chemical Engineering and Biological Engineering

Sangeeta N. Bhatia
Professor of Biological Engineering

Dedicated to Lotte Schregenberger, my Oma,

with all my love

Acknowledgments

This thesis could not have been done without the help of a large number of people. Looking back on my graduate school career and even the events prior I am filled with gratitude for so many people that have helped me along the way. It truly takes a village to arrive at a completed thesis. I believe it is near impossible to thank everyone that has influenced my life to get me to this point but I will try.

Firstly, I must thank my advisor, Prof. Paula Hammond, without whom I would not have been able to complete the work put forth herein. Your belief in me to take me on for such a unique and exciting project with my limited background in the field is greatly appreciated. Your unending optimism and support, even when things were not going our way in the lab has always kept me on the proper path. I must thank you for helping me not only to grow as an independent researcher and scientist during my tenure in the lab but also as a human being. I have always felt that you had my best interests at heart and so for all of the support, encouragement, and advice throughout my thesis I thank you from the bottom of my heart. Your kindness, energy, and positivity serves as an inspiration to me not only in science but in life.

I must also thank my thesis committee, Prof. Darrell Irvine, Prof. Robert Langer, and Prof. Sangeeta Bhatia for helping to guide the work in this dissertation and for the fruitful discussions not only on my thesis work but my career as well. Having the feedback of such an accomplished and diverse group of scientists has made not only the thesis presented here much more well-rounded and complete but also myself as a researcher much more well-rounded and complete. I must especially thank Prof. Irvine who played a large role in the immunological components of this work. It was through our fruitful discussions on immunotherapy targets and collaboration with the Irvine lab that led to a lot of the immune aspects of the work in this thesis from IL-12 as a target molecule for delivery to some of the immune markers we assay for a response. Prof. Langer, thank you for all of your discussions on the research presented here and your pointed feedback. I have always found our discussions to be tremendously helpful, often leaving our meetings with many new ideas and experiments to try. Prof. Bhatia, thank you for the discussions and expertise you brought to this thesis. You have always helped me to view our work through a wider lens and think about the broader implications of our designs. To my entire committee thank you for taking the time to meet with me often and helping me to grow as a researcher.

I must also acknowledge the people who helped put me on the path to graduate school. First, Prof. Warren Seider, my undergraduate research advisor and Cory Silva and Ian Moskowitz, both of whom I had the pleasure of working under. In my time working as a researcher at Penn I learned what it was to be a PhD student and what the path of research looked like. Cory and Ian both showed me what it meant to be a researcher and we had many discussions about the future and what a PhD did beyond graduation which helped to put me on this path. Prof. Seider, thank you for always having the time to talk with me and advise me about my future and for having the belief in me to allow me to take on the projects that you did. My time in your lab at Penn set me up for the path to this thesis and beyond.

I must also thank my colleagues in the Hammond lab who helped shape me as a scientist and helped immensely to make this thesis what it is. As a member of the Hammond lab I learned what it meant to be part of collaborative research efforts as the Hammond lab is truly run on team science. I always felt that not only did everyone have each other's interests at heart but was willing to go the extra mile to help the lab as a whole achieve its goals, rather than being solely invested

in their own research. Erik Dreaden, thank you for helping me to learn many new techniques not only in nanotechnology but in biological research as a whole, and thank you for making the lab such a fun place to be in my early years. Brett Geiger, for the many fruitful discussions not only on how best to focus my research but also for looking ahead to my post-graduation options. Natalie Boehnke for being a valuable resource for all things chemistry and a shining example of what a successful researcher is in the lab. Liz Galoyan and Xiuyun Hou, for helping to keep the lab running smoothly and all your help throughout my time in the Hammond lab. To all of the members of the Hammond lab that I have had the pleasure of working with past and present; Colin, Sheryl, Yanpu, Maylin, Steph, Celestine, Elad, Brandon, Natalie, Joelle, Apoorv, Sean, John, Kevin, Jonathan, Adam, Sarah, Amal, Yamini, Hannah, Chibueze, Archana, Ki-Young, Santi, Daniel, Shuting, Andreas, Betty, Li, Hongkun, Kristiana, Sweeta, Jiahe, Anasuya, Michael, Lawrence, Jouha, Kota, Marianna, Wade, Connie, Ketian, Kaixi, Andrew, and anyone else I may have forgotten thank you for making the lab a place I truly enjoyed being every day.

I must especially acknowledge Santi Correa, who served as my mentor coming into the lab. You showed me countless techniques in the lab and always helped me with any question I had. Seeing how you handled problems and approached your research inspired me and set me up for success in the work of this thesis. I must also especially thank Sean Smith, who served as my immunology and IL-12 mentor in the lab. Starting a relatively new project in the lab was extremely difficult. Sean, not only your expertise in immunology and IL-12 research but also your willingness to share it with me helped to take this work to the next level. Without the two of you I don't know where I would be. Thank you for the countless conversations and hands on help you've given me through the years, and thank you not only for serving as great research mentors to me but also great friends.

I would also like to thank my collaborators in the Irvine lab who were instrumental in this work. Mariane Melo, for the many discussions on immunology as a whole and helping us to make the IL-12 protein used throughout. Heikyung Suh for making the IL-12. Talar Tokatlian for your immense help in finding an efficient technique for encapsulating IL-12 and your help in teaching me many immune assays.

I must also thank the various students I had the pleasure to mentor and who helped in this work. My undergraduate researchers Cathy and Bang for your hard work and dedication, always going above and beyond to reach our project goals. My high school mentee, Alex, who showed an incredible maturity and intellectual curiosity as well as a great aptitude for our research. You all are an inspiration and I hope we get the opportunity to work together in the future.

I would also like to thank the amazing core staff in the Koch Institute who were instrumental in many of the experiments shared here. Specifically, Jaime and Christian in the high throughput core, who were instrumental in helping me streamline a lot of my experiments to test more variables. Glenn from the flow core for helping me to get the best out of my flow cytometry experiments and helping me to understand the intricacies of the techniques. Both Scott and Virginia in the AIPT core for helping me with all of my imaging needs. Eliza, Jeffrey, and Jeff in the microscopy core for their help with taking and processing the microscopy images. A big thank you to the DCM staff at MIT as well who were all instrumental in the animal experiments demonstrated here, especially Nate Rogers and Elizabeth Horrigan who trained me on many animal techniques.

I must also thank my ChemE friends, the lunch train, without whom I likely would not have even made it past first semester. Whether it was working on problem sets, studying for the last

written qualifying exam at MIT ChemE, or getting some much needed relaxation, I greatly value all of our time spent together. Our conversations at lunch were always a highlight of my day, whether they were relevant to our research, current events, or some of our out-there ideas on what we could get funded as “interdisciplinary research”. I could not imagine a better group of people to spend my time at MIT with.

I also must thank my fiancé, Julia. Even though we met during the PhD process you have been incredibly supportive of me and a great resource throughout our time together. You always found a way to help me as stressful situations arose and helped me to relax and have fun.

Finally, I must thank my family, who have been incredibly supportive throughout my schooling and without whom I would not be where I am today. My parents, Yvonne and Tony, for always supporting my interests and turning me on to chemical engineering as a career path. Thank you for your unending support and inspiration. My sister, Andrea, for always being supportive and paving the way for me. Watching your hard work and determination in med school and your career has always given me an excellent example to follow. My entire extended family: aunts, uncles, cousins, and grandparents for making a truly wonderful and supportive family environment. Coming home for family holidays always gave me something to look forward to. You all have always been a wonderful support network for me.

A deep and heartfelt thank you to my grandmother, Lotte Schregenberger, my oma, to whom this is dedicated for all of your support and love in helping me to become the person I am today. Whether it was helping with homework after school or encouraging us to explore our imaginations outside you have shaped my life in a way that I cannot describe and I miss you every day.

To everyone that has supported me and been there for me, my deepest thanks. My sincerest apologies if I forgot anyone.

I would also like to thank the funding sources that made this work possible. This work was supported by the US Department of Defense Congressionally Directed Medical Research Programs (PTH, Teal Innovator Award W81XWH-13-1-0151), the Bridge Project a partnership between the Koch Institute for Integrative Cancer Research at MIT and the Dana-Farber/Harvard Cancer Center, NIH (1-R01-CA235375-01A1), the Marble Center for Cancer Nanomedicine, and a Cancer Center Support (core) Grant P30-CA14051 from the National Cancer Institute, and NIH interdepartmental biotechnology training program. Resources were provided in part by the Koch Institute Support Grant (P30-CA14051) from the National Cancer Institute and the MIT MRSEC Shared Experimental Facilities Grant (DMR-0819762) from the National Science Foundation.

Table of Contents

List of Figures

Figure 3-3. PLE IL-12 NPs maintain efficacy against MC38 (A-D) and HM-1 (E-G) tumors *in vivo*. **A,** Study design. **B,** MC38 tumor volume (mm^3) of indicated treatments. All animals dosed 5 times given weekly intratumorally unless otherwise noted beginning on day 6. **C,** Mean volume (+SEM) from B on day 13 for each group. *** indicates p<.001 as measured by one-way ANOVA using Bonferroni post-hoc test on all pairs of data. **D,** Survival curves of groups from B and C. * indicates p<.05, *** indicates p<.0001 as measured by Log-rank tests between groups. **E,** HM-1 tumor volume (mm^3) of indicated treatments. All animals dosed 5 times given weekly intratumorally beginning on day 6. **F,** Mean volume (+SEM) from E on day 24 for each group. ** indicates p<.01 as measured by one-way ANOVA using Bonferroni post-hoc test on all pairs of data. **G,** Survival curves of groups from E and F. *** indicates p<.0001 as measured by Log-rank tests between groups.

Figure 3-4. Abscopal response to IL-12 therapy. Similar to Figure 3-3, MC38 cells were inoculated in C57Bl/6 mice on both flanks. Mice were treated only on the right flank, and both treated and contralateral tumors were monitored for growth. **A,** Tumor growth in individual mice as measured by caliper measurements with volume calculated at 1/2L*W^2 with L being the longest dimension and W being the shortest dimension. **B,** average tumor sizes from A at day 17. **C,** Survival of cohorts from A.

Figure 3-5. Combined toxicity and efficacy at high doses demonstrates PLE IL-12 NPs are a safer, more effective IL-12 therapy. **A,** Schematic of study. C57Bl/6 mice are inoculated with 5E06 MC38 cells on day 0. Mice are treated twice weekly for 5 doses with serum collected 24 hrs after the first and last dose. Animals are monitored throughout for tumor burden and weight change. **B,** Weight change (Mean+SEM) over initial dosing period,* indicates p<.05, ** indicates p<.01, *** indicates p<.001 compared to PBS as measured by 2-way ANOVA with Bonferroni post-hoc tests comparing all groups to PBS. **C,** Cytokine levels (Mean +SEM) in serum at indicated time points as measured by ELISA. * indicates p<.05, *** indicates p<.001 as measured by 2way ANOVA with Bonferroni post-hoc test comparing all pairs of groups. Comparisons are to PBS where not indicated otherwise. **D,** Tumor volumes of individual animals of indicated treatment groups. **E,** Survival curves of animals from treated and control groups (PBS and PLE NP). ** indicates p<.01, *** indicates p<.001 as measured by Log-rank tests between groups. **F,** Average tumor volumes (mean +SEM) over time for animals from figure 5B low dose experiment (PBS, IL-12 5µg, PLE IL-12 NPs 5µg, PLE IL-12 NPs 7.5µg, PLE IL-12 NPs 5µg 2xweekly) and figure 6D high dose study (IL-12 25µg 2xweekly, PLE IL-12 NPs 25µg 2xweekly, PLE IL-12 NPs 50µg 2xweekly).

Figure 3-6. Flowcytometry analysis shows IL-12 shifts immune populations towards an antitumoral response. **A.** CD3+ T cell gating for CD4 and CD8 T cells in different treatment groups (CD4 y-axis, CD8 x-axis). **B.** Degranulation of CD8+ T cells as measured by CD69 staining in the tumor. **C.** F4/80 staining of CD45+ cells in TDLNs. **D.** DC content as measured by CD11c+ staining in CD45+ cells in TDLNs. **E.** Quantification of chosen T cell populations from A and B. * indicates p<.05 as measured by one way ANOVA with Dunnett posthoc test **F.** Quantification of chosen APC populations flowcytometry. (T=tumor, S=spleen, LN=TDLN)

Figure 4-1. PLE-IL-12-NPs are able to selectively bind to tumor cells and remain localized to cell surfaces, releasing their IL-12 cargo to activate T cells over a 24 hour period. These characteristics make PLE-IL-12-NPs a strong candidate for safe and efficacious systemic delivery of IL-12.

Figure 4-2. Biodistribution of NPs upon systemic delivery. **A**, Schematic of biodistribution study design. **B**, Representative fluorescence results as measured by IVIS in tumors following 4 hour injection of PLE-IL-12-NPs and UL-NPs by both IV and IP delivery route. **C)** Mean percent recovered fluorescence normalized by tissue weight (UL-NPs, PLE-IL-12-NP 24 hr IV n=3; 4 hr and 24 hr IP PLE-IL-12-NPs n=5, error bars denote SEM). IVIS measurements from B were normalized by dextrose control treated subjects and percent recovered fluorescence was calculated with respect to all measured organs (liver, kidney, spleen, and tumor). * indicates p<.05 as calculated by one-tailed t-test. **D,** Correlation of % recovered IL-12/g tissue to % recovered fluorescence/g tissue for both IV (left) and IP (right) delivery. Linear regression

performed using Graphpad PRISM showing 95% confidence ranges and slopes. **** indicates $p<0.0001$ for slope differing from zero.

Figure 4-3. IL-12 toxicity in healthy mice. **A**, Schematic of dosing scheme in healthy animals. Mice were dosed with 5 μg IL-12 in PLE-IL-12-NPs, UL-NPs, or carrier free and compared to 5% dextrose control. **B**, Toxicity of various IL-12 delivery methods administered IV (left) or IP (right) as measured by weight loss during and after dosing. ** indicates $p<0.01$, *** indicates $p<0.001$as measured by 2-way ANOVA with Bonferroni post-hoc test across all groups.

Figure 4-4. PLE-IL-12-NPs improve anti-tumor efficacy of IL-12. **A**, Schematic of dosing scheme in HM-1 tumored animals. Mice were dosed with 5 μg IL-12 in PLE-IL-12-NPs, UL-NPs, or carrier free and compared to 5% dextrose control 7 days after IP inoculation of HM-1 tumor cells. **B**, Survival curves of 5 μg IL-12 treated mice for IV (left) and IP (right) delivery routes. Colored arrows indicate toxicity related deaths during and immediately following dosing.

Figure 4-5 | PLE-IL-12-NPs improve efficacy of IL-12 at reduced toxicity with high dose systemic delivery. **A,** Animal weights upon daily dosing of 10 μg of IL-12 for 5 doses from PLE-IL-12-NPs (red), UL-NPs (green), or carrier-free (blue) compared to vehicle control (black). **B,** Survival of mice with orthotopic HM-1 tumors treated 7 days after inoculation with 5 daily doses of IL-12 from different vehicles similar to A. * indicates $p<0.05$ compared to UL-NPs ## indicates $p<0.01$ compared to Dextrose as measured by Mantel-Cox test between indicated groups. **C,** Serum levels of IL-12 and IFN-γ as measured by ELISA from serum collected 3 hours after the final dose from subjects in A for healthy mice (left) and subjects in B for tumored mice (right) * indicates $p<0.05$, *** indicates $p<0.001$ as measured by 2way ANOVA with Bonferroni post hoc test between all treatments and carrier-free IL-12.

Figure 4-6 | PLE-IL-12-NPs show an equivalent immune response to carrier-free IL-12. **A,** Experimental design for immune profiling. Mice were inoculated with orthotopic HM-1 tumors and dosed with 10 μg IL-12 IP in PLE-IL-12-NPs, UL-NPs, or carrier-free and compared to vehicle control for 3 daily doses 14 days after inoculation. **B-K,** Immune population statistics found within the tumor environment as measured by flow cytometry following gating in Fig C-7. **L-N**, Immune suppressive markers found in indicated organs (tumor, spleen) as measured by flow cytometry following gating in Fig C-7.

Figure 4-7| T cell exhaustion in response to IL-12 therapy. MFI of various exhaustion markers in CD8+ T cells in either the ascites (A) or tumor (T). * indicates $p<0.05$, ** indicates $p<0.01$ as measured by one way ANOVA with Dunnett's multiple comparison post hoc test comparing all groups to dextrose control.

Figure 5-1. Formulation of c.mPLE-IL-12-NPs. **A,** Schematic of particle formulation. Similar formulation details to PLE-IL-12-NPs with the exception of a change in linker chemistry. **B,** Encapsulation efficiency (% recovered IL-12 in NPs from IL-12 added) and loading efficiency (mg IL-12/(mg lipid + mg IL-12)) of different NP formulations.

Figure 5-2. FRET experiments demonstrate mechanism and kinetics of deconstruction of PLE-IL-12-NPs. Schematic of NP structure for FRET kinetic release studies (left). FRET readouts for intact NPs (right, top) and degraded NPs (right, bottom). A mix of these states is also possible, ie IL-12 remains on the surface (high efficiency) while polymers erode (low efficiency).

Figure 5-3 FRET efficiency shows different kinetics and mechanism of action with changing linker chemistry. **A,** Normalized FRET efficiency overtime for NPs. NPs were tested under two media conditions: water (storage media, dashed curves) and spent media (MC38 media cultured on cells for at least 48 hours as an *in vivo* mimic, solid curves). FRET efficiencies were measured for the erosion of the polymer layers as measured by FRET pairing with the acceptor fluorophore on PLR (red) and release of IL-12 as measured by FRET pairing with the acceptor fluorophore on IL-12 for both PLE-IL-12-NPs (blue) and c.mPLE-IL-12-NPs (black). **B,** schematic of PLE-IL-12-NP break down as indicated by release data from B, shows that polymer layers erode from the NP surface initially, revealing IL-12 beneath that is subsequently released. **C,** schematic of c.mPLE-IL-12-NP break down as indicated by release data from B, shows that polymer

layers erode from the NP surface initially, revealing IL-12 beneath that remains bound to the liposomal surface.

Figure 5-4 *in vitro* activity of c.mPLE-IL-12-NPs compares with that of PLE-IL-12-NPs. Dose response curves of IL-12 (left) demonstrate approximately equivalent efficacy in triggering IFN-γ production from B6C3F1 splenocytes in both c.mPLE-IL-12-NPs and PLE-IL-12-NPs, with minimal change in EC50 value for half maximal IFN-γ response (right).

Figure A-1|scIL-12 protein construct. The described single chain IL-12 from Lieschke *et al* contains the murine IL-12p40 subunit with signal peptide attached to the murine IL-12p35 subunit without the leader (signified as delta-mIL12p35) by a (G4S)x3 linker. Attached at the c-terminus is a His tag for purification and chemical handle purposes.

Figure A-2|Subcellular localization of LbL-CML-NPs fluorescence microscopy was done at 6 hr time periods for both MC38 and HM-1 cell lines and 24 hr time period for HM-1 cells. While both PLE and HA NPs are external at 6 hours, by 24 hours the HA NPs show a greater degree of internalization.

Figure A-3| Dose response curves of *in vitro* activity of IL-12 NPs IFN-γ responses. IFN-γ levels in response to various IL-12 therapies both in splenocyte only assays and co-cultured with MC38 cells. Used to calculated EC50 values.

Figure B-1|Flowcytometry gating strategy

Figure B-2|Immune population changes upon IL-12 treatment

Figure C-1. Sample Images from IVIS BioD studies of all collected organs.

Figure C-2. Biodistribution in the kidney and spleen as measured by fluorescence

Figure C-3. IL-12 and IFN-γ recovery upon systemic IL-12 delivery

Figure C-4. 5 μg dosed IL-12 tumor bearing mice toxicity

Figure C-5. 5 μg dosed IL-12 tumor burden

Figure C-6. 10 μg dosed IL-12 tumor bearing mice toxicity. Arrows indicate toxicity induced deaths.

Figure C-7. Gating strategy for immune profiling

Figure C-8. Summary of immune profiling data.

Chapter 1. Introduction and Background

1.1 Immunotherapy in cancer

Immunotherapy has become a tremendously attractive option for cancer treatment since the success of checkpoint inhibitors, dating to the approval of ipilumimab in 2011. Checkpoint inhibitor therapies were able to show diverse efficacy, creating long lasting effects in subsets of patients[2]. Indeed, the checkpoint inhibitor ipilumimab was able to show extended survival responses in metastatic melanoma patients, the first therapy of any kind to achieve this result[3], leading to an explosion of immunotherapy approvals centered around checkpoint inhibitors (Fig 1-1)[1]. Melanoma and lung cancer have shown the greatest success with these therapies; however, most epithelial tumors have been much more difficult to treat using immunotherapies like ipilumimab to date. The initial success and puzzling limitations of immunotherapy have led to a large surge in immunotherapy research in cancer to both better understand the cancer immune response and also better utilize the immune system for treatment.

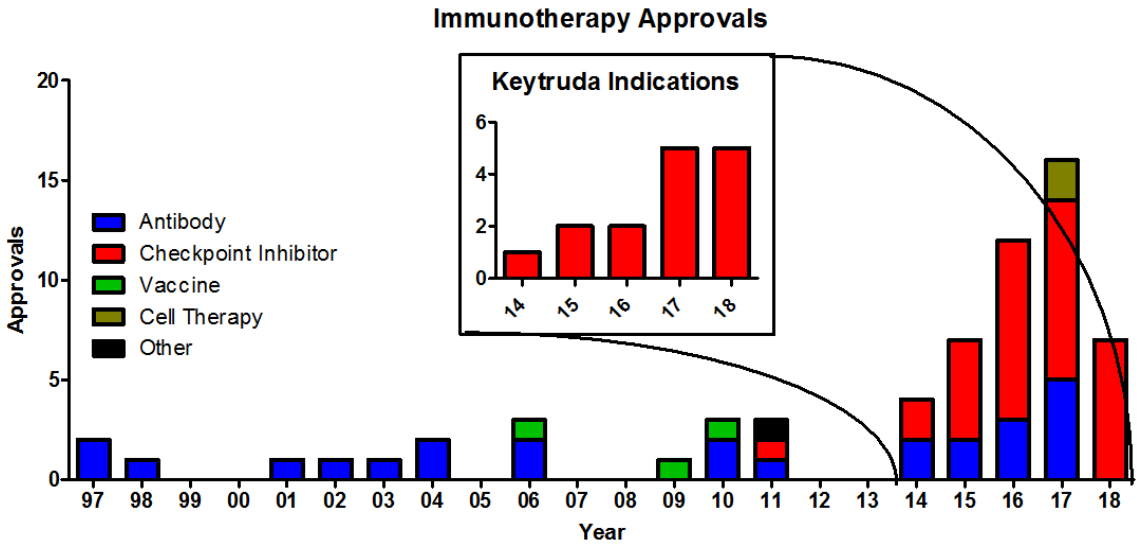

Fig 1-1. Approvals of immunotherapies for cancer by year. Adapted from CRI[1].

This research has led to a significantly improved understanding of an effective immune system interaction with cancer, eloquently described as the cancer immunity cycle[4,5]. The cancer immunity cycle consists of many steps, including antigen release, antigen presentation, priming of T cells and antigen presenting cells (APCs), trafficking to and infiltration of the tumor, and

recognition and activity against the malignancy. These steps of the immune response are in a delicate balance and can either be arrested or driven forward by a variety of factors. For example, the checkpoint inhibitor ipilumimab is targeted towards CTLA-4, a protein that certain cancers overexpress to turn off the immune response in the tumor microenvironment. Checkpoint inhibitors prevent the arrest of the cycle, which works well for some malignancies that have sufficient tumor specific immune populations present; however, "cold" tumor environments need additional therapies to drive the cycle forward, such as proinflammatory cytokines to increase the number and activity level of tumor specific immune cells both locally in the tumor microenvironment and systemically in order to see an improved immune response.

1.2 Tumors suppress the immune system; immunotherapy reverses suppression

One of the reasons cancer is so difficult to treat is the tumors ability to hide from the immune system. This occurs in part through a process by which the tumor tailors its immune environment and the immune environment of the surrounding tissue to a Th2 type immune response over its Th1 counterpart[6-8]. The Th1 and Th2 immune responses are termed this way in reference to the actions of CD4+ helper T cells. A Th1 immune response is generally more adapted to fighting intracellular infection and is associated with high levels of cytokines including interferon-gamma (IFN-γ) and IL-12. This response is often referred to as the inflammatory response or cell-mediated immunity and is shown to be cytotoxic towards tumors. However, the Th2 response, or antibody mediated response, tends to promote tumor growth and metastasis[9]. Tumors have many mechanisms for initiating and maintaining a Th2-like immune environment that are currently being studied to help guide future attempts at immunotherapy in cancer treatment . This ability is one of many that allow tumors to effectively hide from the host's immune system and makes immunotherapies more challenging.

In order to combat the immunosuppression in the tumor environment some key aspects of the switch between Th1 and Th2 immunity and how it is changed in cancer must be better understood. One of the main ways that cancer affects the host immune system is by affecting the terminal populations of myeloid cells. Myeloid cells lead to the populations of dendritic cells, granulocytes, and macrophages[6,7]. For example, it is well understood that tumor associated macrophages (TAMs) play an important role in prognosis for many cancers and are capable of aiding in the treatment of the tumor[8,9]. TAMs are generally classified as being either M1 or M2 type

macrophages, corresponding with Th1 and Th2 type immune responses. The M1 type TAMs can be stimulated by IFN-γ and exercise a cytotoxic effect on tumor cells, while the M2 type cells tend to promote tumor growth and metastasis. Indeed, it has been shown that a higher M1/M2 ratio in ovarian cancer correlates with better 5 year prognosis[9]. Taking advantage of this tumor suppressive versus tumor promoting phenotypic switch can be an important area for tumor immunotherapy and can potentially be exploited to treat many diverse cancer types. In particular, this work looks at stimulating M1 type macrophages, T-cells, and natural killer (NK) cells to kill tumor cells by using cytokines, specifically IL-12, to produce a potent IFN-γ response (a hallmark of Th1 immunity) in the tumor environment.

Once it was established that tumors high jacked the immune system the question became how to override that tumoral control and use the immune system in treatment. Immunotherapy is generally classified by the American Cancer Society as any treatment that stimulates a patient's own immune system to fight disease[10]. The American Cancer Society classifies immunotherapies into four categories; monoclonal antibodies, checkpoint inhibitors, cancer vaccines, and general immune stimulators. This work focuses on general immune stimulators. In particular, it focuses on cytokines that are designed to stimulate the host's immune system in a nonspecific way, simply activating all nearby immune cells in the tumor environment to a Th1 type response. This class of therapy is attractive in that it can trigger a very potent response without reliance on any particular aspects of the tumor, such as overexpression of a specific checkpoint, but it is often challenged with high off target toxicity.

Nonspecific immunotherapy is an attractive means of therapy due to the diversity of different cancers. There are hundreds of different mutations that can accumulate in tumor tissue, driving the oncogenic process. These mutations coupled with tissue of origin differences mean that there are thousands of different types of cancer. Nonspecific immune stimulation is attractive in that it can treat many different types of cancers since it does not rely on targeting characteristics that differ from tumor to tumor, unlike other immune strategies such as checkpoint inhibitors which rely on the overexpression of a specific checkpoint for efficacy. One important consideration for treatment using immunotherapies is the immunogenicity of the tumor, which is often correlated to the mutational burden of the cancer. Immunogenicity is a measure of how effectively the immune system can recognize and kill tumor cells. The immune system must be able to recognize a tumor

cell as non-host or diseased to act against it. The more mutations present in the tumor, the easier it is to recognize as being diseased and thus the higher immunogenicity. Lawrence *et al* show that ovarian cancer is among the more immunogenic cancer types and should react favorably to immune stimulation[11]. This work focuses on developing a delivery mechanism for cytokines (specifically IL-12) in the treatment of ovarian cancer to exploit this immunogenicity in the diverse setting of ovarian cancer, a "cold" tumor that has been refractory to checkpoint inhibition[12-14].

1.3 Interleukin-12 drives a pro-inflammatory immune response but is plagued by toxicity

IL-12 was first identified as natural killer cell stimulating factor in 1989 by Kobayashi *et al* for its activity in stimulating an immune response from Epstein-Barr virus and LPS[15]. IL-12 is a 70 kDa heterodimeric protein. It is made up of a 40 kDa subunit and a 35 kDa subunit that are held together by a covalent linkage. It has been shown that both subunits are required for biological activity. IL-12 shows highest activity on a membrane receptor identified on both activated T-cells and activated NK cells. It has been found that resting populations of these same cells do not contain the receptor at measurable levels, but stimulation of these populations with IL-12 also shows high biological activity, suggesting their rapid activation[16-19]. The fact that IL-12 shows its main activity on a membrane receptor poses a potential issue for nanoparticle (NP) delivery since most NP formulations to date have been designed for internal delivery of payload. Specific aim 2 of this project includes tailoring the delivery of the cytokine to the extracellular space using LbL particle design to maintain high biological activity.

IL-12 exhibits a plethora of biological functions when present in cell populations with its receptor. Most of the IL-12 functions found to date correlate to the triggering of a strong Th1 type immune response. The IL-12/IL-4 ratio is one of the main deciding factors in a response to infection as to whether a Th1 or Th2 immune response is followed, thus having high levels of IL-12 triggers a strong Th1 response[17,19]. The most notable biological activity of IL-12 is its induction of T-cells and NK cells to produce certain cytokines, chiefly IFN-γ. IL-12 is required for optimal IFN-γ production and is the most potent stimulator of IFN-γ production, requiring very low concentrations of IL-12 to reach a substantial IFN-γ response. This is critical for IL-12 function against tumors as IFN-γ has been identified as one of the chief driving cytokines of a Th1 type immune response, which has been proven to be anti-tumoral as discussed previously. The stimulation of IFN-γ production is what this work uses as a proxy for biological activity of IL-12

throughout. IL-12 also stimulates T and NK cells to produce many other cytokines at lower levels, including IL-2, GM-CSF, and TNF-α, although these production rates are dwarfed by the ability of IL-12 to stimulate IFN-γ production[16-19].

IL-12 also shows many effects on proliferation and activation status of different immune cell populations. As stated previously, IL-12 drives activated CD4 helper T cells to a Th1 differentiated state. IL-12 also drives the proliferation of activated CD4 and CD8 T cells and activated NK cells; however, little proliferation is induced by IL-12 in the non-activated populations of these cell types. Another important biological function of IL-12 is the ability to promote and enhance cytolytic activity of NK and T cells *in vivo*[16-19]. IL-12 has been shown to be a more potent cytolytic stimulator than other cytokines such as IL-2 and IFN-α, showing enhancement at much lower concentrations than these cytokines require; however, the maximal enhancement of cytolytic activity achieved by IL-12 is lower than that induced by IL-2. All of these additional functions add to the ability of IL-12 to stimulate a cell mediated, Th1 type immune response, and act in an anti-tumor capacity.

The potent immune stimulatory effects discussed above indicate that IL-12 could be a promising treatment for cancer. Based on this knowledge, many preclinical *in vitro* and *in vivo* studies were carried out to determine the anti-tumor effect of IL-12 with great success[18-22]. These studies have included IL-12 effects on *in vitro* anti-tumor activity of patient derived lymphocytes, SCID mouse xenografts, and full syngeneic animal models of many different cancer types. Many studies have been done showing the efficacy of IL-12 in inducing cytolytic activity of patient lymphocytes against tumor cells *in vitro*, including a study showing that picomolar concentrations of IL-12 were able to induce cytolytic activity of tumor infiltrating lymphocytes in ovarian cancer patients[18,22]. These results were followed by a large array of murine models that showed strong efficacy of IL-12, including models for mammary tumors, colon tumors, and melanoma[19,20]. Importantly, some of these trials showed that an important factor in the efficacy of IL-12 treatment was the ability of the stimulated IFN-γ response to act as an anti-angiogenesis factor in mice in addition to the immunological effects discussed previously[20]. One of the best examples of preclinical efficacy comes from Brunda *et al*[21], showing efficacy of IL-12 in treating both syngeneic melanoma and Renca tumor models. Brunda's work also studied the cell populations needed in the anti-tumor response and found that the efficacy of the IL-12 treatment was dependent upon the presence of

CD8 T cells and not NK cells. These promising preclinical results led to the rapid escalation of IL-12 treatments to clinical trials.

The first clinical trials of IL-12 as a cancer immunotherapy were sobering, as they showed that IL-12 had a very narrow therapeutic window upon systemic delivery. Early trials were plagued with very high levels of systemic toxicity, related to IL-12's ability to stimulate IFN-γ production outside of the tumor environment when delivered systemically, with limited efficacy at acceptable doses[19,20,23-25]. An initial phase I trial was conducted using an initial test dose of IL-12 followed by a schedule of daily dosing for 5 days every 3 weeks. This study found a maximum tolerated dose of 500 ng/kg and quickly went to a phase II study. The phase II study employed only the schedule tested in the first study without the initial dose. This study had to be stopped due to severe toxicity including two deaths. It was hypothesized and later confirmed that the reason for this toxicity was the change in schedule, namely elimination of the test dose. These toxic effects were linked to higher levels of IFN-γ when the test dose was eliminated[26-28]. This complex reliance on scheduling in conjunction with the high toxicity and limited efficacy at tolerable doses found across these trials make systemic delivery of IL-12 infeasible as a treatment for most malignancies. These results make showing reduced toxicity and higher efficacy over free IL-12 treatment important for any future IL-12 therapies to be seriously considered for clinical applicability. These preclinical and clinical results obviate the need for a delivery vehicle that can tightly spatio-temporally control the administration of IL-12 to both avoid activity of the cytokine systemically while also concentrating IL-12 to effective doses within the tumor environment.

After these initial poor results some other techniques for using IL-12 were developed and tested that were thought to surpass the issues behind systemic delivery. These new techniques included targeting IL-12 to the tumor microenvironment, cancer vaccines using IL-12 as an adjuvant, and IL-12 genetherapy with improved results over systemic free drug[26-28]. It was hypothesized that these new methods of IL-12 treatment would avoid the main issues behind systemic dosing. The main issue with systemic IL-12 delivery was identified as an inability for the treatment to overcome the immune suppression in the tumor micro environment at doses that showed acceptable toxicities in the rest of the body. Another issue identified was a difficulty to reliably produce a high IFN-γ response with continued IL-12 treatment. Gene therapy was proposed using either viral vectors, DNA plasmids, or genetically modified CAR-T cells to create IL-12 producing

cells in the tumor environment, eliminating the issue of a stunted, transient response in systemic delivery[29,30]. Another popular technique that has gained prominence in recent studies is combining IL-12 as an adjuvant with tumor derived peptides in cancer vaccines. Finally, various strategies have been used to potentiate local IL-12 therapy, designed to keep intratumorally injected IL-12 in the tumor, such as chitosan co-formulations[31-34] and collagen binding proteins[35,36]. Many of these techniques are still undergoing extensive testing and their feasibility as cancer treatments should become more apparent in the near future. Of note, many of these techniques fail to spatio-temporally control the administration of IL-12 from a systemically deliverable package. In this work we explore the use of systemically administrable NP formulations to address the need for pronounced spatio-temporal control of IL-12 delivery to avoid toxicity at enhanced efficacy while maintaining the possibility of systemic delivery.

1.4 Nanoparticles show promise for limiting off-target toxicity, increasing efficacy

NPs have been making their way into the research field and have been established as a clinically effective means of lowering systemic toxicities without affecting efficacy of a variety of therapeutics including chemotherapies and small molecule inhibitors. Many preclinical studies show that NP formulations are even capable of enhancing efficacy of certain therapeutics. Recent reports show promising results for using NP technology for immune therapy applications as well.

NPs are already proven to ameliorate the high toxicity associated with many frontline therapies by controlling biodistribution and minimizing exposure outside of the target tissue. Reduced off target toxicity has been noted by many recent studies comparing encapsulated chemotherapies to their carrier free form in non-inferiority, reduced toxicity trials[37-40]. For example, Boulikas *et al*[37] and Stathopoulos *et al*[38] both report greatly reduced nephrotoxicity, neuropathy, nausea and vomiting in clinical trials of lipoplatin, a liposome encapsulated form of cisplatin, over carrier free cisplatin in both mono and combination therapies. Notably, Boulikas reported a 10-200 fold increase in platinum concentration in tumors compared to surrounding tissue in patients in the clinic, as determined by atomic absorption spectroscopy of patient biopsies. According to preclinical data, biodistribution can be further improved through active targeting by attaching surface ligands that target specific cell types and tissues. Bertrand *et al*[40] show that active targeting can increase the particles retention and uptake in the cells and tissues of therapeutic interest. Overall, these combined properties make nanotechnology a promising means of controlling the

pharmacokinetics and biodistribution of drug payloads which could reduce off-target side effects and could improve efficacy of the drugs by providing greater accumulation in tumor tissue. This is particularly important for cytokine delivery, which has been plagued by off target toxicity as discussed above, as it could offer a means of increasing the tolerated dose and expanding the therapeutic window.

In light of the promising results with frontline therapies, NPs have recently been expanding to immunotherapy delivery as well, as reviewed by Shao *et al*[41] and shown in many preclinical reports[42-44]. In one such report, Visaria *et al*[42] use gold NPs coated with PEG to deliver tumor necrosis factor alpha (TNF-α) with the purpose of enhancing thermal therapy. This work shows enhanced tumor growth delay with TNF-α particle delivery in conjunction with photothermal therapy (PTT) over PTT alone in a subcutaneous mammary tumor model in the hind flanks of A/J mice. This combination of cytokine and thermal therapy was not possible previously due to the high toxicity of systemically delivered cytokines. This work uses the antivascular activity of TNF-α to potentiate thermal therapy by limiting heat dissipation by blood flow through the tumor environment. This work stands as a motivating example for cogent combinations of cytokines and proteins with other therapies based on their biological activity. Cui *et al*[43] demonstrate successful *in vitro* delivery of a cytokine, TRAIL, using an albumin core particle decorated with layer-by-layer (LbL) functionalization. This work develops an LbL particle designed to co-deliver doxorubicin and TRAIL to enhance cytotoxicity. The design shows TRAIL externally and uses TRAIL binding to death receptor as a means of increasing particle internalization and efficacy in cancer cells. The translation of this particle design into *in vivo* studies and as a functioning therapeutic could prove problematic, as systemic delivery of an uncovered, functional TRAIL domain could lead to high off target toxicities, as is often the case with systemic delivery of most cytokines. While positive *in vitro* results such as the design presented by Cui are important for the field, careful thought must be put forward for translation of such particles into *in vivo* studies. This is particularly important for cytokines and other proteins that require external delivery and show pronounced systemic toxicities.

One of the issues with using NPs for cytokine delivery is that NPs are usually designed for intracellular delivery of payload but cytokines require external delivery for efficacy due to the fact that most cytokines are active on cell surface receptors. Some techniques have been proposed to

overcome this difficulty including targeting ligands associated with receptors that prevent internalization[45] and using larger particles with cytokines on the outside delivered directly to the tumor environment[46,47]. This work looks to build on these previous techniques to create a particle that is capable of external cytokine delivery while being introduced systemically, rather than *in situ*. Cytokine delivery by NPs has grown in prominence in recent years and shows promise in making cytokine therapy routinely seen in the clinic a realizable goal.

As NP therapy expands into the immunotherapy space some particle designs incorporating our cytokine of interest, IL-12, have been reported with varying degrees of success[48-53]. These techniques exploit the hypothesized methods for increased clinical impact of IL-12 discussed above, namely *in situ* delivery and combination with other therapies. One of the first particle formulations of IL-12 came from Egilmez *et al*[48] who devised a polymeric core particle encapsulating the cytokine and delivered it into the tumor. This particle formulation made use of micron-scale sized particles and reported increased efficacy over other administration routes. They report complete primary tumor regression and prevented metastatic activity in a syngeneic lung tumor model. Importantly, this study identified a prolonged release of IL-12 from the particles over 12 days, which was one of the hypothesized methods to improve IL-12 therapy. This study was later expanded to include a combination treatment with GM-CSF which showed improved efficacy over the monotherapy[49]. Many additional combination therapies have been tested in murine models with increased efficacy[48-51,54]; however, it must be noted that systemic monotherapy with IL-12 also showed promise in initial animal models. These studies often show increased efficacy over a control of systemic delivery which inspires hope for a better clinical outcome in the future. However, these studies were limited to micron-scale particles which eliminate the possibility of systemic administration. Other particles on the nano-scale have been reported[52,53] as well; however, these studies relied on passively targeting NPs to tumors and noticeably lacked sufficient toxicology studies to demonstrate reduction of toxicity for IL-12.

Optimally engineered NPs offer an evident opportunity to improve IL-12 therapy as it has been shown that localized IL-12 delivery is of great importance for a successful therapy.[32,34,55] The use of a NP delivery system is particularly attractive because a properly designed NP therapy allows for the possibility of systemic delivery with limited off-target exposure of the IL-12 payload as well as concentration of IL-12 in the tumor microenvironment. Nevertheless, IL-12 poses unique

design challenges for optimal NP delivery vehicles that have not yet been met in the field: 1) Cytokines are labile proteins and have been historically difficult to deliver using traditional encapsulation techniques; 2) NPs are often internalized by cells into endosomal compartments; however, IL-12 and other cytokines must engage external receptors to be effective and are rendered useless and often degraded upon internalization; 3) IL-12 is designed to be secreted and act locally in natural immune responses and is very toxic when allowed to circulate systemically, which necessitates a high degree of tumor association and display of IL-12 only within the tumor. Meeting all of these design criteria in the same NP delivery vehicle is paramount to the success of an IL-12 NP therapy.

1.5 Layer-by-layer (LbL) nanoparticles offer unique opportunity to improve cytokine delivery

LbL assembly is a simple, modular engineering approach for the surface modification of NPs, which provides the means to address each of the design requirements defined above. LbL is a water-based, electrostatic method for layering polymer materials onto surfaces[56,57] to generate a thin film of material that can modulate the material properties of the carrier. This work focuses on the use of LbL NP technology to enhance targeted delivery of IL-12; reducing off target toxicity and increasing efficacy. LbL NP technology has been recognized as an effective means of tailoring NP delivery vehicles to have desirable properties *in vivo*, including targeting abilities, pharmacokinetic and biodistribution control, and decreased toxicity in the body. LbL particles have been established as a diversely applicable delivery system for many therapeutics as reviewed by Correa *et al*[58]. LbL NPs are formulated by incorporating diverse materials in thin films around a particle core using any number of alternating interactions including electrostatics, which is the focal technique of this work. This technique is very versatile and can be applied to a variety of core particles such as liposomes, polymer cores, and mesoporous silica cores as long as they carry a strong enough charge. The benefit of this technique, as described by Correa, is the ability to make use of different materials to add diverse functionalities to the particles, including ligand affinity targeting of the particle, controlling drug release profiles from the particle, and enhancing stability and circulation time of the particle *in vivo*. This NP design offers many advantages including multiple drug compartments with the potential for sequential cargo release, the ability to tailor surface chemistry with polymer layers to affect targeting and biodistribution, and improved pharmacokinetics.[58-67] In particular, the LbL technique offers the ability to easily alter and screen

for surface chemistries that can meet particular design criteria to address the many challenges presented by optimal IL-12 NP construction. In this work, an LbL particle construction approach was used to systematically engineer an optimized NP for IL-12 delivery against cancer. These particles were shown to meet each of the design criteria including 1) high loading and release of active IL-12, 2) localization of NPs on the surface of tumor cells maintaining payload availability to membrane receptors, and 3) high association with tumor cells, concentrating NPs and payload in tumors resulting in increased efficacy and decreased systemic exposure and toxicity.

1.6 Ovarian cancer is an area of high need for systemic immunotherapy improvement

Ovarian cancer is the eleventh most common cancer in women, but corresponds to the fifth highest cancer in terms of death toll in this population, making it the deadliest gynecological cancer according to the Ovarian Cancer Research Alliance[68]. These data suggest that current treatments of ovarian cancer are lacking and require reinforcements. While other tumor types have seen significant improvements in patient outcomes with the previously described immunotherapy strategies ovarian cancer has remained largely unresponsive[69]. Particularly, ovarian tumors are among the worst responders to checkpoint inhibition, likely due to their presentation as an immunologically "cold" tumor environment[12-14]. One possible area for improving the treatment of ovarian cancer is in immunotherapy using immune stimulating agents to drive the immune response forward in these tumors. However, research in this area has often been plagued by off target toxicities and limited therapeutic efficacy at tolerable doses as discussed here. This issue is made more difficult in ovarian cancers due to their presentation. Ovarian cancers often present as dispersed metastatic burden throughout the peritoneal space. This makes local injection of potent immune stimulators difficult, necessitating the need for a systemic delivery option. However, many potent immune stimulators have struggled to achieve an acceptable therapeutic window with systemic delivery due to high toxicity driven by activity outside of the tumor microenvironment. NPs offer a unique way of combating this issue by targeting therapy to the tumor and limiting exposure of the therapies outside of the tumor environment upon systemic delivery. For these reasons treating ovarian cancer is the driving example in this thesis for testing the use of LbL NPs for IL-12 delivery.

1.7 Specific aims of the thesis

The goal of this work is to create a well characterized LbL NP for cytokine delivery with the intent of treating ovarian cancer. This work uses IL-12 as a sample cytokine for its high potency and anti-tumor activity in preclinical models. The following aims, loosely correlating to the discussed engineering challenges for IL-12 delivery from a NP carrier, support the end goal of creating an LbL particle aimed at optimal IL-12 delivery to ovarian tumors for immunotherapy:

1. **Optimizing IL-12 encapsulation into LbL nanoparticles**- Efficiently encapsulating IL-12 is the first step to delivering an IL-12 therapy with NPs. Protein encapsulation in NPs has proven to be an issue in the past due to instability of proteins in many of the processes required for NP formulation such as heat, sonication, and pressure driven extrusion. This must be overcome to effectively deliver IL-12 using a NP.
2. **Delivering bioactive IL-12 to the extracellular space in the tumor**- Once IL-12 has been efficiently encapsulated, it must be shown that the IL-12 delivered from the particle is still bioactive for the therapy to be effective. Tumor targeting is important to prevent off target toxicity upon systemic delivery. The extracellular space must be targeted to maintain high activity of IL-12 on its membrane receptor. This could be a significant challenge as NPs are often designed for internal delivery.
3. **Show reduced toxicity and increased efficacy *in vivo***- The main issue with IL-12 therapy in the past has been high off target toxicity and reduced efficacy at tolerable doses. For a NP delivery method to be successful it must show reduced toxicity and increased efficacy over a free drug treatment in a syngeneic animal model.

1.8 Thesis overview

This thesis, as introduced and supported above, intends to develop an optimized delivery vehicle for cytokine therapy in the treatment of cancer. The focus of this thesis is centered on using IL-12 as a model cytokine to demonstrate the value of the proposed vehicle for a highly potent, yet toxic cytokine. The LbL technique is used to adjust the materials properties of the NP delivery vehicle to meet the demands of effective cytokine delivery. Namely, the LbL NP is used to optimally control the spatio-temporal delivery of IL-12 from a systemically deliverable package. The focus throughout this thesis is in testing these NP delivery vehicles for their ability to reduce toxicity and enhance efficacy of the cytokine payload due to these engineered material properties.

Moreover, this thesis focuses on the effects of the described therapy in ovarian cancer, with the goal of potentiating future success of immunotherapy in this difficult to treat tumor type.

Chapter 2 focuses on the development of the NP design and materials characterization *in vitro*. We demonstrate efficient protein encapsulation in NPs using association to a liposomal surface. It is further demonstrated that using poly-L-glutamic acid (PLE) outer layer coatings lead to enhanced tumor cell binding. Moreover, PLE coatings were shown to preferentially localize on tumor cell surfaces compared to other coatings which were rapidly internalized. These results were then shown to correlate to increased *in vitro* activity of IL-12 as measured by IFN-γ production in a tumor mimic model compared to internalized NPs or carrier-free IL-12 therapy.

Chapter 3 expands on the findings in chapter 2 by testing the designed PLE NPs (PLE-IL-12-NPs) *in vivo* for their ability to reduce toxicity and enhance efficacy of IL-12 therapy. We show that PLE-IL-12-NPs show significantly reduced toxicity upon local administration both with and without tumors (subcutaneous or intra tumoral injections respectively). Moreover, we demonstrate that the PLE-IL-12-NPs show no reduction in anti-tumor efficacy compared to carrier free cytokine. Finally, we probe the strength and duration of the immune response triggered by PLE-IL-12-NPs, demonstrating an active immune response over 7 days that is no less potent than carrier-free IL-12 delivery in triggering a proinflammatory immune response as measured by immune profiling within the tumor, tumor draining lymph node, and spleen.

Chapter 4 takes the results of chapters 2 and 3 further by focusing on systemic delivery of PLE-IL-12-NPs. This chapter focuses on the application to ovarian tumors by both intravenous and intraperitoneal injections, demonstrating both reduction in toxicity and enhancement of antitumor efficacy from PLE-IL-12-NPs not only compared to carrier-free cytokine but also compared to a simpler NP design that does not incorporate the LbL technique (UL-NPs). We further demonstrate that the PLE-IL-12-NPs are capable of concentrating IL-12 in tumors and avoiding clearance in other organs such as the liver compared to UL-NPs. Finally, we also demonstrate that the PLE-IL-12-NPs are capable of generating an equivalent immune response in ovarian tumors compared to carrier-free IL-12 and exceeding that of UL-NPs.

Chapter 5 expands on earlier chapters by probing the method of activity from the LbL NPs further. This chapter uses intricate FRET *in vitro* studies to show that IL-12 is first exposed on the liposome surface then released to the surrounding tissue over time. This finding is then used to

hypothesize alternate linker chemistries of IL-12 to liposomes to further enhance IL-12 therapy. It is demonstrated that altering the linker chemistry can prevent IL-12 from dissociating with the particle and that this new design holds the same *in vitro* activity as the PLE-IL-12-NPs proposed and tested in chapters 2-4.

Chapter 6 summarizes the main findings of the previous chapters. Additionally, chapter 6 offers possible future directions and applications of the work discussed in this thesis.

Chapter 2. Formulation and characterization of IL-12 containing LbL-NPs

Adapted from:

Barberio, A.E., Smith, S.G., Correa, S., Nguyen, C., Nhan, B.T., Melo, M., Tokatlian, T., Suh, H., Irvine, D.J., Hammond, P.T., 2020. Cancer Cell Coating Nanoparticles for Optimal Tumor-Specific Cytokine Delivery. ACS Nano, *Under Revision*.

2.1 Introduction to IL-12 NP design challenges

An effective immune response against cancer requires a complex series of steps, eloquently described as the cancer immunity cycle[4,5], which include tumor antigen release, dendritic cell priming of T cells in tumor-draining lymph nodes, and effector T cell homing to the tumor. These steps of the immune response are in a delicate balance and can either be arrested or driven forward by a variety of therapeutic approaches. Checkpoint inhibitors prevent the arrest of the cycle, which works well for some malignancies that have sufficient pre-existing tumor-specific immune populations present. For example, melanoma and lung cancer have shown some of the greatest success with these therapies; however, many epithelial tumors have been much more difficult to treat using immunotherapies to date. This is particularly true of cancers that are known to have a "cold" immune microenvironment such as advanced serous ovarian cancer, for which the concentration of prognostic leukocytes such as CD8+ T cells is low and the signaling cascade to elicit an immune response is greatly lowered or missing.[12-14] Such "cold" tumor environments need additional therapies to drive the cycle forward, such as proinflammatory cytokines to increase the number and activity level of tumor specific immune cells both locally in the tumor microenvironment and systemically. One promising candidate for driving a proinflammatory response is interleukin-12 (IL-12). An extremely potent cytokine, IL-12 bridges innate and adaptive immunity and drives an antitumoral Th1 type immune response, mediated in large part by inducing the production of interferon-γ (IFN-γ) that acts as the main downstream product of IL-12 signaling.[17-20] IL-12 has been used in multiple preclinical models to great effect against various tumor types,[21] which led to the initiation of multiple clinical trials of this cytokine for cancer therapy.[23-25] Although initial trials found a well-tolerated dose, subsequent trials found high toxicity at the same dose with slightly altered schedule. It was found that these high, schedule-dependent toxicities were linked with the appearance of high IFN-γ levels in blood plasma.

Recently, many new delivery methods have been tested to improve IL-12 therapy. These methods have focused largely on local delivery techniques including microparticle delivery[48-50,70] and chitosan co-formulations[32-34] designed to keep IL-12 in the injected tumor; however, these methods require an accessible tumor to inject and cannot be translated to systemic delivery as is required for metastatic diseases that lack a main tumor such as ovarian cancer. Additional delivery methods have used gene therapy to induce IL-12 production in the tumor.[29,30] Finally, simple NP delivery vehicles have been tested to deliver IL-12 protein[52,53] relying on passive targeting, and notably lacking in sufficient toxicology studies demonstrating the reduction of toxic side effects for this potent therapy, a critical aspect of bringing the promise of IL-12 back to clinical relevance. All of these approaches lack the ability to spatio-temporally control the delivery of cytokine in the tumor environment from a systemically deliverable package; which is critical for meaningful success in the delivery of a highly potent and systemically toxic therapy such as IL-12 and other cytokines.

Optimally engineered NPs offer an evident opportunity to improve IL-12 therapy as it has been shown that localized IL-12 delivery is of great importance for a successful therapy.[32,34,55] The use of a NP delivery system is particularly attractive because a properly designed NP therapy allows for the possibility of systemic delivery with limited off-target exposure of the IL-12 payload as well as concentration of IL-12 in the tumor microenvironment. Nevertheless, IL-12 poses unique design challenges for optimal NP delivery vehicles: 1) Cytokines are labile proteins and have been historically difficult to deliver using traditional encapsulation techniques; 2) NPs are often internalized by cells into endosomal compartments; however, IL-12 and other cytokines must engage external receptors to be effective and are rendered useless and often degraded upon internalization; 3) IL-12 is designed to be secreted and act locally in natural immune responses and is very toxic when allowed to circulate systemically, which necessitates a high degree of tumor association and display of IL-12 only within the tumor. Meeting all of these design criteria in the same NP delivery vehicle is paramount to the success of an IL-12 NP therapy.

Layer-by-layer (LbL) assembly is a simple, modular engineering approach for the surface modification of NPs, which provides the means to address each of the design requirements defined above. LbL is a water-based, electrostatic method for layering polymer materials onto surfaces[56,57] to generate a thin film of material that can modulate the material properties of the carrier. This NP

design offers many advantages including multiple drug compartments with the potential for sequential cargo release, the ability to tailor surface chemistry with polymer layers to affect targeting and biodistribution, and improved pharmacokinetics.[58-66,71] In particular, the LbL technique offers the ability to easily alter and screen for surface chemistries that can meet particular design criteria to address the many challenges presented by optimal IL-12 NP construction. In this chapter, an LbL particle construction approach was used to systematically engineer an optimized NP for IL-12 delivery against cancer and extensively characterized *in vitro*. These particles were shown to meet each of the design criteria including 1) high loading and release of active IL-12, 2) localization of NPs on the surface of tumor cells maintaining payload availability to membrane receptors, and 3) high association with tumor cells. Importantly, these LbL NPs showed efficacy in ovarian cancer, one of the more challenging tumor types to treat with immunotherapy as it often presents as a "cold" tumor that is difficult to treat using current approaches. Thus we demonstrate a marked improvement in the ability to control and improve IL-12 therapy compared to current delivery methods.

2.2 Materials and Methods

Materials

1,2-dioleoyl-sn-glycero-3-[(N-(5-amino-1-carboxypentyl)iminodiacetic acid)succinyl] (nickel salt) (DGS-NTA (Ni)), 1,2-distearoyl-sn-glycero-3-phosphocholine (DSPC), Cholesterol, and 1-palmitoyl-2-oleoyl-sn-glycero-3-phospho-(1'-rac-glycerol) (sodium salt) (POPG) 1,2-dioleoyl-sn-glycero-3-phosphoethanolamine (DOPE) were purchased from Avanti Polar Lipids and used without modification. PLR and PLE were purchased from Alamanda Polymers and used without modification. Single chain IL-12 was produced in house from HEK-293 cells.

Protein Synthesis and Purification

Single chain IL-12 sequence[72] was synthesized as a genomic block (Integrated DNA Technologies) and cloned into gWIZ expression vector (Genlantis). Plasmids were transiently transfected into Expi293 cells (ThermoFisher Scientific). After 5 days, cell culture supernatants were collected and protein was purified in an ÄKTA pure chromatography system using HiTrap HP Niquel sepharose affinity column, followed by size exclusion using Superdex 200 Increase 10/300 GL column (GE Healthcare Life Sciences). Endotoxin levels in purified protein was

measured using Endosafe Nexgen-PTS system (Charles River) and assured to be < 5EU/mg protein.

Particle Formulation and Characterization

LbL NP assembly was performed as described previously[63] with minor modifications. Briefly, liposomes were prepared by the rehydration/extrusion method. A lipid solution containing 5% DGS-NTA (Ni), 65% DSPC, 23.9% Cholesterol, and 6.1% POPG by mole in chloroform was dried at 20 mbar for 1 hr by rotovap and desiccated under vacuum overnight. The lipid film was then reconstituted in PBS to a concentration of 1 mg/mL under sonication at 65ºC for 30 minutes. Rehydrated liposomes were extruded through 50 nm filters (Whatman) using Avestin Liposofast-50 pressure driven extruder at 65ºC until they reached a size of appx 60 nm as measured by number average diameter by DLS (Malvern ZS90). Single chain IL-12 was added to liposomes in a 28:1 Ni:His ratio by mole overnight at 4C. Particle buffer was switched to water by tangential flow filtration (TFF) by 5x washing through a 100 kDa membrane (Spectrum Labs). Particles were added to a bath of PLR solution in glass vial under sonication at 0.1 weight equivalent of polymer compared to lipid and allowed to equilibrate on ice for 1-2 hours. Excess polymer was purified by TFF through a 100 kDa membrane (Spectrum Labs) and characterized for size and charge by DLS. Similarly, for terminal layer polyanion, particles were then added to a bath of polymer in glass vial under sonication at 1 weight equivalent of polymer compared to lipid and allowed to equilibrate on ice for 1-2 hours. Particles were purified by TFF and characterized for size and charge by DLS.

Encapsulation characterization

Encapsulation of scIL-12 in particles at various stages of the particle manufacture process was characterized by breaking up particles in 1% triton-100 (Sigma), 0.1% BSA (Sigma) under vortex for 1 min. IL-12 content was then measured by ELISA (Peprotech) and compared to initial amount of IL-12 added to the NPs (measured by nanodrop at time of addition) for encapsulation efficiency. Final particle lipid concentration was measured by Stewart assay[73] using chloroform dissolved lipid mixture from liposome formulation to produce a standard curve and weight percent encapsulation was calculated using IL-12 and lipid concentrations (mg IL-12/(mg lipid+mg IL-12)).

Fluorescence Imaging

Chambered cover slips (LabTek) were coated with 50 μg/mL rat tail collagen (corning). Cells were seeded on coverslips at 5000 cells per well and allowed to establish for 24 hours. Cells were treated at different time points at 6.2 μg/mL particles. Fluorescent core carboxy modified latex particles (Thermo Fisher F8803) layered with PLR and indicated terminal layer polyanions were used in place of scIL-12 liposome cores for visualization. Cells were incubated for 4 or 24 hours after particle treatment. Cells were fixed with 4% formaldehyde for 15 minutes and stained with wheat germ agglutinin-AF647. Cells were then fixed again for 2 minutes and permeabilized with 0.2% triton x-100 and stained with Hoechst solution at 1.25 μg/mL. After staining, wells were protected with Vectashield and imaged on an Applied Precision DeltaVision Spectris Imaging System with Softworx deconvolution software. Images were further analyzed in FIJI.

Cell Culture

MC38 cells were a gift from the laboratory of Darrell Irvine. HM-1 cells were acquired through Riken BRC. Cells were cultured in DMEM or α-MEM respectively, supplemented with 10% FBS and penicillin/streptomycin or as recommended by the supplier in a 5% CO_2 humidified atmosphere at 37C. All cell lines were murine pathogen tested and confirmed mycoplasma negative by Lonza MycoAlert™ Mycoplasma Detection Kit regularly throughout experiments.

***In vitro* activity experiments**

Constructed scIL-12 LbL NPs were tested for bioactivity by ability to stimulate an IFN-γ response. Briefly, splenocytes were isolated from appropriate background strain mice (based on the tumor cell line being used; MC38 paired with C57Bl/6 mice and HM-1 paired with B6C3F1) by pushing spleens through 70 μm strainers, lysing red blood cells via ACK lysis buffer and resuspending splenocytes in RPMI containing 10% FBS, 1% penicillin/streptomycin, 1% sodium pyruvate, and 0.0005% β-mercaptoethanol. Splenocytes were cultured for 24 hours or less to prevent changes in populations from culture. Splenocytes were either dosed with varying doses of scIL-12 in particles or soluble form or added to cancer cell cultures that had been dosed for 6 hrs previously with varying doses of scIL-12 in particle or soluble form for 18 hours. Supernatants were then tested for IFN-γ content by ELISA (peprotech). Data were analyzed in Graph Pad PRISM 5 to find EC50 values based on dose response curves.

Tumor selectivity studies

MC38 cells were seeded in 96 well plates at 50000 cells per well and cultured for 24 hours. Splenocytes were harvested similar to *in vitro* activity experiments and added to wells (1:1 ratio with MC38 cells) containing subcultured MC38 cells for a total volume of 90 µl. Wells were then dosed with 10 µl of 0.1 mg/mL or 0.01 mg/mL Cy5 NPs at varying timepoints. Cy5 NPs were made by addition of 5% DOPE by mol replacing 5% by mol DSPC in original liposome formulation. These liposomes were then tagged with sulfo-Cy5 NHS ester (Lumiprobe 13320) following manufacture protocol. Briefly, 8 fold molar excess of dye was added to NP solution titrated to pH 8.5 and allowed to react at 4C overnight under agitation. Excess dye was purified off the NPs using TFF. NP solution was washed until the permeate from TFF showed <5% fluorescence as compared to the start of purification. IL-12 and polymer layering was then carried out similar to previous formulations. After NP incubation cultures were processed and stained for live/healthy cells (Biolegend 423114) and CD45 (BD 564279). Immunostained cells were run on an LSR Fortessa HTS with FACSDIVA software and analyzed using FlowJo V10.5.3.

Statistical Analysis

GraphPad PRISM 5 was used to perform statistical analyses. Multiple comparisons were performed using multiple t tests, one-way ANOVA, or two-way ANOVA followed by post-hoc tests as indicated in figures.

Data Availability

The data for this study are available within the thesis. Raw data are available upon reasonable request from the corresponding author.

2.3 Results and Discussion

IL-12 encapsulation

A single chain version of IL-12 originally described by Lieschke *et al*[72] was used for this work due to its enhanced stability and ease of production. This construct was engineered with a 6x His tag at the C-terminus for purification and encapsulation (Fig A-1). The presence of the His tag was further utilized to attach the single chain IL-12 (scIL-12, IL-12) construct onto liposome surfaces via Ni-His interactions with nickel bearing head groups from 1,2-dioleoyl-sn-glycero-3-[(N-(5-

amino-1-carboxypentyl)iminodiacetic acid)succinyl] (nickel salt) (DOGS-NTA (Ni)) on the liposome surface (Fig 2-1A).[74] This attachment was performed using a simple overnight incubation of formed liposomes with IL-12, preserving the integrity and activity of the labile cytokine by avoiding liposome processing which requires heat, sonication and high pressure with the protein in solution. The IL-12 loaded liposomes were then further modified with a polyelectrolyte bilayer using the well-established LbL process, in which polymer layers of alternating charge are adsorbed to the particle surface and excess polymers removed using tangential flow filtration.[63] These polymer layers serve two important purposes. First, the external anionic layer can be altered to tailor the targeting of the particles to particular cell types and cellular compartments. Second, the polymers act as a shield to the underlying IL-12, limiting its systemic exposure and toxicity. The initial cationic polymer layer on the particles was chosen to be poly-L-arginine (PLR) for its low toxicity and well-established use in LbL systems.[65,75] For the external layer, both hyaluronic acid (HA) and poly-L-glutamic acid (PLE) were chosen to test based on their interactions with immune and cancer cells and dense negative charge[76] (Fig 2-1A).

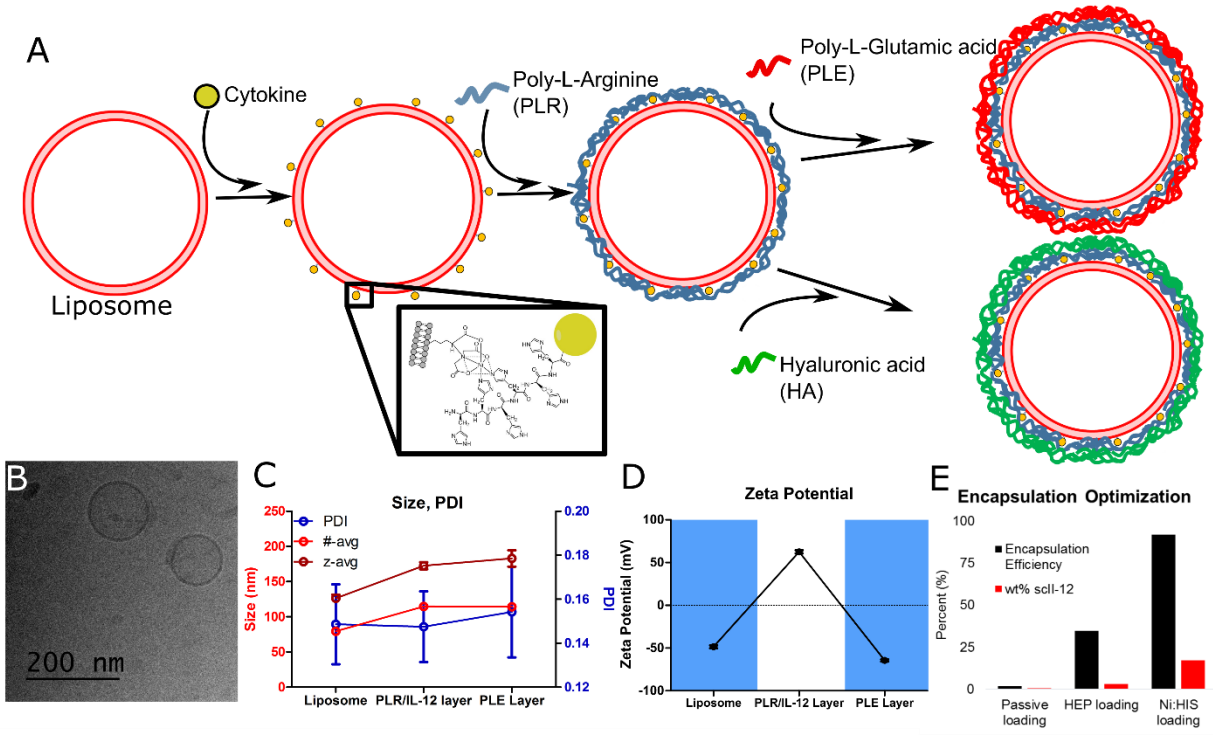

Figure 2-1. IL-12 is formulated into monodisperse LbL-NPs. **A,** Schematic of layer-by-layer buildup of particle and cytokine attachment. **B**, cryoEM image of LbL-NPs shows layered liposome structures 80-120 nm in diameter. **C,** Dynamic light scattering measurements show

effective layering of particles by diameter increase and **D,** charge reversal through layering process, resulting in ~110nm negatively charged particles. Data presented for PLE terminal polyanion layer particles, other external polymers showed similar results by DLS. **E,** Encapsulation of scIL-12 in LbL-NPs as measured by ELISA for different encapsulation techniques (passive, heparin layering interaction (HEP), Ni His tag interaction (Ni:His)).

HA was chosen for its known ligand/receptor interaction with CD44 which has been utilized in the past to target cancers that overexpress CD44, such as triple negative breast cancer, non-small cell lung cancer and ovarian cancer.[60,61,77-80] PLE was chosen based on its strong association and binding to ovarian cancer cells and immune cells of interest, as well as its subcellular localization to cell membranes.[76] The resulting NPs were verified to be monodisperse and successful LbL constructs via cryoEM and dynamic light scattering (DLS) analysis (Fig 2-1B-D). LbL-NPs showed a number average radius of approximately 110 nm and an approximately -60mV zeta potential for both surface chemistries irrespective of IL-12 loading. These particles showed efficient loading of cytokine, especially when compared to more traditional passive loading or loading via heparin binding of IL-12[81] in the layers of the particle (Fig 2-1E), with 90% loading of IL-12 resulting in 13% IL-12 by weight in the final formulation as compared to lipid weight. Using approximations based on lipid head group size, diameter, and monolayer thickness an estimation for number of lipid molecules in a unilamellar liposome can be generated and combined with the loading efficiency of IL-12 from Fig 2-1 to find that each LbL-NP contains approximately 50 IL-12 molecules (Calculation A-1).

NP cellular and subcellular targeting

It is critical that the NPs associate primarily with tumor cell populations to prevent off-target toxicities; however, the receptor-mediated endocytosis achieved with typical selective binding to cells is not desirable for cytokine delivery, as it prevents the payload's access to membrane receptors. Thus, we hypothesize that NP delivery vehicles with extended cell surface membrane localization will improve IL-12 activity by allowing for greater interaction with its membrane receptor. To this end, fluorescence microscopy was used to probe the subcellular localization of both PLE and HA terminal layer LbL-NPs in target cells. Fluorescence microscopy showed that HA terminal layer NPs were internalized in both MC38 colon carcinoma and HM-1 ovarian cancer cell lines by 24 hrs, while PLE terminal layer NPs remained bound to the surface membrane of the

cells for extended periods without significant internalization in multiple cell lines (Fig 2-2, A-2), consistent with recently reported work.[76] Overall these results show promise for PLE as the terminal layer for IL-12-LbL-NPs as the increased cell surface localization on cancer cells has the potential to prolong IL-12 activity from the particles in the tumor microenvironment as compared to particles that are rapidly internalized.

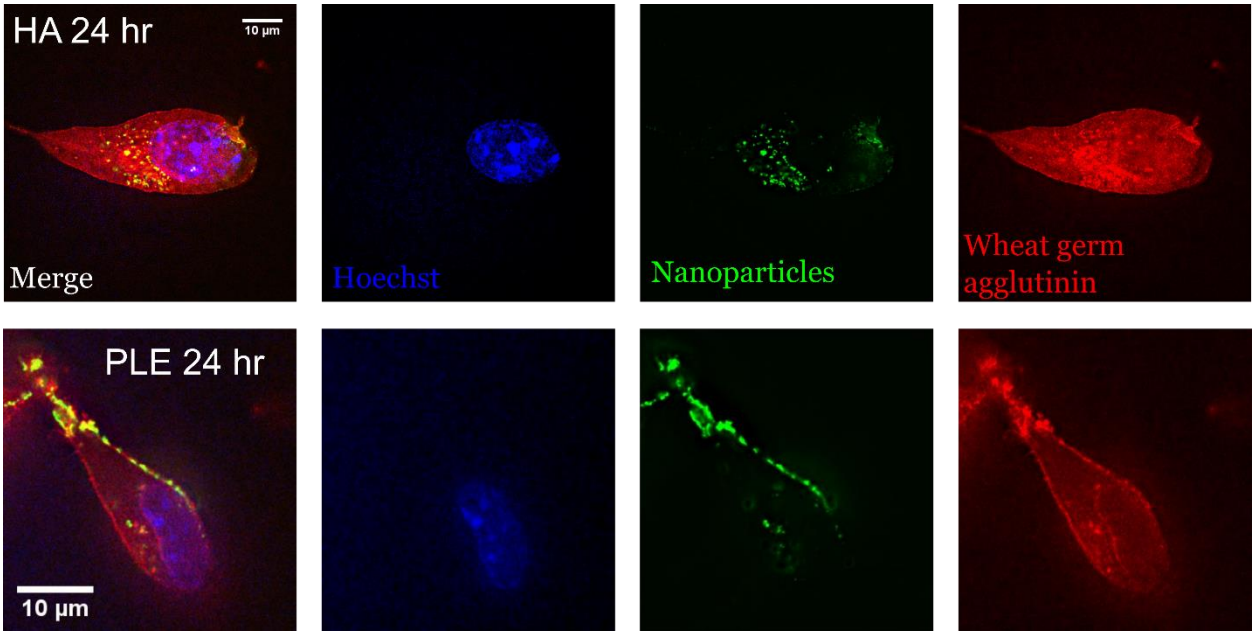

Figure 2-2. LbL-NPs demonstrate differential interactions with cancer cells based on surface chemistry. Fluorescence imaging of MC38 tumor cells incubated with fluorescent carboxy-modified latex core LbL-NPs with either HA or PLE terminal layers for 24 hours. Blue indicates Hoechst nuclear stain, green is LbL-NP fluorescence, red marks wheat germ agglutinin membrane stain.

In addition, the identified PLE-IL-12-NPs were tested for their selectivity in binding to tumor cells over immune cells as an initial *in vitro* test for viability of systemic delivery for such a NP system (Fig 2-3). It is critical that IL-12 be prevented from systemic activity for a successful IL-12 delivery strategy as off target toxicity is the most pronounced limit to IL-12 success in the clinic. To that end, it is paramount that an IL-12 delivery vehicle not only prevent systemic activity by preventing association with immune cells in circulation but also associate with tumor cells to concentrate NPs and their IL-12 payload in the tumor microenvironment. The described PLE-IL-12-NPs demonstrate this selectivity for tumor cell association as measured by flowcytometry using

fluorescently tagged NPs dosed on a co-culture of splenocytes and MC38 tumor cells (Fig 2-3). These data demonstrate that the layering on the PLE-IL-12-NPs enhances NP uptake as compared to an unlayered construct and that NP association is highly (>92%) selective for tumor cells. These data together with the tumor cell membrane association show strong evidence that the described NP meets the design challenges for effective IL-12 delivery.

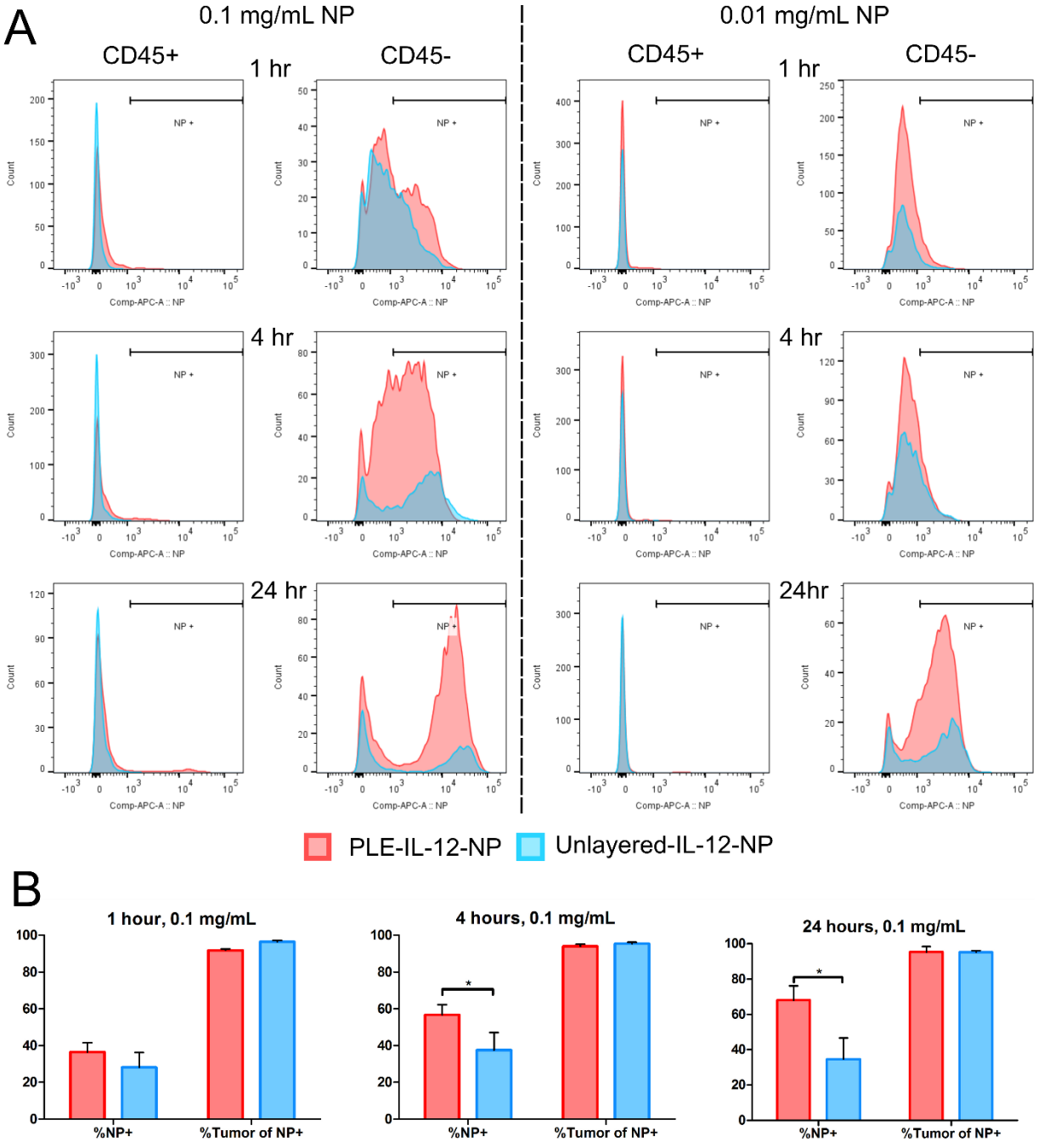

Figure 2-3. NP selectivity for tumor association in tumor-splenocyte co-culture**.** A co-culture containing C57Bl/6 splenocytes and MC38 tumor cells was dosed with fluorescently tagged PLE-IL-12 NPs and assessed for selective uptake in different cell types by flowcytometry. **A)** Histograms of NP signal by dose and time showing differential NP association based on the presence or absence of polymer layers in tumor cells or immune cells. **B)** Quantification (+SEM) of populations in A showing % NP+ cells and of those cells associating with NPs % tumor cells. * indicates $p<0.05$ as measured by two-tailed unpaired t test.

In vitro activity of IL-12 NPs

To evaluate the importance of extended membrane localization for IL-12 delivery via the NP carrier, the biological activity of the LbL-IL-12-NP constructs was probed and compared to free IL-12. To demonstrate biological activity, the IL-12 NPs' efficacy was tested *in vitro* by measuring their ability to stimulate an IFN-γ response from primary splenocytes[17] (Fig 2-4A). In an assay involving direct application to splenocyte culture, the IL-12 NPs showed less activity than an equivalent amount of free IL-12 as measured by the EC50 calculated from dose response curves (Fig 2-4C, A-3). This result is expected, as binding and encapsulation of the cytokine on the NPs should reduce activity, and is indeed relied upon to ameliorate off-target toxicity when the particles are delivered *in vivo* by preventing systemic IL-12 exposure. However, this experimental design does not fully mimic the tumor microenvironment the NPs experience *in vivo* upon delivery, which includes many more tumor cells than immune cells.

Having demonstrated activity directly on target immune cells, it is critical to show that the designed IL-12 NPs are able to maintain activity in the event that they are exposed to tumor cells before these target populations, as is likely *in vivo*. To this end, IL-12 NPs or free cytokine were first incubated with cancer cells before washing off media and adding splenocytes to the culture (Fig 2-4B). In this way, only therapies bound to cancer cells following the washing step, which mimics clearance, are still available to deliver cytokine to immune cells. PLE terminal layer LbL-IL-12-NPs (henceforth called PLE-IL-12-NPs) maintained the highest activity as measured by the lowest calculated EC50 value (Fig 2-4D, A-3), outperforming both free IL-12 and HA terminal layer LbL-IL-12-NPs. Indeed even in this simulated worst-case scenario, PLE-IL-12-NPs maintained the activity of IL-12 in comparison to their direct activity on the target immune populations approximately 10x more than carrier free IL-12 and 2x more than readily internalized

HA-IL-12-NPs (Fig 2-4E). This is likely due to the extended membrane localization of PLE-IL-12-NPs (Fig 2-2). Overall, these results indicated PLE-IL-12-NPs were the formulation most likely to maintain the activity of IL-12 within the tumor microenvironment, supporting our hypothesis that extended membrane localization is important for a cytokine delivery vehicle.

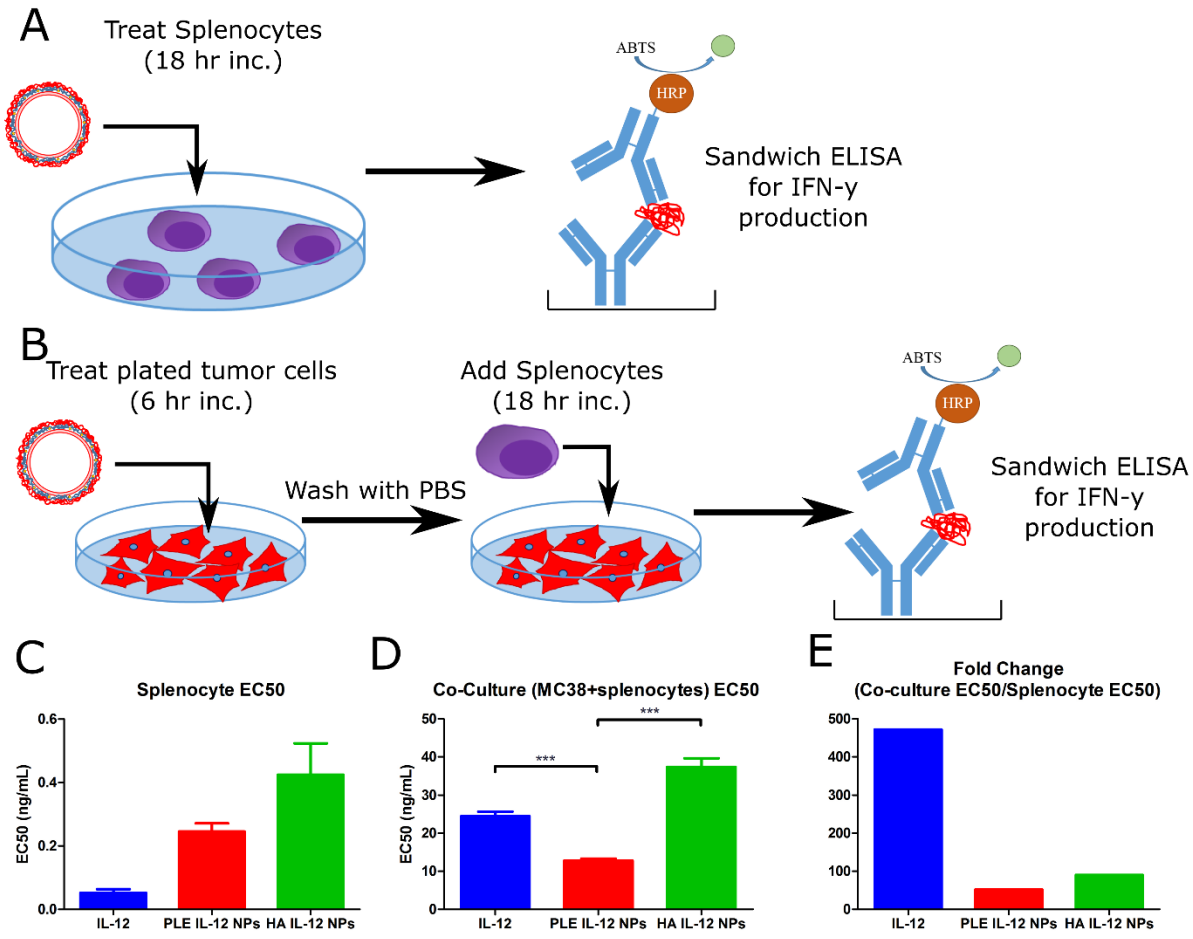

Figure 2-4. LbL-IL-12-NPs demonstrate enhanced efficacy *in vitro*. **A,** Schematic of *in vitro* efficacy test on splenocyte culture. **B,** Schematic of *in vitro* efficacy test in tumor mimic co-culture. **C,** EC50 of IFN-γ response of splenocytes treated with varying IL-12 therapies from A. **D,** EC50 (+SEM) of IFN-γ response of co-cultured MC38 cells and splenocytes treated with varying IL-12 therapies from B. *** indicated $p<.001$ calculated by one-way ANOVA with Bonferroni post hoc test across all groups. **E,** Fold change of activity between C and D.

Activity in gynecologic cancer

Showing efficacy in the MC38 model is an excellent first-pass indicator of the viability of the described PLE-IL-12-NPs as an effective cytokine delivery vehicle. However, the MC38 cell line is known to be an immune infiltrated or "hot" tumor model. Ovarian tumors have proven much more difficult in their response to immunotherapies.[12-14] As a further measure of IL-12 efficacy and test for viability of cytokine delivery via PLE-NPs, their activity in HM-1 tumors (murine ovarian tumors known to be heavily infiltrated with myeloid derived suppressor cells and poorly infiltrated with T-cells) was tested similarly to the characterizations done in MC38.[82,83] Initially, the subcellular localization of PLE-IL-12-NPs in this tumor model were tested similar to the studies carried out in Fig 2-2. These experiments showed that the surface localization of PLE-IL-12-NPs is present in these cells as well (Fig A2). This model was then tested using the same *in vitro* assays described for the MC38 model in Fig 2-4. Similar responses in the *in vitro* efficacy tests in both the splenocyte only and co-culture models were obtained with HM-1 cells (Fig 2-5). As a further test of the diverse applicability of the described PLE-IL-12-NPs their activity in co-culture with 4T1 breast cancer cells was tested as well; again demonstrating an improvement in cytokine response as compared to carrier-free therapy. The pronounced responses found in all of these diverse tumor models demonstrates the wide applicability of the described PLE-IL-12-NPs for cytokine therapy. These data together with toxicity reduction suggest that PLE-IL-12-NPs show promise for treatment of multiple tumor types, including those traditionally less responsive to immunotherapy such as ovarian cancer.

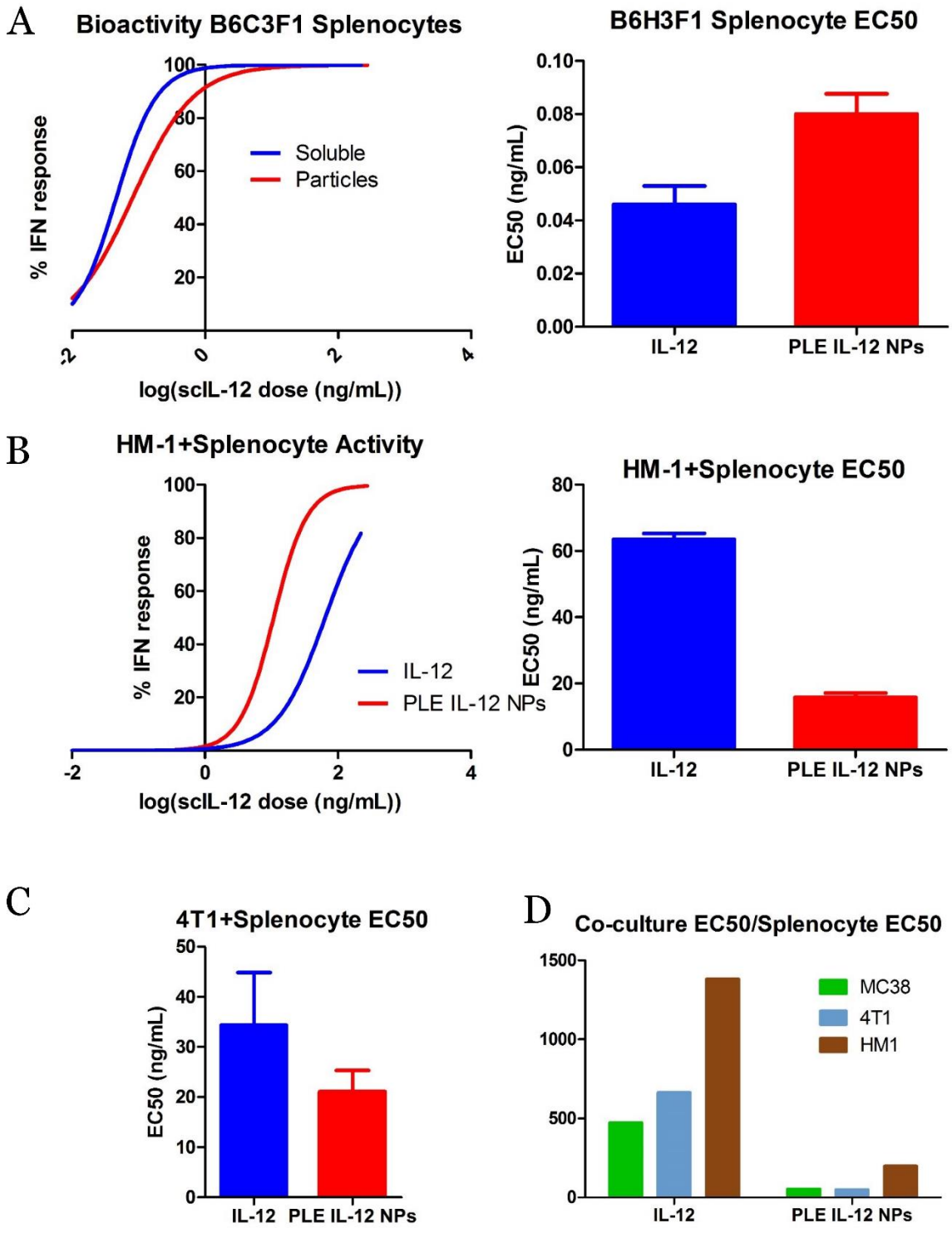

Figure 2-5|*In Vitro* activity of IL-12 NPs in various cancer models A, IFN-γ response to IL-12 therapies in splenocytes from B6C3F1 mice (background of HM-1 tumors). EC50 calculated from

dose response curves. **B,** IFN-γ response to IL-12 therapies in co-culture of HM-1 cells and B6H3F1 splenocytes. EC50 calculated from dose response curves. **C,** EC50 of IL-12 therapies in 4T1 tumor model co-culture experiments. **D,** Fold change of activity for various tumor models of IL-12 therapy calculated similar to figure 3: (co-culture EC50)/(splenocyte EC50)

2.4 Conclusions and future work

In this chapter we have shown the rational engineering of an LbL NP delivery vehicle for the potent but toxic cytokine IL-12. The PLE-IL-12-NP met all of the key design criteria for cytokine delivery including efficiently encapsulating and releasing the cytokine, maintaining cytokine activity on external cell receptors, selectively interacting with tumor cells, and achieving immune efficacy in multiple tumor models. We have demonstrated that the described PLE-IL-12-NPs have a pronounced ability to encapsulate IL-12, showing a 90% encapsulation at 13% by weight in stable particles (Fig 2-1). We have shown that PLE-IL-12-NPs maintain the efficacy of IL-12 in its ability to stimulate IFN-γ production from target cells, and indeed exceed the activity of free IL-12 in a worst-case tumor mimic *in vitro* model, likely due to the distinctive ability of PLE-IL-12-NPs to localize on tumor cell membranes and act as a drug depot (Fig 2-2, 2-3). We have also demonstrated that PLE-IL-12-NPs show a high selectivity for association with tumor cells over other cell types, a critical finding for potential success in systemic delivery.

One limitation of the current study is that it relies on *in vitro* studies to assess therapeutic activity. Future chapters and ongoing work explore the application of this delivery system *in vivo* for both local and systemic administration, focusing on ovarian tumor models to bring the promise of immunotherapy to this difficult to treat malignancy. Indeed the extensive characterization and *in vitro* work here shows promise for a successful systemic cytokine delivery platform. Firstly, the described PLE-IL-12-NPs showed selective association with tumor cells both in this work (Fig S4) and previous studies,[76] which is critical for concentrating NPs and payload in the tumor microenvironment. This is a critical phenomenon for potential success *in vivo*, particularly for systemic delivery, as the main limiting factor for IL-12 is on-target, off-tumor activity, or activating a potent pro-inflammatory immune response throughout the body, also known as cytokine storm. Therefore, a successful IL-12 delivery vehicle must demonstrate pronounced selectivity for interacting with tumor cells over other cell types, particularly immune cells in circulation, in order to concentrate the therapeutic effect to tumors while limiting systemic

exposure of the potent IL-12 payload. Moreover, once NP and payload are within the tumor environment the activity of the IL-12 payload must be kept intact. This is not trivial from a NP vehicle which is often internalized as IL-12 binds to an extracellular receptor. To this end the subcellular fate of the NP delivery vehicle is key. A NP that stays on the cell membrane for an extended period (Fig 2-2) is more likely to maintain payload activity on nearby immune cells than one that is internalized and degraded. Taken together, the *in vitro* characterizations of IL-12 loading (Fig 2-1), subcellular localization (Fig 2-2), tumor cell association selectivity (Fig 2-3), and biological activity (Fig 2-4) demonstrate a NP platform that meets all the criteria for a successful systemically deliverable cytokine therapy.

Additionally, these initial studies show significant promise in important areas for expanding the usefulness of immunotherapy in previously unresponsive cancers. Most notably through the demonstration of activity in ovarian cancer. Ovarian cancer has proven to be refractory to many immunotherapeutic treatments like checkpoint inhibitors, likely due to its common presentation as a "cold" immune environment. This can potentially be ameliorated by delivery of proinflammatory agents like IL-12. In this chapter we demonstrate the *in vitro* ability of PLE-IL-12-NPs to trigger proinflammatory responses in an ovarian tumor mimic. Potentiating immunotherapy for ovarian cancer is especially attractive, as immunotherapy offers the promise of systemic anti-cancer responses. Ovarian cancer often presents as dispersed metastatic burden throughout the peritoneal space, making local therapy very difficult. Immunotherapy offers a path of treatment to circumvent this issue by demonstrating therapeutic effect outside of directly treated lesions. However, to bring this promise to ovarian cancer the therapeutic must also be contained in a systemically deliverable package, such as the described PLE-IL-12-NPs. This promising activity in ovarian tumors is discussed further in the coming chapters.

Another critical aspect of the work presented in this chapter for furthering the field of cancer immunotherapy is the ability to deliver multiple agents from the same vehicle. While we demonstrate the use of the described NP system using IL-12, no IL-12 specific processes are used to make the NPs. This allows for the potential future expansion of the platform to deliver a plethora of other immunotherapies such as cytokines and checkpoint inhibitors as long as they incorporate an appropriate binding ligand. This is critical as the future success of immunotherapy has increasingly pointed to combination therapy to achieve the greatest effect. Indeed, many studies

also indicate that not only the combination of therapies but also the timing between the deliveries of those therapies is critical for the greatest success. The described particle offers a platform to not only deliver multiple therapies at once but also adjust the relative ratios and kinetic delivery of those therapies, as has been done in previous LbL NP work.

Chapter 3 *In vivo* activity and immune response of PLE-IL-12-NPs

Adapted from:

Barberio, A.E., Smith, S.G., Correa, S., Nguyen, C., Nhan, B.T., Melo, M., Tokatlian, T., Suh, H., Irvine, D.J., Hammond, P.T., 2020. Cancer Cell Coating Nanoparticles for Optimal Tumor-Specific Cytokine Delivery. ACS Nano, *Under Revision*.

3.1 Introduction

In the previous chapter, we demonstrate the creation of a NP delivery vehicle for IL-12. The described PLE-IL-12-NPs are thoroughly characterized for materials properties and immune activity *in vitro*. Critically, we find that the PLE-IL-12-NPs are capable of highly efficient protein encapsulation, minimizing cytokine waste; specifically interacting with tumor cells, targeting activity to the tumor environment; localizing to tumor cell surfaces, keeping the cytokine payload available to its extracellular receptor on nearby lymphocytes; and demonstrating pronounced activity *in vitro* in producing an IFN-γ response, most notably in a worst-case tumor mimic model in which therapies first experience tumor cells before target lymphocytes. Importantly, in the previous chapter's activity tests we demonstrate that in the situation in which therapies first interact with tumor cells prior to exposure to target lymphocytes PLE-IL-12-NPs demonstrate a more potent immune activity compared to carrier free cytokines. This is critical as target lymphocytes are often rare cell populations in tumors, particularly in immunologically "cold" tumors, where the proinflammatory response from IL-12 is most critical in potentiating immunotherapy. Therefore, it is imperative that an IL-12 delivery vehicle maintain the activity of this potent anticancer agent in the event that exposure to tumor populations precludes lymphocyte exposure. These data suggest a highly effective IL-12 therapy using PLE-IL-12-NPs.

In this chapter we further demonstrate the effect of PLE-IL-12-NPs using *in vivo* toxicity and efficacy tests. These studies focus on intratumoral delivery to establish reduction of toxicity of IL-12 therapy at equivalent efficacy from PLE-IL-12-NPs compared to carrier-free IL-12. In addition, we probe the intensity and duration of immune response triggered by IL-12 delivery within tumors from both PLE-IL-12-NPs and carrier-free IL-12 delivery. Most critically, we demonstrate that PLE-IL-12-NPs significantly reduce the toxicity profile of IL-12 upon intratumoral delivery. This

is paramount to any IL-12 therapy as toxicity has been the main limiting factor in progression of IL-12 in the clinic[23-25].

3.2 Materials and Methods

Materials

1,2-dioleoyl-sn-glycero-3-[(N-(5-amino-1-carboxypentyl)iminodiacetic acid)succinyl] (nickel salt) (DGS-NTA (Ni)), 1,2-distearoyl-sn-glycero-3-phosphocholine (DSPC), Cholesterol, and 1-palmitoyl-2-oleoyl-sn-glycero-3-phospho-(1'-rac-glycerol) (sodium salt) (POPG) 1,2-dioleoyl-sn-glycero-3-phosphoethanolamine (DOPE) were purchased from Avanti Polar Lipids and used without modification. PLR and PLE were purchased from Alamanda Polymers and used without modification. Single chain IL-12 was produced in house from HEK-293 cells.

Protein Synthesis and Purification

Single chain IL-12 sequence[72] was synthesized as a genomic block (Integrated DNA Technologies) and cloned into gWIZ expression vector (Genlantis). Plasmids were transiently transfected into Expi293 cells (ThermoFisher Scientific). After 5 days, cell culture supernatants were collected and protein was purified in an ÄKTA pure chromatography system using HiTrap HP Niquel sepharose affinity column, followed by size exclusion using Superdex 200 Increase 10/300 GL column (GE Healthcare Life Sciences). Endotoxin levels in purified protein was measured using Endosafe Nexgen-PTS system (Charles River) and assured to be < 5EU/mg protein.

Particle Formulation and Characterization

LbL NP assembly was performed as described previously[63] with minor modifications. Briefly, liposomes were prepared by the rehydration/extrusion method. A lipid solution containing 5% DGS-NTA (Ni), 65% DSPC, 23.9% Cholesterol, and 6.1% POPG by mole in chloroform was dried at 20 mbar for 1 hr by rotovap and desiccated under vacuum overnight. The lipid film was then reconstituted in PBS to a concentration of 1 mg/mL under sonication at 65ºC for 30 minutes. Rehydrated liposomes were extruded through 50 nm filters (Whatman) using Avestin Liposofast-50 pressure driven extruder at 65ºC until they reached a size of appx 60 nm as measured by number average diameter by DLS (Malvern ZS90). Single chain IL-12 was added to liposomes in a 28:1

Ni:His ratio by mole overnight at 4C. Particle buffer was switched to water by tangential flow filtration (TFF) by 5x washing through a 100 kDa membrane (Spectrum Labs). Particles were added to a bath of PLR solution in glass vial under sonication at 0.1 weight equivalent of polymer compared to lipid and allowed to equilibrate on ice for 1-2 hours. Excess polymer was purified by TFF through a 100 kDa membrane (Spectrum Labs) and characterized for size and charge by DLS. Similarly, for terminal layer polyanion, particles were then added to a bath of polymer in glass vial under sonication at 1 weight equivalent of polymer compared to lipid and allowed to equilibrate on ice for 1-2 hours. Particles were purified by TFF and characterized for size and charge by DLS.

Animal Studies.

All animal experiments were approved by the Massachusetts Institute of Technology Committee on Animal Care (CAC) and were conducted under the oversight of the Division of Comparative Medicine (DCM).

***In vivo* toxicity tests**

To test toxicity, C57Bl/6 mice (Taconic) were injected subcutaneously (healthy mice) on the flank with varying doses as indicated of PLE-IL-12-NPs, lipid dose matched LbL-NPs without IL-12, dose matched soluble IL-12, or PBS and monitored daily for weight change. Serum was collected after 5 days and assayed using multiplex inflammatory cytokine assay (done by Abcam).

***In vivo* temporal immune response tests**

C57Bl/6 (Taconic) mice were inoculated subcutaneously with 5E05 MC38 cells in a 1:1 PBS:matrigel solution. Tumors were allowed to establish for 6 days prior to treatment. Subjects were treated with 5 ug IL-12 from PLE-IL-12-NPs injected intratumorally. Subjects were euthanized at different time points and tumors extracted for protein processing. Tumors were digested using RIPA lysis buffer with HALT protease inhibitor (thermoscientific) and 1% active silicon (Y-30, Sigma) at 50 mg tissue/mL buffer. Samples were processed on a miltenyi biotec gentleMACS dissociator using protocol protein-01 in M tubes (miltenyi). Digested tissues were spun at 4000 rcf for 5 minutes and supernatants collected for further protein analysis. Cytokine content in tumors was measured using ELISAs; peprotech 900-K97 to measure all IL-12, peprotech 900-K98 to measure IFN-γ, and peprotech 900-K97 replacing detection antibody with HIS tag detection antibody (R&D systems, cat# MAB050H) diluted at 1:10000. Full IL-12 ELISA

quantification was then corrected for HIS-tagged exogenous IL-12 to calculate endogenous IL-12 delivery.

In vivo efficacy tests

C57Bl/6 (Taconic) or B6C3F1 (Jackson Labs) mice as appropriate for tumor type were injected subcutaneously with 5E05 (MC38) or 1E06 (HM-1) cells in 1:1 PBS:Matrigel (Corning) mixture. Tumors were allowed to establish for 6 days prior to treatment. Mice were treated intratumorally with scIL-12 LbL-NPs, lipid dose matched LbL-NPs without IL-12, dose matched soluble scIL-12, or PBS either weekly or 2x weekly for a maximum of 5 doses. Mice were monitored 2x weekly for tumor growth as measured by digital calipers (Vernier) taking tumor volume to be L*W^2*1/2 where L is the longest diameter and W the shortest diameter of the tumor. Mice were euthanized when volume exceeded 1000 mm^3. For combined toxicity/efficacy studies mice were monitored daily for weight changes over the dosing period and serum was collected 24 hours after the first and last dose and analyzed for IFN-γ and IL-12 content via ELISA (Peprotech) in addition to the above.

Abscopal Response

C57Bl/6 mice were injected subcutaneously with 5E05 cells in 1:1 PBS:matrigel mixture on the right flank and 1E05 cells in 1:1 PBS:matrigel mixture of the left flank. Tumors were allowed to establish for 6 days prior to treatment. Mice were treated intratumorally with PLE-IL-12-NPs, dose matched soluble IL-12, or PBS weekly for 5 doses in the right tumor only. Mice were monitored 2x weekly for tumor growth as measured by digital calipers (Vernier) taking tumor volume to be L*W^2*1/2 where L is the longest diameter and W the shortest diameter of the tumor. Mice were euthanized when volume exceeded 1000 mm^3.

Immune Profiling

Immune profiling studies were carried out similar to *in vivo* efficacy tests. Mice were inoculated with 5E05 (MC38) cells in 1:1 PBS:Matrigel (Corning) mixture. Tumors were allowed to establish for 6 days prior to treatment. Mice were treated intratumorally with 5 ug IL-12 from scIL-12 LbL-NPs, lipid dose matched LbL-NPs without IL-12, dose matched soluble scIL-12, or PBS 2x weekly for 3 doses. 24 hours after the third dose mice were sacrificed and tumors, tumor draining lymphnodes (TDLNs), and spleens were harvested and processed to sinfle cell suspension. Tumors

were digested to single cell suspension using mouse tumor dissociation kit (Miltenyi, 130-096-730) and gentleMACS octo-dissociator following recommendations of supplier. Briefly, tumors were diced into 1-2mm sections and added to C tubes (Miltenyi) and processed on tissue dissociator using protocol m_imptumor_02. Tubes were then incubated at 37C in nutating incubator for 40 minutes and processed on dissociator using m_imptumor_03 twice. Tumors were then pushed through 70 μm strainers to form single cell suspensions. Cells were treated with ACK lysis buffer to remove red blood cells. Spleens and TDLNs were processed similar to splenocyte isolation in chapter 2. Briefly, spleens and TDLNs were forced through 70 μm strainers to form single cell suspensions. Cells were treated with ACK lysis buffer to remove red blood cells. Single cell suspensions were then treated for flow cytometry studies.

Flowcytometry

Antibodies used for immunostaining were against CD69 (biolegend 104545), CD25 (biolegend 102041), NK-1.1 (biolegend 108753), CD3 (biolegend 100232), CD4 (biolegend 100423), CD8a (BD biosciences 566410), FoxP3 (biolegend 126404), CD45 (biolegend 103112), Ly-6C (biolegend 128032), Ly-6G (biolegend 127633), CD274 (biolegend 124331), F4/80 (biolegend 123110), CD11c (BD biosciences 566504), CD11b (biolegend 101217), CD86 (biolegend 105037) CD103 (biolegend 562722). FoxP3 intracellular staining was carried out using FoxP3 intracellular staining kit (Thermo 00-5523-00) following manufacture protocol. Immunostained cells were run on an LSR Fortessa HTS with FACSDIVA software and analyzed using FlowJo V10.5.3.

Statistical Analysis

GraphPad PRISM 5 was used to perform statistical analyses. Multiple comparisons were performed using multiple t tests, one-way ANOVA, or two-way ANOVA followed by post-hoc tests as indicated in figures.

Data Availability

The data for this study are available within the thesis. Raw data are available upon reasonable request from the corresponding author.

3.3 Results and Discussion

PLE-IL-12-NPs reduce the toxicity of IL-12 therapy

The most critical aspect of any IL-12 therapy is the ability to control systemic activity and limit toxicity outside the tumor microenvironment as this has been the largest limitation of this potent class of cytokines in the clinic[23-25]. PLE-IL-12-NPs were tested for their toxicity in healthy C57Bl/6 mice which were dosed subcutaneously with 5 μg doses of either the free cytokine or the PLE-IL-12-NP, as well as a group treated with 7.5 μg of IL-12 in PLE-IL-12-NPs, each dosed daily for 5 days. These groups were compared to PBS dosing and lipid concentration-matched PLE NPs without IL-12 as controls (Fig 3-1). Mice given free IL-12 rapidly lost weight over the dosing period, losing approximately 10% of starting body weight by day 5, indicating a highly toxic therapy. In contrast, mice showed little weight change compared to controls over the dosing period when given PLE-IL-12-NPs, even at 1.5x the dosing of the free IL-12 (Fig 3-1B). These data demonstrate that PLE-IL-12-NPs reduce the systemic toxicity associated with IL-12 therapy.

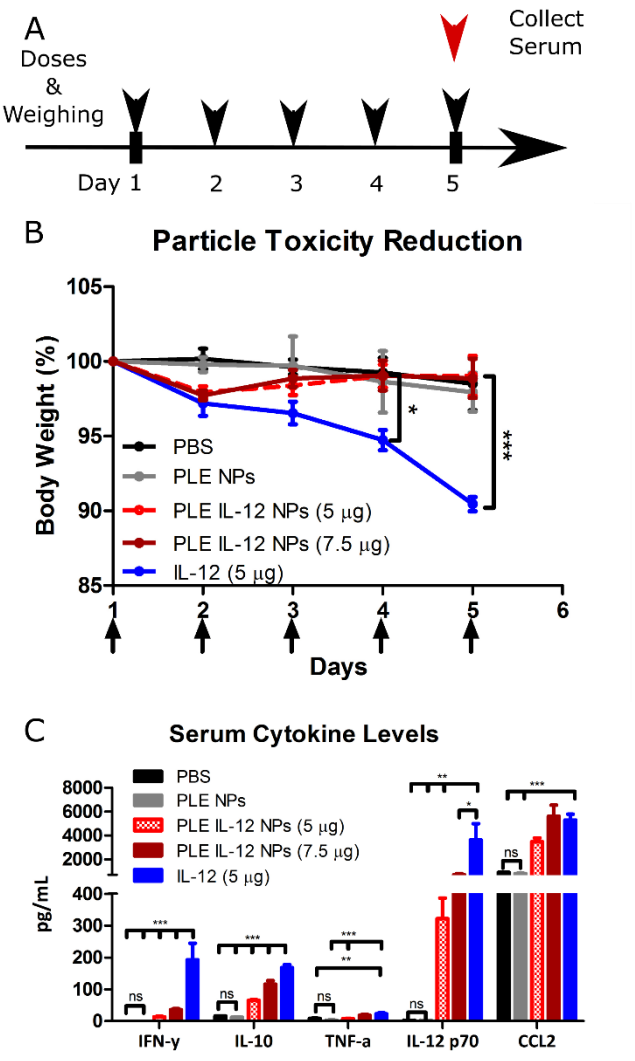

Figure 3-1. PLE IL-12 NPs reduce toxicity of IL-12 therapy *in vivo*. **A,** Schematic of experimental design **B,** Body weight change (Mean+SEM) of healthy animals treated as indicated subcutaneously (PLE IL-12 NPs 5μg n=5, n=3 all other groups). * indicates p<.05, *** indicates p<.001 as measured by 2-way ANOVA with Bonferroni post-hoc test across all groups. **C**, Cytokine response (Mean+SEM) in serum taken after dose 5 from B as measured by multiplexed assay. * indicates p<.05, ** indicates p<.01, *** indicates p<.001 as measured by One way ANOVA on individual cytokine groups with Bonferroni post-hoc test comparing all groups to IL-12 (5μg) and PBS to PLE NPs.

As an additional test of toxicity, serum was collected from the subjects 3 hours after the final dose and analyzed for a panel of systemic inflammatory cytokines. This panel included IL-12 and

IFN-γ which are the direct downstream products of IL-12 signaling and most often associated with toxicity as well as CCL2 which acts as a chemoattractant for T cells, IL-10 which acts as the antithesis of IL-12 and is upregulated to slow down an inflammatory response, and TNF-α which is an immune regulatory molecule. Carrier-free IL-12 therapy showed much higher levels of systemic cytokines IFN-γ and IL-12 than PLE-IL-12-NPs, (Fig 3-1C), again indicating that PLE-IL-12-NPs are able to reduce the systemic toxicity of IL-12. Of note, when comparing the PLE-IL-12-NPs, specifically at the higher dose of 7.5 μg, to free IL-12 many of the positive aspects of the systemic immune response remain engaged, such as chemoattraction of monocytes via CCL2, while the highly toxic IFN-γ is drastically reduced in systemic circulation by the NP carrier even at the higher dose. This demonstrated reduction of systemic toxicity is critical for a successful IL-12 therapy.

PLE-IL-12-NPs show an immune response lasting up to one week

Once full characterization and activity of the PLE-IL-12-NPs was established *in vitro* in the previous chapter and they were confirmed to impart a toxicity benefit, their release and activity *in vivo* was probed to find an appropriate dosing schedule for cancer treatments. C57BL/6 mice bearing MC38 tumors were treated intratumorally with PLE-IL-12-NPs (5 μg IL-12) and sacrificed at different time points. Tumors were then homogenized and assessed for levels of delivered scIL-12, endogenous IL-12, and IFN-γ by ELISA on tumor supernatants (Fig 3-2). Kinetic release of exogenously delivered scIL-12 was found to have a short lag followed by burst release between 4 and 24 hours, followed by a peak response of endogenous IL-12 and a later peak of IFN-γ. These data suggest an active immune response to PLE-IL-12-NPs over a seven day period, with the expected cascade of activation and interferon generation anticipated for an IL-12 therapy (Fig 3-2). Critically these data also demonstrate release of the IL-12 payload while the NPs are still localized to the cell surface (Fig 2-2) These data indicate that a dosing schedule of at least weekly or more frequent dosing of PLE-IL-12-NPs may be required to maintain an active immune response *in vivo* capable of treating cancer.

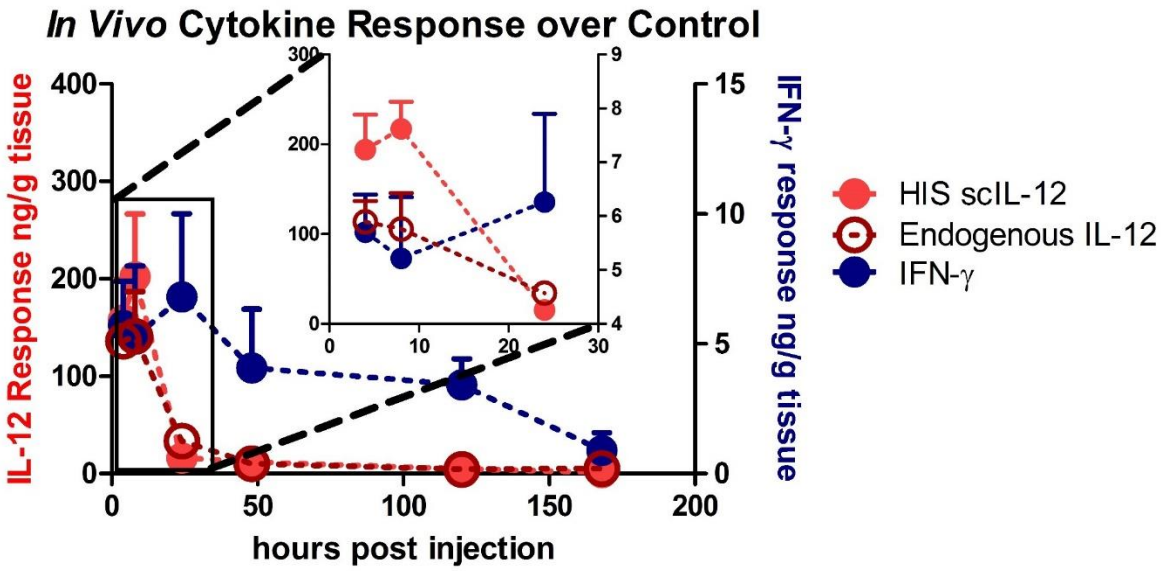

Figure 3-2. Temporal *in vivo* immune response to PLE-IL-12-NPs Established MC38 subcutaneous tumors were treated with 5 μg PLE-IL-12-NPs or PBS at t=0. Mice were sacrificed at indicated time points, tumors homogenized and measured for cytokine signal by ELISA. HIS scIL-12 was measured using IL-12 capture antibody and HIS detection antibody in sandwich ELISA. Endogenous IL-12 was measured using a standard IL-12 sandwich ELISA and correcting for HIS scIL-12 values, and IFN-γ was measured by standard sandwich ELISA. Data shown are the difference between cytokine values in PLE-IL-12-NP treated tumors and PBS treated tumors (n=4 per time point)

PLE-IL-12-NPs maintain efficacy of IL-12 therapy in multiple tumor models

To determine whether safer IL-12 delivery from the described NP carrier continued to provide antitumor efficacy, PLE-IL-12-NPs were tested for their ability to slow tumor growth and prolong survival in two flank tumor models, MC38 colon cancer and the more difficult to treat HM-1 ovarian cancer, as a test of anti-tumor response. As an initial test, MC38 cells were implanted subcutaneously in C57BL/6 mice and vascularized tumors were allowed to form (6 days). Once tumors were established, mice were treated intratumorally with both free IL-12 and PLE-IL-12-NPs and compared to appropriate controls (PBS and PLE NPs without IL-12) (Fig 3-3A). Mice were monitored for tumor response both by growth of tumor size (Fig 3-3B, C) and overall survival (Fig 3-3D). Subjects receiving 5 μg weekly injections of both carrier-free IL-12 and PLE-IL-12-

NPs showed slowed tumor growth and prolonged survival compared to both the PBS and PLE NP control groups in a statistically significant manner by the thirteenth day of tumor growth. Importantly, subjects treated with free IL-12 and PLE-IL-12-NPs showed no differences in therapeutic response from each other. Also, increasing the dose and dosing frequency of PLE-IL-12-NPs enabled a further improvement in tumor responses, as demonstrated with 7.5 μg dosing of the PLE-IL-12-NPs or increased 2x weekly frequency of dosing; both of these conditions elicited slower tumor growth and a statistically significant survival benefit as compared to 5 μg weekly doses of IL-12 in both the PLE NP encapsulated form and free drug (Fig 3-3B-D). These data together with the previously discussed reduction in toxicity demonstrate a widening of the therapeutic window for this potent yet toxic therapy.

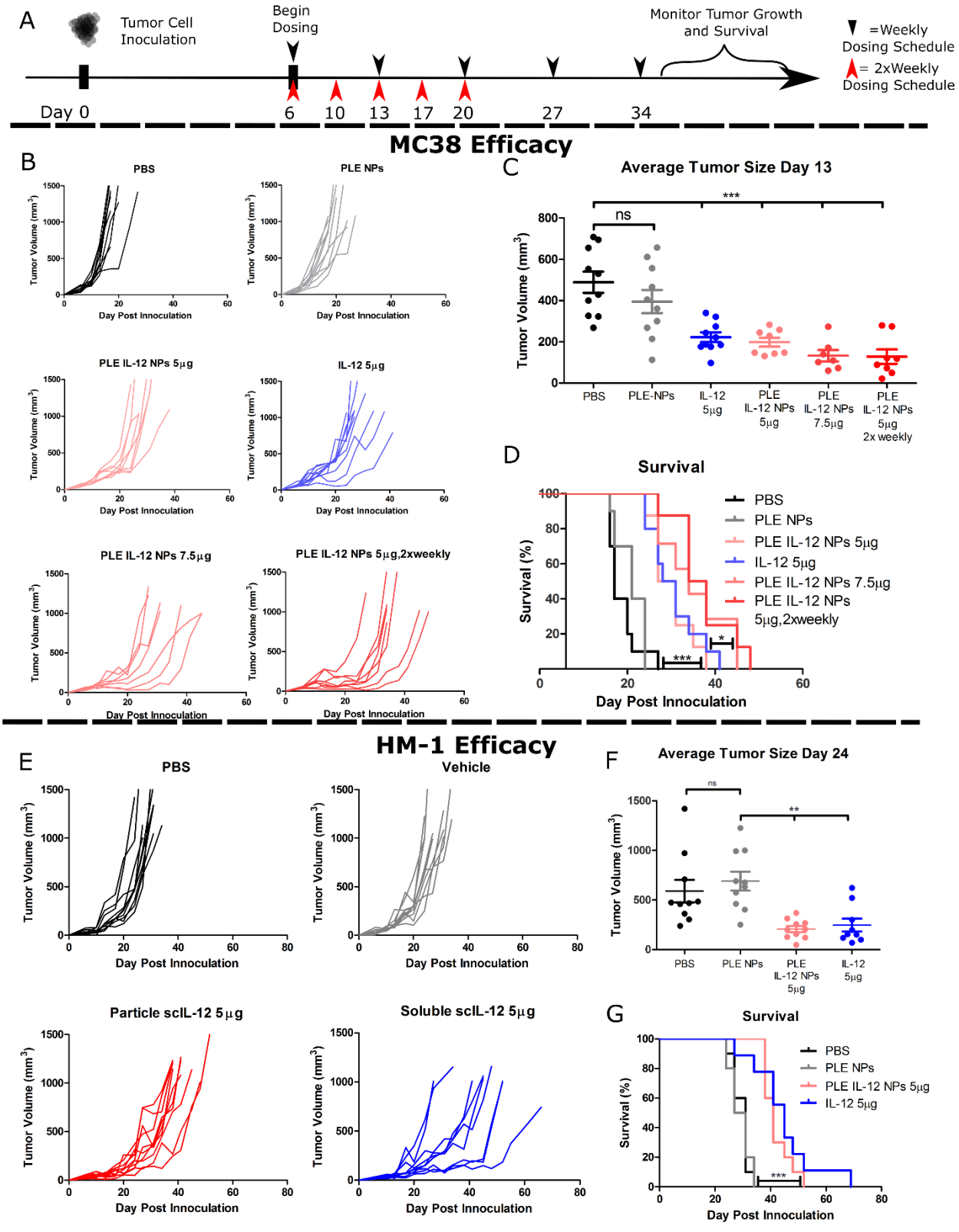
A
Tumor Cell Inoculation
Begin Dosing
Monitor Tumor Growth and Survival
=Weekly Dosing Schedule
= 2xWeekly Dosing Schedule
Day 0
6
10
13
17
20
27
34
MC38 Efficacy
B
PBS
PLE NPs
PLE IL-12 NPs 5μg
IL-12 5μg
PLE IL-12 NPs 7.5μg
PLE IL-12 NPs 5μg,2xweekly
Tumor Volume (mm3)
Day Post Innoculation
C
Average Tumor Size Day 13
ns
***
Tumor Volume (mm3)
PBS
PLE-NPs
IL-12 5μg
PLE IL-12 NPs 5μg
PLE IL-12 NPs 7.5μg
PLE IL-12 NPs 5μg 2x weekly
D
Survival
Survival (%)
PBS
PLE NPs
PLE IL-12 NPs 5μg
IL-12 5μg
PLE IL-12 NPs 7.5μg
PLE IL-12 NPs 5μg,2xweekly
*
***
Day Post Innoculation
HM-1 Efficacy
E
PBS
Vehicle
Particle scIL-12 5μg
Soluble scIL-12 5μg
Tumor Volume (mm3)
Day Post Innoculation
F
Average Tumor Size Day 24
ns
**
Tumor Volume (mm3)
PBS
PLE NPs
PLE IL-12 NPs 5μg
IL-12 5μg
G
Survival
Survival (%)
PBS
PLE NPs
PLE IL-12 NPs 5μg
IL-12 5μg
***
Day Post Innoculation

Figure 3-3. PLE IL-12 NPs maintain efficacy against MC38 (A-D) and HM-1 (E-G) tumors *in vivo*. **A,** Study design. **B,** MC38 tumor volume (mm^3) of indicated treatments. All animals dosed 5 times given weekly intratumorally unless otherwise noted beginning on day 6. **C,** Mean volume (+SEM) from B on day 13 for each group. *** indicates p<.001 as measured by one-way ANOVA using Bonferroni post-hoc test on all pairs of data. **D,** Survival curves of groups from B and C. * indicates p<.05, *** indicates p<.0001 as measured by Log-rank tests between groups. **E,** HM-1 tumor volume (mm^3) of indicated treatments. All animals dosed 5 times given weekly intratumorally beginning on day 6. **F,** Mean volume (+SEM) from E on day 24 for each group. ** indicates p<.01 as measured by one-way ANOVA using Bonferroni post-hoc test on all pairs of data. **G,** Survival curves of groups from E and F. *** indicates p<.0001 as measured by Log-rank tests between groups.

Showing efficacy in the MC38 model is an excellent indicator of the viability of the described PLE-IL-12-NPs as an effective cytokine delivery vehicle. However, the MC38 cell line is known to be an immune infiltrated or "hot" tumor model. Ovarian tumors have proven much more difficult in their response to immunotherapies.[12-14] As a further measure of IL-12 efficacy and test for viability of cytokine delivery via PLE-NPs, their efficacy in HM-1 tumors (murine ovarian tumors known to be heavily infiltrated with myeloid derived suppressor cells and poorly infiltrated with T-cells) was tested.[82,83] This tumor model also showed improvement in tumor responses both by slowing of tumor growth (Fig 3-3 E, F) and survival (Fig 3-3G) when treated with IL-12, with PLE-IL-12-NPs achieving equivalent efficacy to the more toxic carrier-free therapy. These data together with toxicity reduction suggest that PLE-IL-12-NPs show promise for treatment of multiple tumor types, including those traditionally less responsive to immunotherapy such as ovarian cancer.

In addition to the described single tumor efficacy tests, the ability of PLE-IL-12-NPs to provoke an abscopal immune response was tested in a two flank model (Fig 3-4). Mice were inoculated with MC38 tumor cells subcutaneously on both flanks, with a smaller (5x less inoculant) tumor inoculation on the untreated (left) flank. Tumors on the right flank were treated with PBS, PLE-IL-12-NPs, or free IL-12 at 5 μg weekly doses and both tumors were monitored for response. Treated tumors responded equally well to PLE-IL-12-NPs and free IL-12; however, the abscopal untreated tumor growth was slowed by both PLE-IL-12-NPs and free IL-12 with a slightly better

(statistically insignificant) response to the free IL-12. This is likely due to the greater systemic activity of the carrier-free treatment shown in Fig 3-1. Notably there is still a trend in abscopal response to the PLE-IL-12-NPs compared to controls suggesting a systemic immune response against the tumor. Coupled with reduced toxicity (Fig 3-1) the equivalent efficacy of PLE-IL-12-NPs to carrier-free IL-12 demonstrates an improvement in IL-12 therapy using the described PLE-IL-12-NPs.

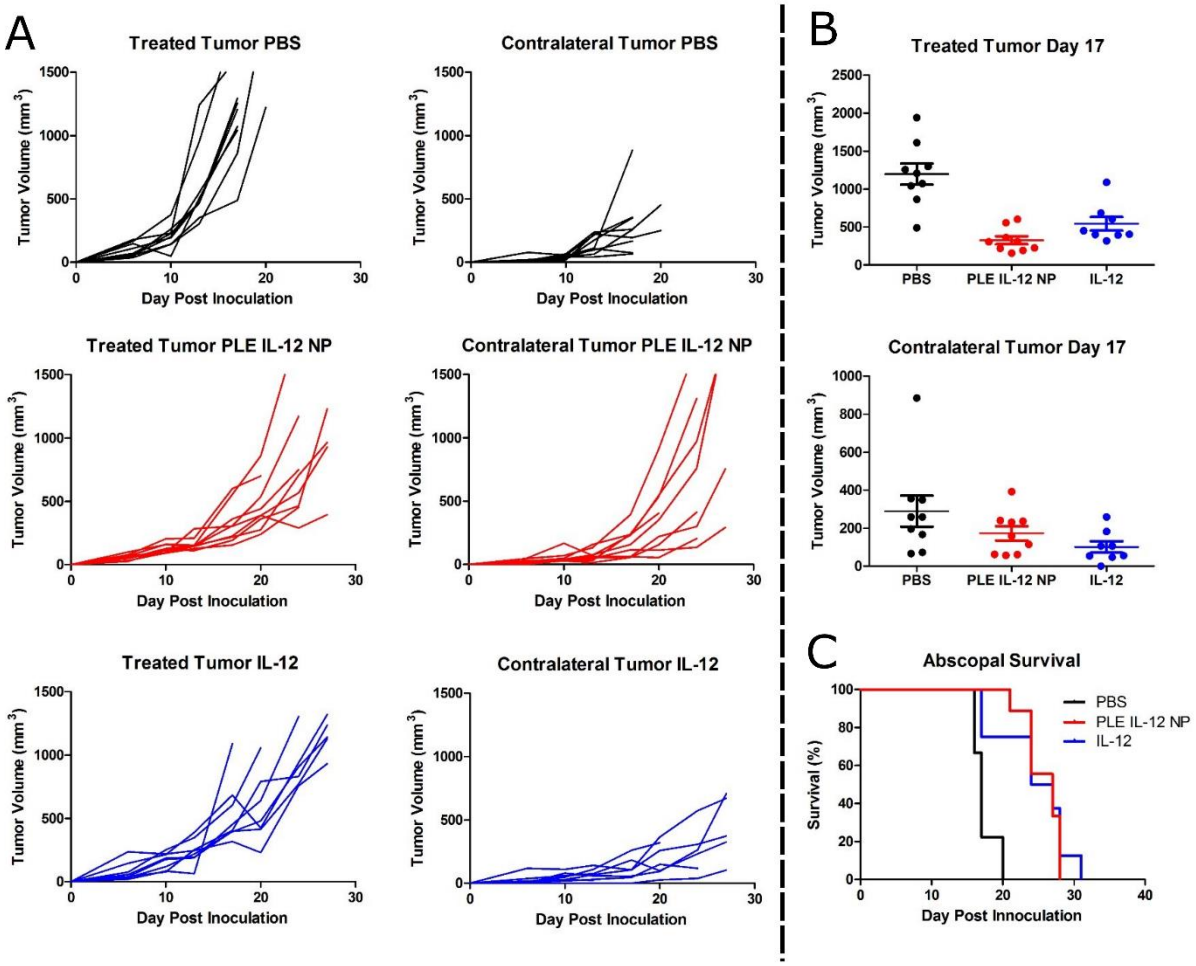

Figure 3-4. Abscopal response to IL-12 therapy. Similar to Figure 3-3, MC38 cells were inoculated in C57Bl/6 mice on both flanks. Mice were treated only on the right flank, and both treated and contralateral tumors were monitored for growth. **A,** Tumor growth in individual mice as measured by caliper measurements with volume calculated at 1/2L*W^2 with L being the longest dimension and W being the shortest dimension. **B,** average tumor sizes from A at day 17. **C,** Survival of cohorts from A.

As a further test of the LbL-NP's ability to improve IL-12 therapy, PLE-IL-12-NPs were tested against carrier-free delivery for both toxicity and efficacy at greatly increased dosing levels to further demonstrate the described widening of the therapeutic window. For these tests, subjects were treated with PLE-IL-12-NP doses increased to 25 μg (5x the normal dose from Fig 3-3) and 50 μg (10x the normal dose) given twice weekly (as opposed to weekly dosing in Fig 3-3) for five doses and compared to 25 μg and 50 μg free IL-12 given twice weekly. Tumor growth and survival was analyzed for efficacy and weight change over the dosing period and serum cytokine levels after the first and last treatments were analyzed for toxicity (Fig 3-5A). Groups treated with free IL-12 lost weight after each dose, with the 50 μg treated mice losing significant weight (~10% body weight) following the first treatment, thus reaching the level of weight loss that exceeds that of the maximum tolerated dose as defined for these studies, evidencing a highly toxic therapy. Conversely, groups treated with PLE-IL-12-NPs continued to gain weight with the controls (Fig 3-5B) at the same dosing levels. In addition, both IL-12 and IFN-γ levels in the serum were higher in the free IL-12 treated mice after the first and last dose, particularly at the higher dosing level of 50 μg. At this dose the free IL-12 treated groups showed significant differences to the PLE-IL-12-NP groups throughout the dosing period, especially in the toxic systemic IFN-γ levels (Fig 3-5C), again demonstrating the systemic toxicity of free cytokine in these subjects. These data suggest that PLE-IL-12-NPs greatly reduce the toxicity of IL-12 treatment even at very high doses. Taking this study further, the group treated with the 25 μg dosing level of the PLE-IL-12-NPs showed equivalent efficacy compared to the group dosed with free IL-12 in terms of both tumor growth arrest and survival (Fig 3-5D, E). Moreover, the group dosed with the 50 μg PLE-IL-12-NPs showed significantly longer survival compared to the group dosed with 25 μg of free IL-12, which was the highest tolerated dose of free cytokine tested, at reduced toxicity. Furthermore, the PLE-IL-12-NP (50 μg) resulted in a cured mouse which rejected a rechallenge with 1 x 10^6 tumor cells 85 days after treatment, indicating a memory response. Combining these data with Fig 3-3, the dose response achieved by IL-12 therapy both in free and PLE NP form is evident (Fig 3-5F). These data show that the rationally engineered PLE-IL-12-NPs make a significant improvement for IL-12 therapy by allowing for increased dosing levels with reduced toxicity over what is achievable with carrier-free cytokine with no loss in efficacy of the IL-12 treatment. The ability to effectively treat epithelial cancers including ovarian cancers at tolerated doses with proinflammatory cytokines such as IL-12 is critical in potentiating the promise of

immunotherapies in these tumors, as these therapies are capable of driving immune infiltration and activity in these difficult to treat tumors.

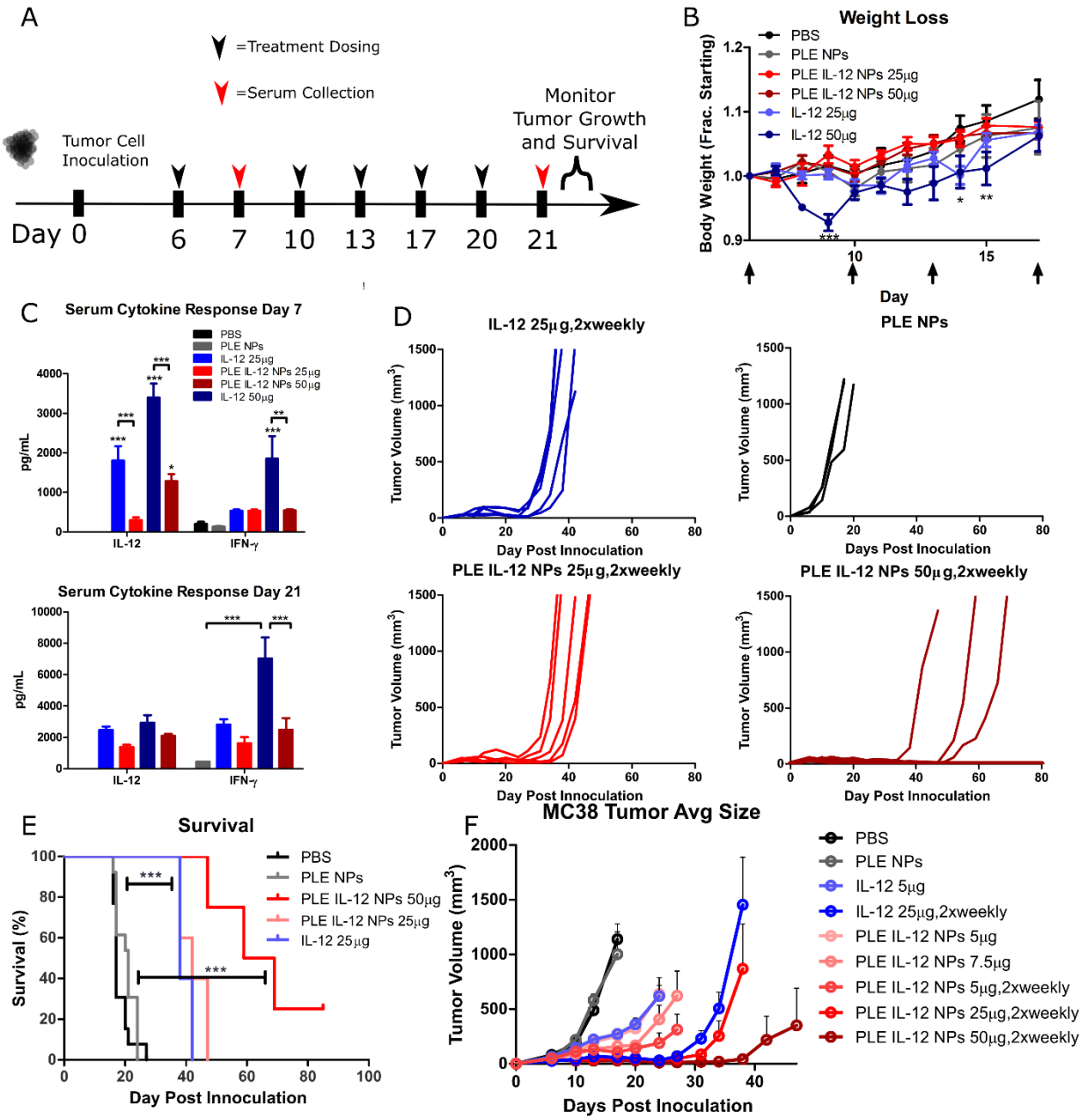

Figure 3-5. Combined toxicity and efficacy at high doses demonstrates PLE IL-12 NPs are a safer, more effective IL-12 therapy. **A,** Schematic of study. C57Bl/6 mice are inoculated with 5E06 MC38 cells on day 0. Mice are treated twice weekly for 5 doses with serum collected 24 hrs after the first and last dose. Animals are monitored throughout for tumor burden and weight change. **B,** Weight change (Mean+SEM) over initial dosing period,* indicates p<.05, ** indicates p<.01, ***

indicates p<.001 compared to PBS as measured by 2-way ANOVA with Bonferroni post-hoc tests comparing all groups to PBS. **C,** Cytokine levels (Mean +SEM) in serum at indicated time points as measured by ELISA. * indicates p<.05, *** indicates p<.001 as measured by 2way ANOVA with Bonferroni post-hoc test comparing all pairs of groups. Comparisons are to PBS where not indicated otherwise. **D,** Tumor volumes of individual animals of indicated treatment groups. **E,** Survival curves of animals from treated and control groups (PBS and PLE NP). ** indicates p<.01, *** indicates p<.001 as measured by Log-rank tests between groups. **F,** Average tumor volumes (mean +SEM) over time for animals from figure 5B low dose experiment (PBS, IL-12 5μg, PLE IL-12 NPs 5μg, PLE IL-12 NPs 7.5μg, PLE IL-12 NPs 5μg 2xweekly) and figure 6D high dose study (IL-12 25μg 2xweekly, PLE IL-12 NPs 25μg 2xweekly, PLE IL-12 NPs 50μg 2xweekly).

PLE-IL-12-NPs enhance lymphocyte activity in tumors and tumor draining lymph nodes

After showing that the described PLE-IL-12-NPs were capable of reducing toxicity with comparable anti-tumor efficacy compared to free cytokine, flowcytometry was used to probe the immunological mechanisms of the treatments in the MC38 model. As described above, vascularized tumors were allowed to establish before starting therapy (6 days). Tumors were then treated intratumorally with biweekly doses of 5 μg IL-12 either in PLE-IL-12-NP form or carrier-free, PLE-NPs with matched lipid dose, or PBS. Tumors, spleens, and tumor draining lymph nodes (TDLNs) were prepared for flowcytometry 24 hours after the third dose which was chosen as an endpoint based on significant differences in tumor sizes occurring between treatment groups at that time as shown in Fig 3-3. Flowcytometry was used to distinguish different cell populations in the isolated tissues (gating strategy Fig B-1, all data Fig B-2).

As expected, both IL-12 therapies caused large shifts in lymphocyte populations indicative of a more active antitumor immune response in the tumor microenvironment. The main impact from IL-12 therapy both in carrier-free and PLE-IL-12-NPs was a shift towards higher CD8+ T cell populations in the tumor (Fig 3-6A). This is evidenced not only by a higher CD8+ fraction of T cells in the tumor, but also by a higher ratio of CD8+/CD4+ T cells in the tumor (Fig 3-6E). Moreover, IL-12 therapy yielded more active CD8+ T cells in the tumor, as measured by degranulation markers (CD69+) (Fig 3-6B,E). Importantly, the PLE-IL-12-NPs showed no difference in CD8+ T cell or degranulated CD8+ T cell populations compared to free IL-12, indicating the same gains in immune activation state in the tumor microenvironment as the free

drug, despite the therapy's encapsulation. These T cell shifts are expected from an IL-12 therapy and indicative of a shift toward a more active, antitumoral Th1 type immune response in the tumor. In addition, the monocyte populations in the tumor undergo a shift from more monocytic (Ly6C+) to more granulocytic (Ly6G+) (Fig B-2) indicating a polarization of monocytes to neutrophils and a more active local immune response.

In addition to these intratumoral T cell shifts, the IL-12 therapies showed a shift towards greater APC migration to TDLNs. Both DC and macrophage populations were increased in TDLNs with both the PLE-IL-12-NPs and free IL-12 (Fig 3-6C,D,F). This migration of APCs to the TDLNs is again indicative of a more active immune response to the tumor. Migration of APCs to the lymph node is an expected step in the immunity cycle in response to an IL-12 therapy driving the cycle forward.[4,5]

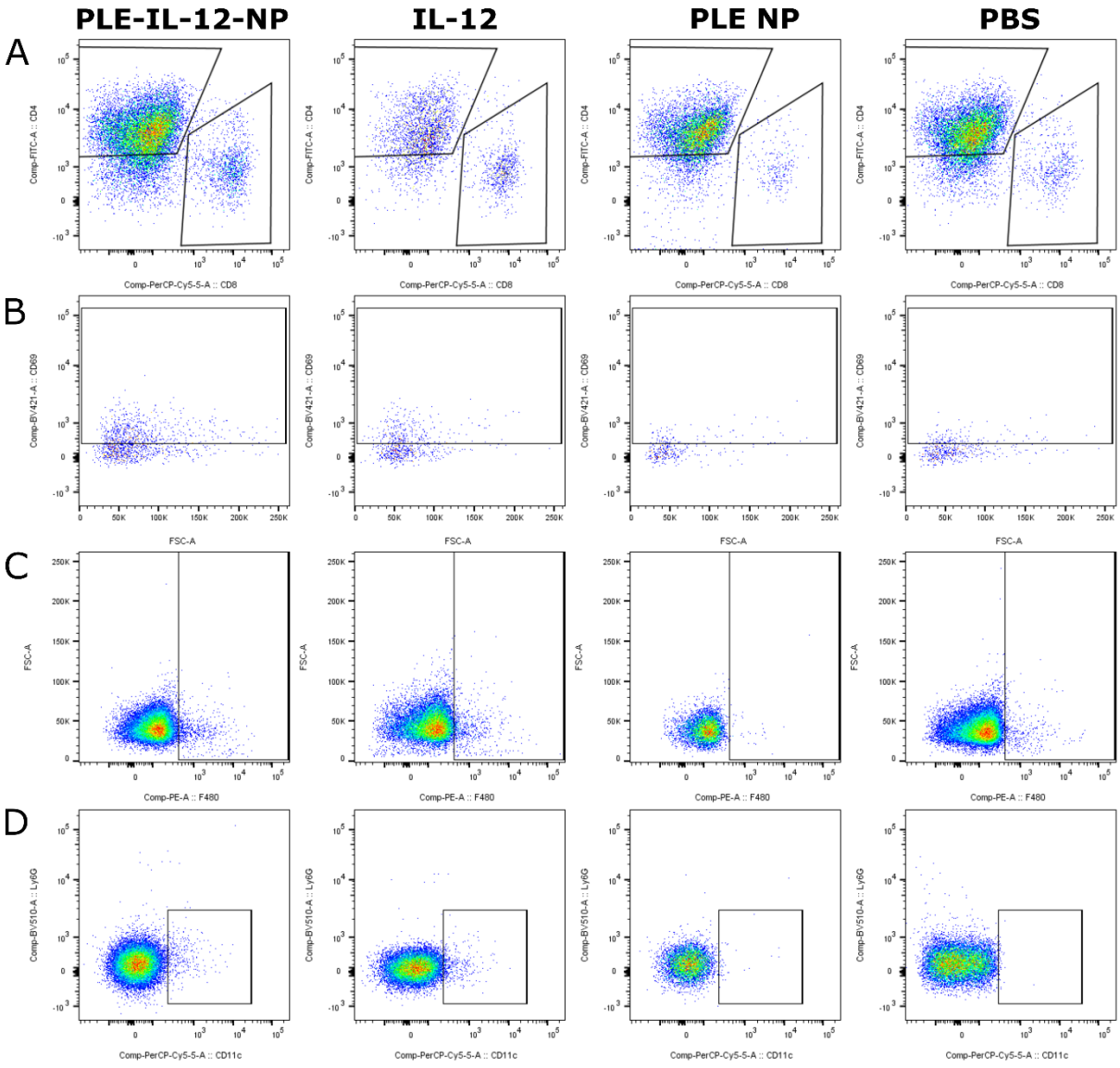
PLE-IL-12-NP
IL-12
PLE NP
PBS
A
B
C
D
Comp-FITC-A :: CD4
Comp-PerCP-Cy5-5-A :: CD8
Comp-BV421-A :: CD69
FSC-A
Comp-PE-A :: F480
Comp-BV510-A :: Ly6G
Comp-PerCP-Cy5-5-A :: CD11c

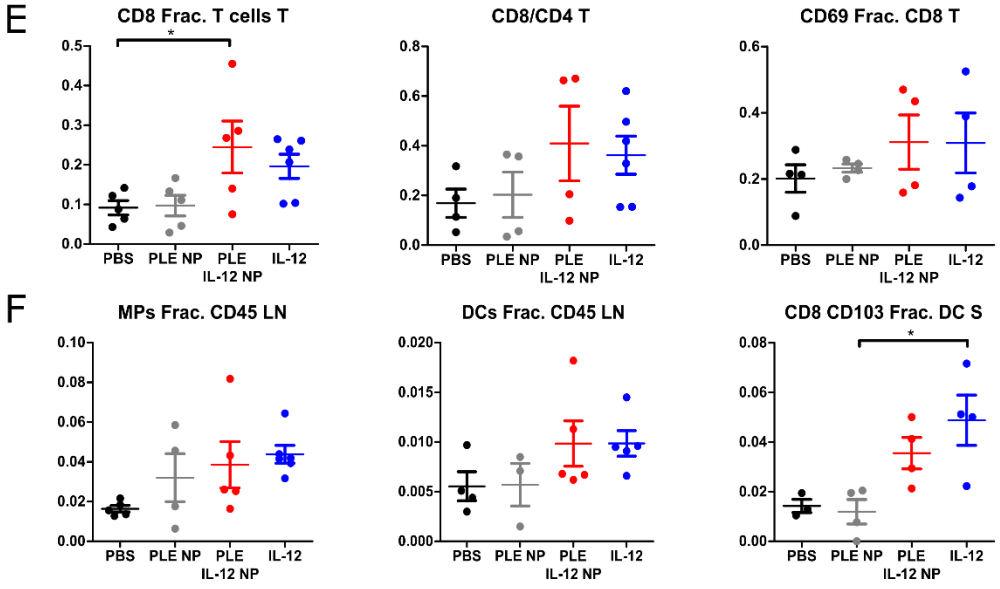
E
CD8 Frac. T cells T
CD8/CD4 T
CD69 Frac. CD8 T
F
MPs Frac. CD45 LN
DCs Frac. CD45 LN
CD8 CD103 Frac. DC S
PBS
PLE NP
PLE
IL-12
IL-12 NP
*

Figure 3-6. Flowcytometry analysis shows IL-12 shifts immune populations towards an antitumoral response. **A.** CD3+ T cell gating for CD4 and CD8 T cells in different treatment groups (CD4 y-axis, CD8 x-axis). **B.** Degranulation of CD8+ T cells as measured by CD69 staining in the tumor. **C.** F4/80 staining of CD45+ cells in TDLNs. **D.** DC content as measured by CD11c+ staining in CD45+ cells in TDLNs. **E.** Quantification of chosen T cell populations from A and B. * indicates $p<.05$ as measured by one way ANOVA with Dunnett posthoc test **F.** Quantification of chosen APC populations flowcytometry. (T=tumor, S=spleen, LN=TDLN)

Little changes were seen in the spleen of treated mice, with the sole differences between IL-12 therapy and the control being an increase in neutrophil populations and a slight decrease in CD45+ leukocyte fractions in the treated groups (Fig B-2). Taken together, these immune population changes upon treatment with IL-12 both within PLE-IL-12-NPs and carrier-free show a shift towards a more active and antitumoral Th1 type immune response in the tumor microenvironment and local lymphoid tissue, as is expected from an IL-12 therapy. These data demonstrate that PLE-IL-12-NPs are able to trigger a potent immune response and drive the cancer immunity cycle forward equivalently to carrier free IL-12 at significantly reduced toxicity.

Additional leukocyte population shifts indicate a shift towards a less suppressive immune microenvironment with IL-12 therapy. The PLE-IL-12-NP treatment showed a reduced number of regulatory T cells (Tregs) in the tumor coupled with a higher ratio of CD8/Treg cells in the TDLN. In addition, PLE-IL-12-NPs showed a trend towards reduced expression of PD-L1 (CD274) on CD45+ cells as compared to free IL-12. This difference is mainly from macrophage expression differences in PD-L1, as there is little difference in the DC population PD-L1 expression (Fig B-2). Together, these data indicate that PLE-IL-12-NPs are capable of reducing the immune suppressive tumor microenvironment, particularly in the macrophage population, potentially beyond what is achievable with free cytokine, which could prove to be a potentially helpful enhancement in treatment.

3.4 Conclusions

This chapter focuses on furthering the characterization and analysis of PLE-IL-12-NPs by testing their toxicity and efficacy *in vivo.* We demonstrate significantly reduced toxicity from PLE-IL-12-NPs as compared to carrier-free cytokine in multiple studies. Importantly, we demonstrate that this reduction in toxicity comes at no cost to efficacy against multiple tumor challenges,

standing as an improvement in IL-12 therapy. Most notably we demonstrate in the same study that PLE-IL-12-NPs show no discernable toxicity at a dose where carrier-free IL-12 is not tolerated in the subjects. Moreover, at this dose the PLE-IL-12-NPs show significantly higher efficacy than the highest tolerated dose of carrier-free cytokine. This increase in accessible dosing levels at no cost to efficacy stands as a significant improvement for cytokine delivery.

Most importantly for IL-12 therapy, we have demonstrated in multiple studies the ability of the described PLE-IL-12-NPs to reduce the systemic toxicity of IL-12 at multiple schedules and doses. Indeed, we have demonstrated that the PLE-IL-12-NPs offer a safer therapy, even at higher doses than the free cytokine (Fig 3-1,3-5), which in turn yields a more effective therapy due to the ability to access higher dosing levels as compared to carrier free cytokine with the two delivery strategies showing equivalent efficacy at equivalent dosing. This is of utmost importance for any IL-12 therapy as toxicity has been the largest factor in preventing IL-12 from progressing in the clinic as evidenced by the severe toxicity, including two deaths in previous trials.[23-25] Other approaches to IL-12 therapy were hypothesized and tested with limited success, including IL-12 gene therapy, microparticles and co-formulations limited to local delivery, and simple passive targeting NPs. These approaches still allow systemic exposure and fail to adequately control delivery of this complex therapy which can lead to toxicity and/or insufficient dosing at the tumor site to elicit an effective antitumor response. The described PLE-IL-12-NPs address these issues by reducing toxicity while maintaining antitumoral efficacy of IL-12 therapy, as described above, likely through targeting to the cell surfaces in the tumor microenvironment. This targeting phenomenon is likely to show even greater importance as these therapies progress to systemic administration, where the dosing is not *prima facie* confined to the tumor.

One limitation of the current study is that it relies on an intratumoral approach in *in vivo* studies to deliver the therapeutic. However, overcoming IL-12 based toxicity even from a local injection has remained a challenge clinically and preclinically with several investigations taking a local delivery approach still failing to reduce systemic toxicity when the IL-12 is given at therapeutically relevant dose. Indeed, even in the current study, locally delivered free IL-12 showed significant toxicity at relevant doses. Therefore, even though the reduction in toxicity shown in the current study is thus far only demonstrated for intratumoral administration, this result still stands as a relevant advance for IL-12 delivery. Nonetheless, future chapters and future work will explore the

application of this delivery system for systemic administration, focusing on ovarian tumor models to bring the promise of immunotherapy to this difficult to treat malignancy. Indeed these studies combined with the *in vitro* work in chapter 2 shows promise for a successful systemic cytokine delivery platform. Firstly, the described PLE-IL-12-NPs showed selective association with tumor cells both in this work (Fig 2-3) and previous studies,[41] which is critical for concentrating NPs and payload in the tumor microenvironment. In addition, kinetic immune response studies showed the majority of the IL-12 remains attached to the particle or in the tumors for greater than 4 hours (Fig 3-2), which is longer than similar actively targeted NPs take to concentrate in the tumor microenvironment upon systemic delivery. This delayed IL-12 release is critical for potential success in systemic delivery as it prevents off-tissue exposure of potent cytokine payloads. Equally important, the IL-12 payload is rapidly released thereafter while the NPs remain localized to the cell surfaces, maintaining the cytokine payload activity once in the tumor microenvironment, and causing a potent and long lasting immune response. Taken together, the *in vitro* characterizations of IL-12 loading (Fig 2-1), subcellular localization (Fig 2-2), tumor cell association selectivity (Fig 2-3), *in vivo* biological activity (Fig 3-3, 3-4, 3-5), and immune response of IL-12 (Fig 3-2, 3-6) demonstrate a NP platform that meets all the criteria for a successful systemically deliverable cytokine therapy.

Another significant finding of this study is the efficacy of the PLE-IL-12-NPs in an ovarian tumor model, reinforcing the activity found in the previous chapter *in vitro*. Ovarian cancer generally has not benefitted from the clinically available checkpoint inhibitors, and the exploration of inflammatory molecules such as IL-12 and some other cytokines as a supplement to checkpoint inhibiters has been limited by toxicity concerns. Ovarian cancer usually does not present with a single injectable tumor but instead with many metastatic nodules spread throughout the abdomen, making intratumoral treatment an impractical option clinically. The delivery system described in the current study could open the door to systemic or intraperitoneal application of toxic cytokines in these difficult tumors; as polymer layers not only reduce the toxicity of the cytokine as described herein, but also may provide a significant targeting effect to ovarian tumors *in vivo* that can effectively concentrate the delivery of cytokines to the tumor nodules.[76] Indeed, systemic immunotherapy via cytokine delivery offers a unique promise for widely disseminated metastatic disease such as ovarian cancer as developing a local immune response in some tumors can lead to systemic immunity against the cancer at other metastatic sites. Our PLE-IL-12-NPs demonstrate

this systemic effect in their efficacy against abscopal tumors. Expanding the applications of the described PLE-IL-12-NPs to systemic delivery poses the promise of bringing immunotherapy advancements to the ovarian treatment space.

Finally, while these PLE-IL-12-NPs make use of the potent cytokine IL-12, no IL-12 specific techniques are used for their generation, making them adaptable to many other cytokines or proteins of interest for delivery. Moving forward, these particles can be utilized to deliver any protein with an appropriate binding ligand, or indeed a combination of such molecules. The general design is also easily adaptable to many other conjugation strategies for linking the cytokines to liposomes that can be used to modulate the release rate of delivered proteins. Accordingly, another advantage of the described LbL NP system is easy adaptability to combination therapy. Additional therapeutics can be added to the particle in multiple ways, including adding additional cytokines on the liposome surface, adding small molecules to the liposome core as described previously,[60,66] or including therapeutics such as siRNA within the layers. These particles can also be used to incorporate checkpoint inhibitors such as anti PD-1 or anti CTLA4 in a similar manner to cytokines on the liposome surface or attached to the layers. These combinations could prove to be most effective, because for many malignancies, a combination of immunotherapies is viewed as the most promising path forward. As this approach progresses, the need to deliver combinations of immunotherapeutics in precise ratios and schedules[84] will also need to be controlled - another potential benefit of using the described LbL-NPs, which can be designed to stage release of combination therapies.[62]

Chapter 4. Systemic delivery of IL-12 using PLE-IL-12-NPs

4.1 Introduction

Immunotherapy has become an increasingly attractive treatment option for cancer therapy since the approval of the checkpoint inhibitor ipilumimab in 2011[85]. Checkpoint inhibitors and other immunotherapies offer the promise of prolonged cures in many diseases, including some malignancies with previously very poor prognoses[2,85]. However, current immunotherapies still have many limitations, including only a minor response rate in many tumors. It is becoming clear that immunosuppressive or immune excluded "cold" tumor microenvironments (TME) play a key role in nonresponsive tumors[4,5]. Ovarian cancer is one such malignancy that often presents as a "cold" tumor[12-14] and has been particularly unresponsive to checkpoint inhibition[69]. One method to bring immunotherapy to such immune excluded environments is to use complementary therapeutics to drive lymphocyte infiltration and activation into tumors while preventing immune system arrest using checkpoint inhibition[4].

One class of therapeutics with the potential to drive immune infiltration into "cold" tumors are proinflammatory cytokines such as interleukin-12 (IL-12), which has shown a potent ability to drive lymphocyte infiltration[17-19] and cure preclinical tumors in the past[21]. However, proinflammatory cytokines tend to be highly toxic when given systemically. Indeed, IL-12 showed very high, schedule dependent toxicity in clinical trials, including two deaths[23-25], motivating the need for any future IL-12 therapies to have pronounced spatio-temporal control over delivery to keep active concentrations in the TME while limiting its systemic exposure. Many newer delivery methods have been attempted to improve IL-12 therapy such as gene delivery into the tumor[29,30], microparticle delivery[48-50,70] and chitosan-hydrogel co-formulations[32-34] but are limited by a need for local injection. This limits the usability of such treatments in widely disseminated diseases that do not have easily injectable tumors, such as ovarian cancer which often presents as disseminated metastatic tumor burden throughout the peritoneal cavity. Thus there is a need for a properly spatio-temporally controlled IL-12 delivery vehicle that can be systemically administered.

One promising route for controlled IL-12 delivery from a systemically deliverable carrier is the use of an engineered nanoparticle (NP) as demonstrated in previous chapters. Systemically administered strategies using simple NP formulations[52,53] have also been tried, but have failed to spatio-temporally control delivery and significantly reduce toxicity. However, careful engineering

of NP structure and surface chemistry has the potential to eliminate those issues by considering the design criteria for optimal cytokine delivery. For IL-12 those criteria include 1) high loading and release of active IL-12, 2) maintenance of NPs on the surface of tumor cells to allow availability to membrane-bound IL-12 receptors on nearby lymphocytes, 3) high association with tumor cells, and 4) decreased systemic exposure and toxicity.

Previous chapters developed a NP delivery vehicle engineered to meet these design criteria using the LbL technique to adjust the material properties of the particle[58,60,61,65,66,76]. We showed that a liposomal NP with IL-12 bound to the liposomal surface and subsequently covered with a bilayer of PLR and PLE, termed PLE-IL-12-NP, demonstrated >90% loading efficiency of IL-12, extended (>24 hr) localization on the surface of tumor cells, high selectivity for binding to tumor cells over other cell types, and significant antitumor efficacy when administered intratumorally in multiple subcutaneous tumor models at reduced toxicity compared to carrier-free IL-12.

We hypothesized that PLE-IL-12-NPs can also enable the systemic delivery of IL-12 to orthotopic ovarian tumors (Fig 4-1) which require systemic delivery due to presentation as widely disseminated metastasis throughout the peritoneal cavity. Because previous studies with other PLE-layered particles showed targeting of ovarian tumors upon systemic administration[76], it is hypothesized that PLE-IL-12-NPs will also concentrate IL-12 in these tumors. The polymer layers could act as a "shield" to minimize off-target IL-12 exposure while anchoring the NPs to the surface of tumor cells and releasing active IL-12 into the tumor microenvironment. In the current study we use orthotopic HM-1 model of ovarian cancer to show that PLE-IL-12-NPs given intraperitoneally and intravenously concentrate IL-12 within disseminated tumors, increase the therapeutic window of IL-12, produce long-term antitumor immune responses, and induce a distinct immunological profile post administration conducive to combination therapy with checkpoint inhibitors.

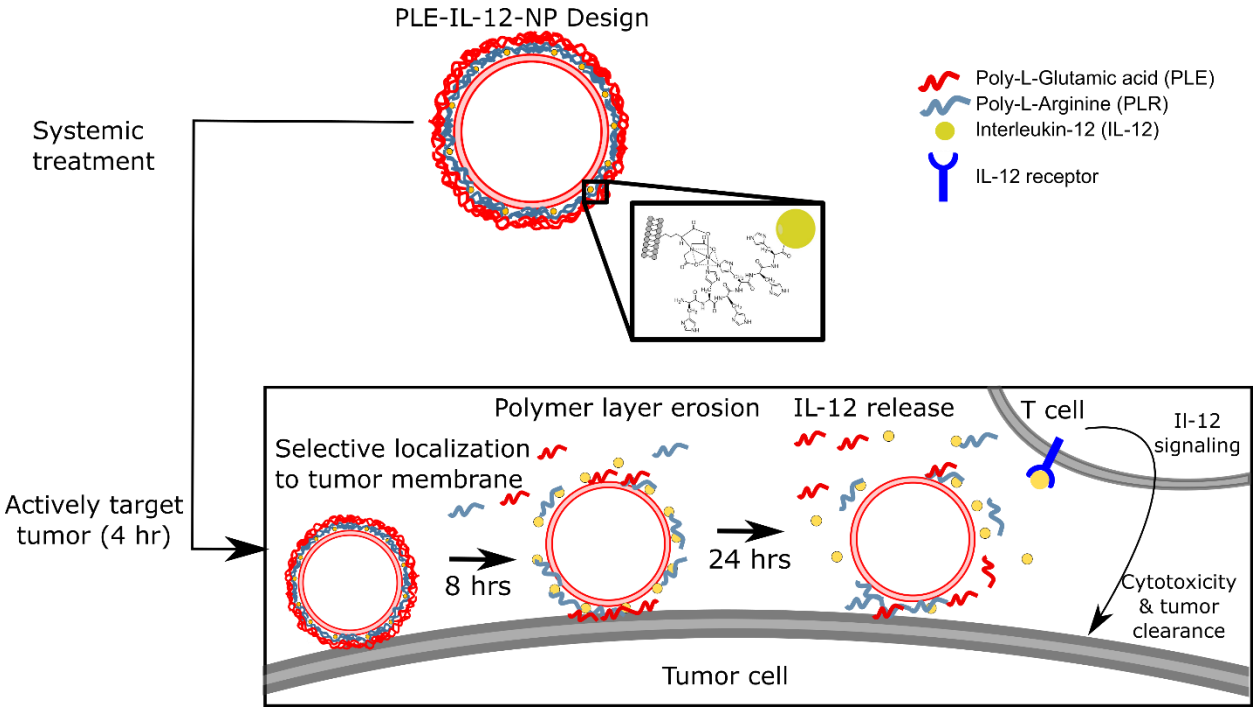

Figure 4-1. PLE-IL-12-NPs are able to selectively bind to tumor cells and remain localized to cell surfaces, releasing their IL-12 cargo to activate T cells over a 24 hour period. These characteristics make PLE-IL-12-NPs a strong candidate for safe and efficacious systemic delivery of IL-12.

4.2 Materials and Methods

Materials

1,2-dioleoyl-sn-glycero-3-[(N-(5-amino-1-carboxypentyl)iminodiacetic acid)succinyl] (nickel salt) (DGS-NTA (Ni)), 1,2-distearoyl-sn-glycero-3-phosphocholine (DSPC), Cholesterol, and 1-palmitoyl-2-oleoyl-sn-glycero-3-phospho-(1'-rac-glycerol) (sodium salt) (POPG) 1,2-dioleoyl-sn-glycero-3-phosphoethanolamine (DOPE) were purchased from Avanti Polar Lipids and used without modification. PLR and PLE were purchased from Alamanda Polymers and used without modification. Single chain IL-12 was produced in house from HEK-293 cells.

Particle Formulation and Characterization

NP formulations were manufactured similar to previous studies[76,86]. Briefly, single chain IL-12[72] was produced via vector cloning and expression in Expi293 cells (ThermoFisher Scintific). Liposome cores were made via lipid film drying (rotovap) followed by rehydration and pressure driven extrusion to 50 nm particle size (Avestin Liposofast-50). Liposomes were comprised of 5%

DGS-NTA (Ni), 65% DSPC, 23.9% Cholesterol, and 6.1% POPG by mole for therapeutic NPs. Fluorescent NP were made by lowering DSPC to 60% and adding 5% DOPE for addition of fluorophore. NHS ester fluorophores were added to free amines on DOPE for fluorescently labeled liposomes via overnight reaction at room temperature at pH 8.5 with 5 molar excess dye. Excess dye was removed via tangential flow filtration (TFF). Lipid films were made by drying the indicated lipid mixtures in chloroform by rotovap at 20 mbar for 30 minutes followed by overnight desiccation under vacuum. 50 nm liposomes were made by first rehydrating films with PBS under sonication at 65C followed by pressure driven extrusion to desired size (50 nm) at 65C. IL-12 was added to extruded particles by overnight incubation under agitation at 4C. Unreacted IL-12 was removed and buffer was exchanged to water via tangential flow filtration through a 100 kDa membrane (Repligen). Unlayered control particle synthesis ended here. PLE-IL-12-NPs were layered with PLR by mixing with a 0.1 wt eq solution of PLR under sonication, removing unlayered PLR by TFF. PLE was added in at similar manner at 1 wt eq. Throughout NP manufacture sizes, PDIs and zeta potentials were measured via dynamic light scattering (Malvern ZS90). NPs were tested for activity *in vitro* via their ability to stimulate production of IFN-γ from splenocytes prior to *in vivo* use. NPs were formulated for systemic injection by mixing 9:1 NP solution:50% Dextrose to make injections isotonic with blood.

Flowcytometry

Antibodies used for immunostaining were against CD69 (biolegend 104545), CD25 (biolegend 102041), NK-1.1 (biolegend 108753), CD3 (biolegend 100232), CD4 (biolegend 100423), CD8a (BD biosciences 566410), FoxP3 (biolegend 126404), CD45 (biolegend 103112), Ly-6C (biolegend 128032), Ly-6G (biolegend 127633), CD274 (biolegend 124331), F4/80 (biolegend 123110), CD11c (BD biosciences 566504), CD11b (biolegend 101217), CD86 (biolegend 105037) CD103 (biolegend 562722). FoxP3 intracellular staining was carried out using FoxP3 intracellular staining kit (Thermo 00-5523-00) following manufacture protocol. Immunostained cells were run on an LSR Fortessa HTS with FACSDIVA software and analyzed using FlowJo V10.5.3.

Cell Culture

HM-1 cells were acquired through Riken BRC. Cells were cultured in α-MEM, supplemented with 10% FBS and penicillin/streptomycin or as recommended by the supplier in a 5% CO_2

humidified atmosphere at 37C. All cell lines were murine pathogen tested and confirmed mycoplasma negative by Lonza MycoAlert™ Mycoplasma Detection Kit.

Animal Studies.

All animal experiments were approved by the Massachusetts Institute of Technology Committee on Animal Care (CAC) and were conducted under the oversight of the Division of Comparative Medicine (DCM).

Biodistribution

1E06 HM-1 mcherry luc2 tumor cells were inoculated in B6C3F1 mice via intraperitoneal injection. Tumors were allowed to establish for 2 weeks. PLE-IL-12-NPs and Unlayered IL-12 NPs were made following the procedure above with Sulfo-Cy7 NHS ester dye (Lumiprobe), and confirmed to have equivalent fluorescent properties via plate reader (Tecan). NPs were injected either intravenously via the retro-orbital route or intraperitoneally at 5 ug doses of IL-12. Mice were euthanized 4 and 24 hours after dosing and liver, kidneys, spleen, and tumors were removed and immediately placed in PBS on ice. Organs were imaged via *In Vivo* Imaging System (IVIS, Perkin Elmer) immediately after removal for NP signal (excitation: , emission:). Organs were frozen immediately following imaging. Data was analyzed using Living Image software. Background fluorescence measurements were made for each organ based on signal from Dextrose only treated mice. Regions of interest (ROIs) were made around treated organs using the contour ROI setting in Living Image. Total radiant efficiencies (TRE) were measured for each treated organ and corrected by the average radiant efficiency from the matching organ in dextrose treated controls. Percent recovered fluorescence for each organ was then calculated as $\frac{TRE(organ)}{\sum_{mouse} TRE}$. These % recovered fluorescence values were then normalized by organ weight. Similar to previously reported studies[76].

Cytokine levels in organs

Following biodistribution studies, organs were further processed to extract all protein from individual organs using Miltenyi Biotech gentleMACS Octo Dissociator following recommended protocol for protein extraction. Briefly, organs were placed in M tubes with enough buffer to make a 50 g tissue/mL buffer solution. Buffer used for tissue homogenization was RIPA lysis buffer

with HALT protease inhibitor cocktail (XXX) and 1% active silicon from Y-30 emulsion (Sigma) for anti-foaming purposes. Organs were then homogenized using gentleMACS Octo Dissociator. Samples were spun at 4000 rcf to remove tissue debris and supernatants were analyzed by ELISA for cytokine content.

In vivo toxicity tests

To test toxicity, B6C3F1 mice (Jackson Labs 100010) were injected either intravenously via the retro-orbital route or intraperitoneally with varying doses as indicated of PLE-IL-12-NPs, dose matched soluble IL-12, dose matched unlayered NPs or PBS for 5 daily doses and monitored daily for weight change. Serum was collected 3 hours after the last dose and assayed for IL-12 and IFN-γ levels via ELISA (peprotech).

In vivo efficacy tests

1E06 HM-1 mcherry luc2 tumor cells were inoculated in B6C3F1 mice via intraperitoneal injection. Tumors were allowed to establish for 1 week. Subjects were treated with 5 ug intravenously via the retro-orbital route or 5 or 10 ug intraperitoneally of IL-12 in PLE-IL-12-NPs, Unlayered NPs, or carrier-free and compared to PBS controls for 5 daily doses. Mice were weighed daily to track toxicity. Serum was collected after the last dose to test for systemic cytokine levels. Mice were tracked for tumor burden twice weekly via IVIS. Mice were sacrificed based on ascites accumulation and/or overall body condition.

Immune Profiling

Immune profiling studies were carried out similar to *in vivo* efficacy tests. Mice were inoculated with 5E05 (MC38) cells in 1:1 PBS:Matrigel (Corning) mixture. Tumors were allowed to establish for 6 days prior to treatment. Mice were treated intratumorally with 5 ug IL-12 from scIL-12 LbL-NPs, lipid dose matched LbL-NPs without IL-12, dose matched soluble scIL-12, or PBS 2x weekly for 3 doses. 24 hours after the third dose mice were sacrificed and tumors, tumor draining lymphnodes (TDLNs), and spleens were harvested and processed to sinfle cell suspension. Tumors were digested to single cell suspension using mouse tumor dissociation kit (Miltenyi, 130-096-730) and gentleMACS octo-dissociator following recommendations of supplier. Briefly, tumors were diced into 1-2mm sections and added to C tubes (Miltenyi) and processed on tissue dissociator using protocol m_imptumor_02. Tubes were then incubated at 37C in nutating

incubator for 40 minutes and processed on dissociator using m_imptumor_03 twice. Tumors were then pushed through 70 μm strainers to form single cell suspensions. Cells were treated with ACK lysis buffer to remove red blood cells. Spleens and TDLNs were processed similar to splenocyte isolation in chapter 2. Briefly, spleens and TDLNs were forced through 70 μm strainers to form single cell suspensions. Cells were treated with ACK lysis buffer to remove red blood cells. Single cell suspensions were then treated for flow cytometry studies.

Statistical Analysis

GraphPad PRISM 5 was used to perform statistical analyses. Multiple comparisons were performed using multiple t tests, one-way ANOVA, or two-way ANOVA followed by post-hoc tests as indicated in figures.

Data Availability

The data for this study are available within the thesis. Raw data are available upon reasonable request from the corresponding author.

4.3 Results and Discussion

PLE-IL-12-NPs are concentrated in tumors upon systemic administration

As a first test of systemic availability and delivery of IL-12 from PLE-IL-12-NPs the biodistribution of the NPs was tested in HM-1 tumor bearing mice. For these studies a Sulfo-Cy7 fluorophore was added to the NP core via NHS ester linkage to an amine carrying lipid head group (1,2-dioleoyl-sn-glycero-3-phosphoethanolamine [DOPE]). Subjects were treated 14 days after tumor inoculation via intravenous (IV) or intraperitoneal (IP) route (Fig 4-2A). Subjects were euthanized 4 or 24 hours after treatment and organs were collected and imaged for NP fluorescence via *in vivo* imaging system (IVIS) (Fig 4-2B, Fig S1). These data demonstrate that the LbL coating plays a critical role in concentrating NPs in the tumors, with accumulation of PLE-IL-12-NPs in tumors exceeding the accumulation achieved with unlayered NPs (UL-NPs) in both the IV and IP delivery routes at both 4 and 24 hour time points. These results are most evidenced in the case of IP delivery in which the PLE-IL-12 NPs showed tumor accumulation 30% and 54% greater than UL-NPs at 4 and 24 hours respectively. Intriguingly, the concentration of PLE-IL-12 NPs in the tumor even exceeded that found in the liver (Fig 4-2B), kidney and spleen (Fig C-2) by 7-fold, 17-

fold, and 4-fold respectively. Indeed, PLE-IL-12-NPs showed less accumulation in the liver, particularly by the 24 hour time point (Fig 4-2C), in both delivery routes in comparison to UL-NPs suggesting a reduced amount of off-target activity from PLE-IL-12-NPs as compared to UL-NPs.

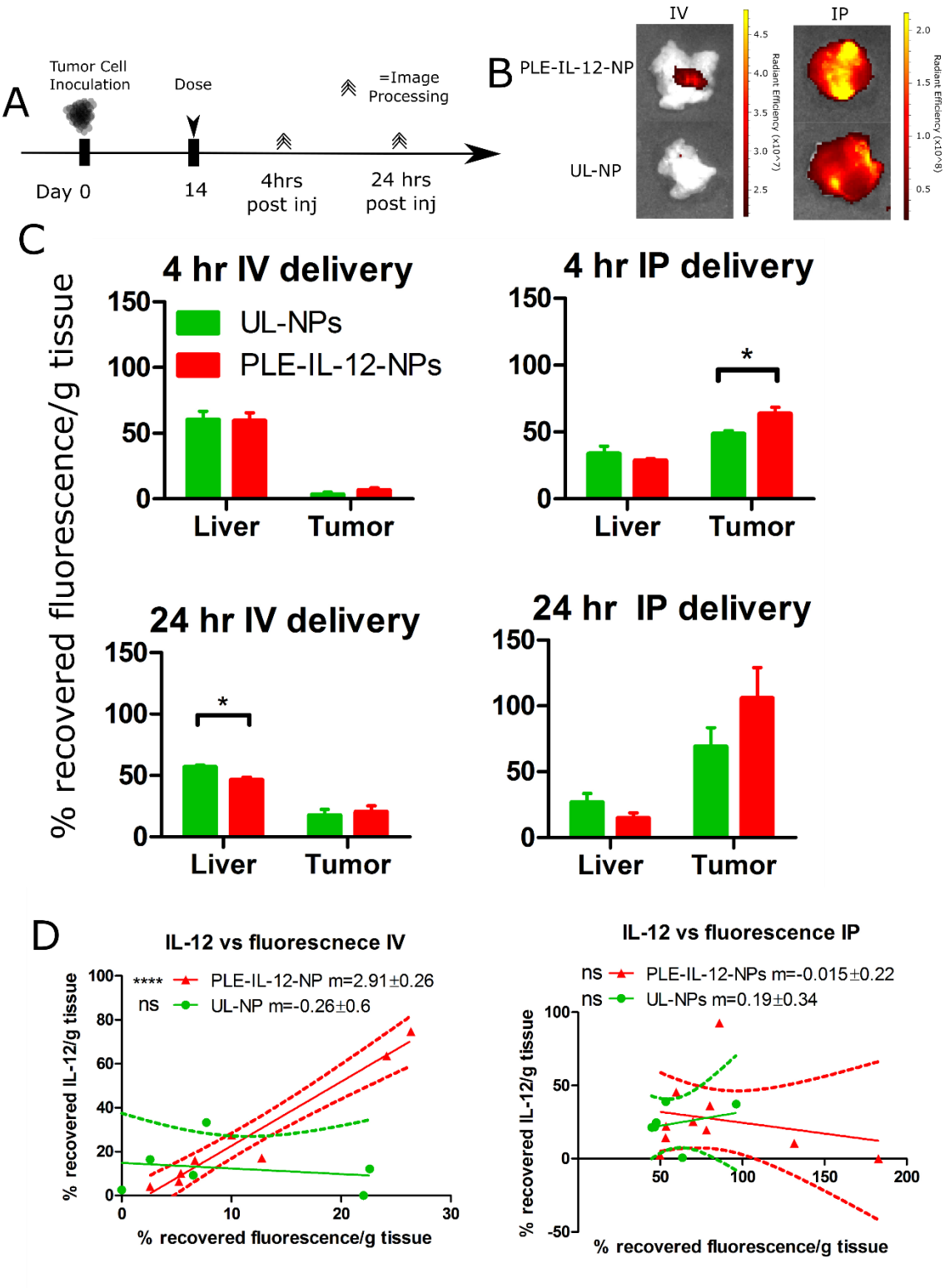

Figure 4-2. Biodistribution of NPs upon systemic delivery. **A**, Schematic of biodistribution study design. **B**, Representative fluorescence results as measured by IVIS in tumors following 4 hour injection of PLE-IL-12-NPs and UL-NPs by both IV and IP delivery route. **C)** Mean percent

recovered fluorescence normalized by tissue weight (UL-NPs, PLE-IL-12-NP 24 hr IV n=3; 4 hr and 24 hr IP PLE-IL-12-NPs n=5, error bars denote SEM). IVIS measurements from B were normalized by dextrose control treated subjects and percent recovered fluorescence was calculated with respect to all measured organs (liver, kidney, spleen, and tumor). * indicates $p<.05$ as calculated by one-tailed t-test. **D,** Correlation of % recovered IL-12/g tissue to % recovered fluorescence/g tissue for both IV (left) and IP (right) delivery. Linear regression performed using Graphpad PRISM showing 95% confidence ranges and slopes. **** indicates $p<0.0001$ for slope differing from zero.

Having demonstrated that PLE-IL-12-NPs are effectively concentrated in tumors by both IV and IP administration the delivery of the IL-12 payload was analyzed in both these cases. Based on previous data, the majority of IL-12 is released from PLE-IL-12-NPs between 4 and 24 hours as demonstrated in the kinetic immune response from chapter 3, which overlaps well with the concentration of NPs in tumors in Fig 4-2B,C. To test the biodistribution of IL-12 payload from both PLE-IL-12-NPs and UL-NPs organs from Fig 4-2B were homogenized and assayed for IL-12 content by ELISA (Fig C-3). These data demonstrate that IL-12 payload delivery tracks well with NP location for both layered and unlayered particles. There is a trend of greater amounts of IL-12 in the tumors and less off target exposure in the liver from PLE-IL-12-NPs as compared to UL-NPs by the 24 hour time point. Note that this recovered IL-12 includes both the delivered IL-12 and endogenously produced IL-12 in response to therapy and thus compounds itself as IL-12 signaling drives further IL-12 production. Taking this further, the correlation between IL-12 recovery and fluorescence recovery in tumors was calculated (Fig 4-2D). In the IP delivery case both PLE-IL-12-NPs and UL-NPs showed little correlation between IL-12 delivery and NP delivery, likely due to the peritumoral location of injection, allowing for dissociated IL-12 to traffic to tumors. However, in the IV case PLE-IL-12-NPs showed a strong correlation for IL-12 delivery with NP delivery while UL-NPs showed no correlation. This indicates that PLE-IL-12-NPs are able to selectively deliver IL-12 to tumors, while UL-NPs likely lose the attached IL-12 in circulation which can then traffic to tumors as carrier-free IL-12. This is a strong indicator that PLE-IL-12-NPs are able to reduce systemic exposure to IL-12 upon systemic delivery. In addition, as a measure of IL-12 activity IFN-γ levels were measured in a similar manner (Fig C-3B). IFN-γ levels followed similar trends to NP distribution as well, demonstrating activity of the NPs upon

systemic delivery. These data demonstrate that the PLE-IL-12-NPs are more capable than UL-NPs at concentrating IL-12 delivery and activity to tumors while limiting its exposure in other organs.

PLE-IL-12-NPs reduce toxicity of IL-12 upon systemic administration

Because the biodistribution of PLE-IL-12-NPs demonstrated concentration of both NP and payload in tumors we hypothesized that they may also limit the IL-12 related toxicities that have been the main limiting factor for IL-12 in the clinic[23-25]. To this end, toxicity studies in healthy mice were performed (Fig 4-3A). Subjects were dosed with 5 μg IL-12 in PLE-IL-12-NPs, UL-NPs, or carrier-free or equivalent volume of 5% dextrose solution either IV or IP and monitored for weight change (Fig 4-3B) as a measure of toxic response to therapy. IL-12 delivery from both UL-NPs and carrier-free IL-12 showed significant toxicity from both IV and IP delivery, with subjects losing ~10% body weight during and immediately after dosing, while delivery from PLE-IL-12-NPs showed no significant weight loss compared to dextrose controls. This demonstrates a significantly safer toxicity profile from PLE-IL-12-NPs not only from carrier-free IL-12 but also from UL-NPs, demonstrating the critical role that layering plays in not only targeting therapy to tumors (Fig 4-2) but also preventing systemic activity of IL-12, thus reducing off target toxicity of this therapy.

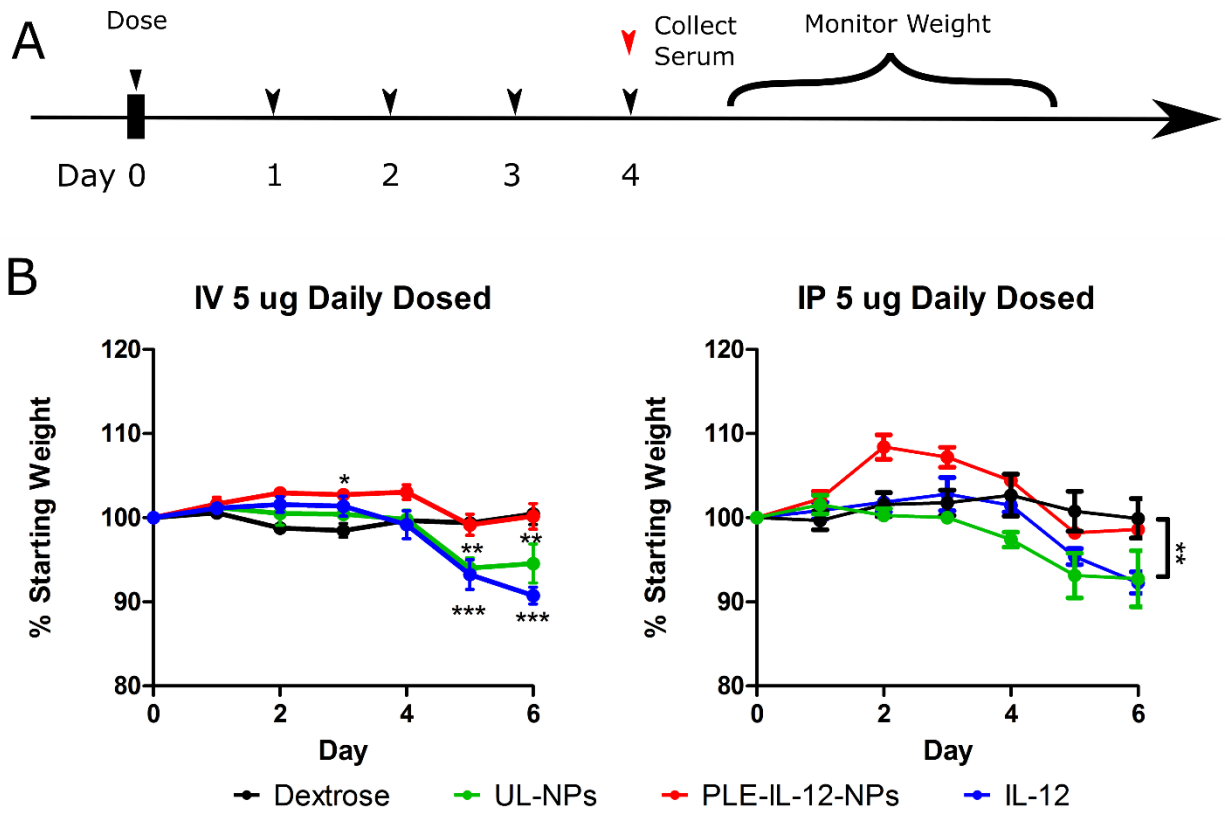

Figure 4-3. IL-12 toxicity in healthy mice. **A**, Schematic of dosing scheme in healthy animals. Mice were dosed with 5 µg IL-12 in PLE-IL-12-NPs, UL-NPs, or carrier free and compared to 5% dextrose control. **B**, Toxicity of various IL-12 delivery methods administered IV (left) or IP (right) as measured by weight loss during and after dosing. ** indicates $p<0.01$, *** indicates $p<0.001$as measured by 2-way ANOVA with Bonferroni post-hoc test across all groups.

PLE-IL-12-NPs enhance high-dose IL-12 efficacy upon systemic administration

Having demonstrated a significant reduction in toxicity of IL-12 therapy from PLE-IL-12-NPs, the activity of IL-12 therapy against a tumor challenge was probed. Mice were inoculated with orthotopic HM-1 tumors that were allowed to form for 7 days prior to 5 daily treatments with 5 µg of IL-12 given carrier free, from PLE-IL-12-NPs, or from UL-NPs (Fig 4-4A) and compared to dextrose controls. Subjects were monitored for toxicity during and immediately after dosing by weight changes (Fig C-4). These data demonstrate that the PLE-IL-12-NP treated animals were healthier than the carrier-free IL-12, though due to the confounding variable of the presence of tumors and ascites toxicity results were more muted than previous studies (Fig 4-3). However, following subjects for tumor burden as measured by fluorescence signal on IVIS (Fig C-5) and

survival (Fig 4-4B) shows that PLE-IL-12-NP delivery is more efficacious in prolonging survival in this orthotopic ovarian tumor than both soluble and UL-NP IL-12 delivery methods upon IP delivery. Indeed, IP delivery of PLE-IL-12-NPs showed the largest improvement over both carrier-free IL-12 and UL-NPs, leading to cures in this malignancy. This is likely due to the enhanced ability of PLE-IL-12-NPs to concentrate IL-12 delivery in the tumors (Fig 4-2) and effectively maintain IL-12 activity through cell surface localization demonstrated previously from the PLE terminal layer. IV delivery showed a more muted response in these tests, with UL-NPs actually showing an enhanced response. This is likely due to the fact that the tumors in these studies were still rather small and so were not fully vascularized. UL-NPs release IL-12 more readily in the blood stream than PLE-IL-12-NPs as evidenced by the toxicity data (Fig 4-3) which likely allows for easier access of this released IL-12 to the tumors as compared to layered NPs. However, this also is a main route of toxicity. It is likely that as larger, more vascularized tumors are treated PLE-IL-12-NPs show better efficacy at the already demonstrated reduced toxicity, similar to the results obtained IP. These data together with the enhanced toxicity profiles (Fig 4-3) demonstrate that the PLE-IL-12-NPs make a significant improvement to IL-12 therapy by both reducing systemic exposure, thus allowing for increased dosing levels, and increasing efficacy against an orthotopic ovarian tumor model. Importantly, these improvements outclass those achieved with UL-NPs in addition to carrier-free cytokine delivery.

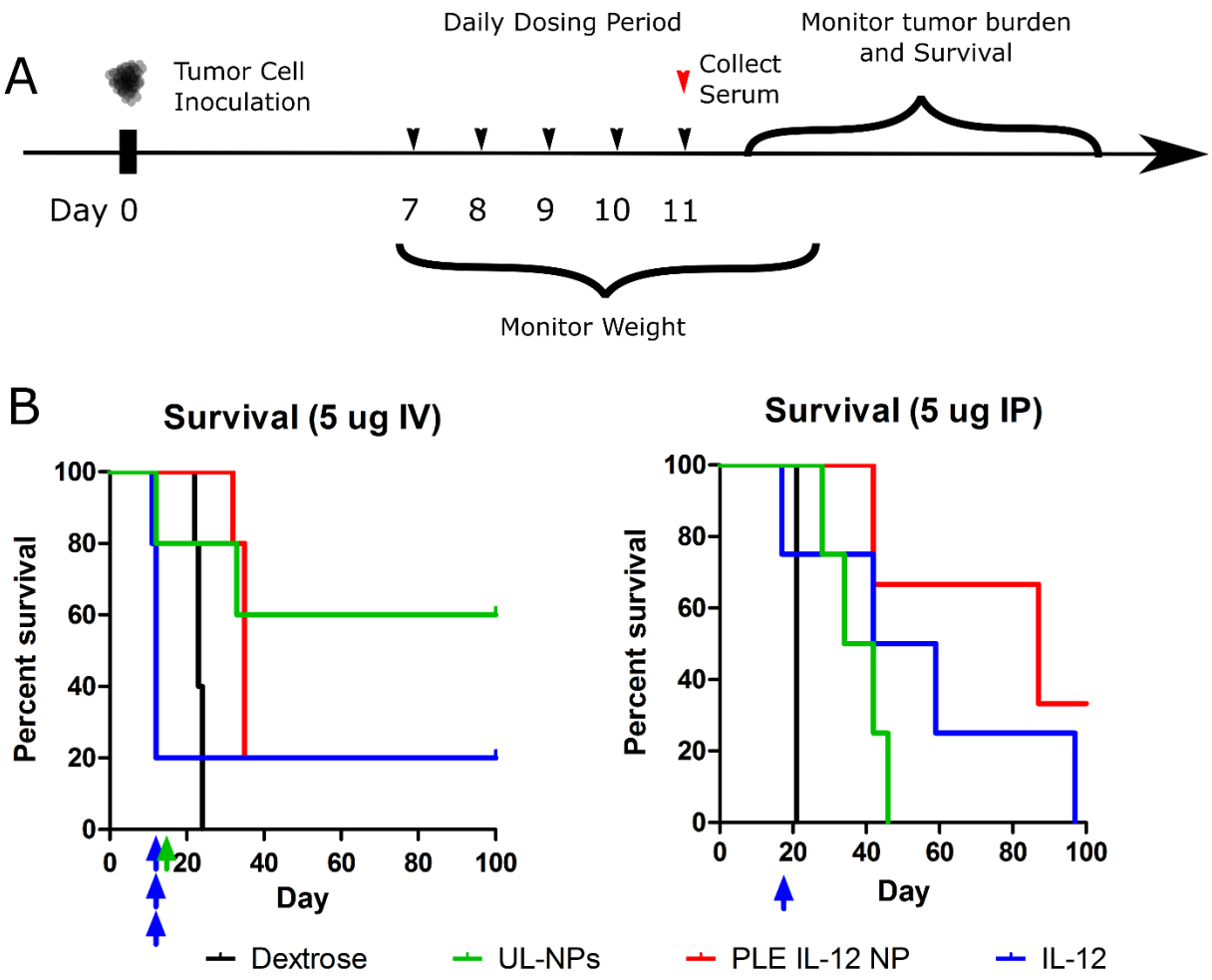

Figure 4-4. PLE-IL-12-NPs improve anti-tumor efficacy of IL-12. **A**, Schematic of dosing scheme in HM-1 tumored animals. Mice were dosed with 5 μg IL-12 in PLE-IL-12-NPs, UL-NPs, or carrier free and compared to 5% dextrose control 7 days after IP inoculation of HM-1 tumor cells. **B**, Survival curves of 5 μg IL-12 treated mice for IV (left) and IP (right) delivery routes. Colored arrows indicate toxicity related deaths during and immediately following dosing.

A further test of the PLE-IL-12-NPs was carried out at higher dosing in the better performing IP delivery case to further demonstrate the pronounced ability of the described delivery vehicle to enhance IL-12 therapy in difficult to treat ovarian tumors. These studies were identical to previous studies (Fig 4-3, 4-4) at an increased dose of 10 μg. At this increased dosing level significant toxicities occurred in both the carrier-free IL-12 and UL-NP treated subjects, with toxicity related deaths occurring during the dosing period in both healthy and tumor bearing subjects. In healthy subjects, all mice treated with carrier-free IL-12 and 50% of the mice treated with UL-NPs needed to be sacrificed during or immediately after dosing due to toxicity as measured by severe (>15%)

body weight reduction, while mice treated with PLE-IL-12-NPs showed little (statistically insignificant) changes in body weight and condition compared to controls (Fig 4-5A). Moving forward, mice bearing HM-1 tumors were treated with PLE-IL-12-NPs, UL-NPs, and carrier free IL-12 and compared to dextrose controls. Again, both carrier-free and UL-NP IL-12 treatments showed significant toxicity in these studies as measured by weight changes (Fig S6), with subjects succumbing to toxicity during the dosing period, while PLE-IL-12-NP treatments were well tolerated (Fig 4-5B). Furthermore, PLE-IL-12-NPs showed prolonged survival (Fig 4-5B) compared to other IL-12 delivery methods in these studies and indeed led to a ~30% cure rate.

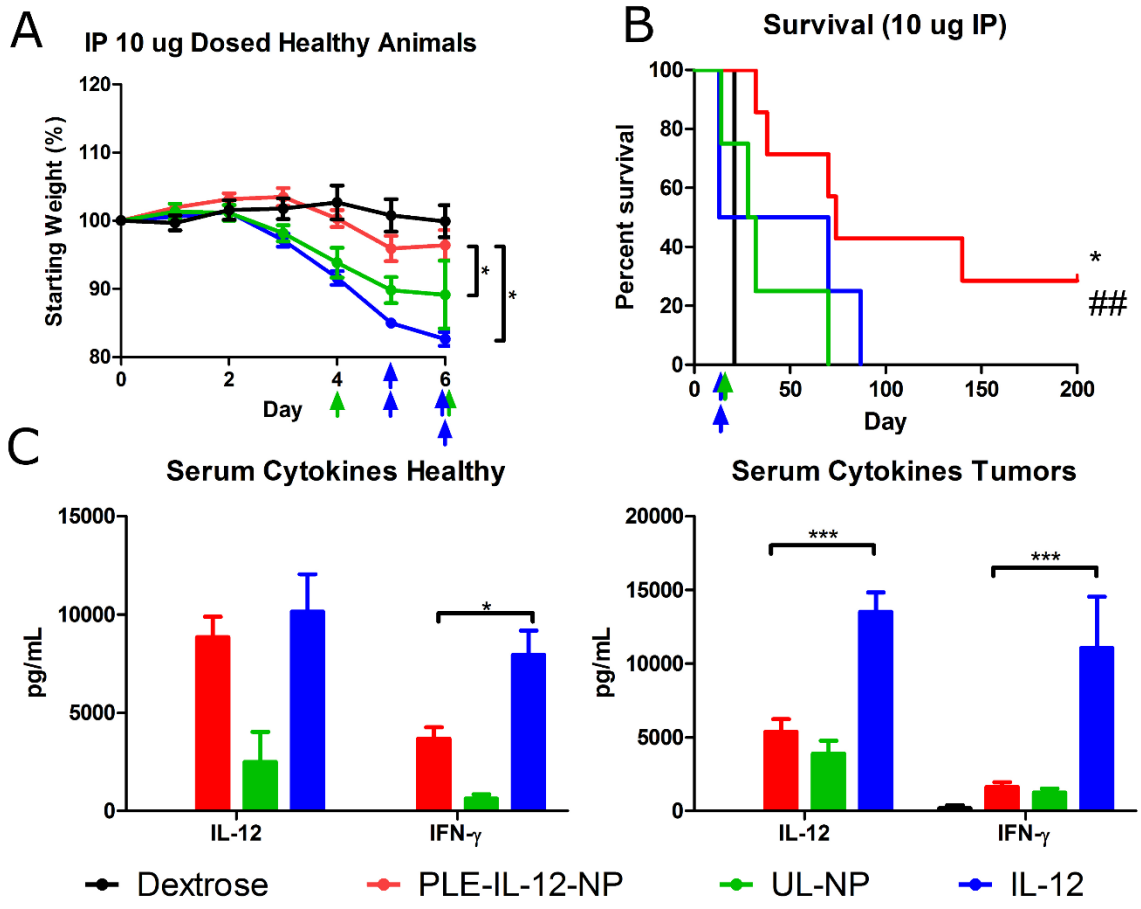

Figure 4-5 | PLE-IL-12-NPs improve efficacy of IL-12 at reduced toxicity with high dose systemic delivery. **A,** Animal weights upon daily dosing of 10 μg of IL-12 for 5 doses from PLE-IL-12-NPs (red), UL-NPs (green), or carrier-free (blue) compared to vehicle control (black). **B,** Survival of mice with orthotopic HM-1 tumors treated 7 days after inoculation with 5 daily doses of IL-12 from different vehicles similar to A. * indicates $p<0.05$ compared to UL-NPs ## indicates $p<0.01$

compared to Dextrose as measured by Mantel-Cox test between indicated groups. **C,** Serum levels of IL-12 and IFN-γ as measured by ELISA from serum collected 3 hours after the final dose from subjects in A for healthy mice (left) and subjects in B for tumored mice (right) * indicates $p<0.05$, *** indicates $p<0.001$ as measured by 2way ANOVA with Bonferroni post hoc test between all treatments and carrier-free IL-12.

Taken further, serum cytokine levels were monitored after treatments in both healthy and tumored mice as an additional measure of toxicity in relation to the different delivery vehicles (Fig 4-5C). In healthy mice, similar levels of IL-12 were present in the serum from both PLE-IL-12-NPs and carrier-free IL-12; however, carrier-free IL-12 delivery was significantly more systemically active as evidenced by the IFN-γ levels present in the serum, with significantly less IL-12 and IFN-γ in the UL-NP case. This is logical as the UL-NPs will be taken up and degraded in the RES system, such as in the liver, to a greater degree than the PLE-IL-12-NPs (Fig 4-2) and carrier-free IL-12. Moreover, while levels of IL-12 are similar in systemic circulation from both the PLE-IL-12-NPs and carrier-free cytokine delivery likely due to the fact that there is no tumor for the NPs to interact with, the PLE coating sufficiently protects the IL-12 from systemic activity as evidenced by the lower systemic levels of IFN-γ from the PLE-IL-12-NPs. However, in subjects bearing malignancies the systemic IL-12 burden is significantly reduced from PLE-IL-12-NPs compared to carrier-free IL-12 which remains at similar levels as seen in healthy subjects. This leads to an even further reduction of toxic systemic IFN-γ levels from PLE-IL-12-NPs as compared to carrier-free IL-12 delivery. These data, together with the weight loss responses (Fig 4-5A) demonstrate a significant reduction in toxicity of IL-12 from PLE-IL-12-NPs upon IP administration at significantly enhanced efficacy (Fig 4-5B). Importantly, the effects of PLE-IL-12-NPs on IL-12 delivery in both toxicity reduction and enhancement of efficacy outpace not only carrier-free IL-12 delivery but also delivery of IL-12 from UL-NPs, demonstrating the pronounced role the LbL polymers play in this system.

PLE-IL-12-NPs enhance immune activity in tumors upon systemic delivery

We next expanded our analysis to the immunological response triggered by these IL-12 based therapies. In these studies, HM-1 tumors were allowed to establish for 14 days after IP implantation before treating with 10 μg of IL-12 for 3 daily doses from PLE-IL-12-NPs, UL-NPs, or carrier free IL-12 and compared to dextrose control (Fig 4-6A). 24 hours after the final treatment, ascites,

tumors, and spleens were harvested and analyzed using flow cytometry. Samples were profiled for diverse T-cell phenotypes including CD4/8 subtypes, activity markers, effector/memory markers, and a library of exhaustion markers. Samples were also assayed for a variety of myeloid populations including macrophages, dendritic cells (DCs), and monocyte derived suppressor cells (MDSCs) (gating strategy Fig C-7, full data sets Fig C-8).

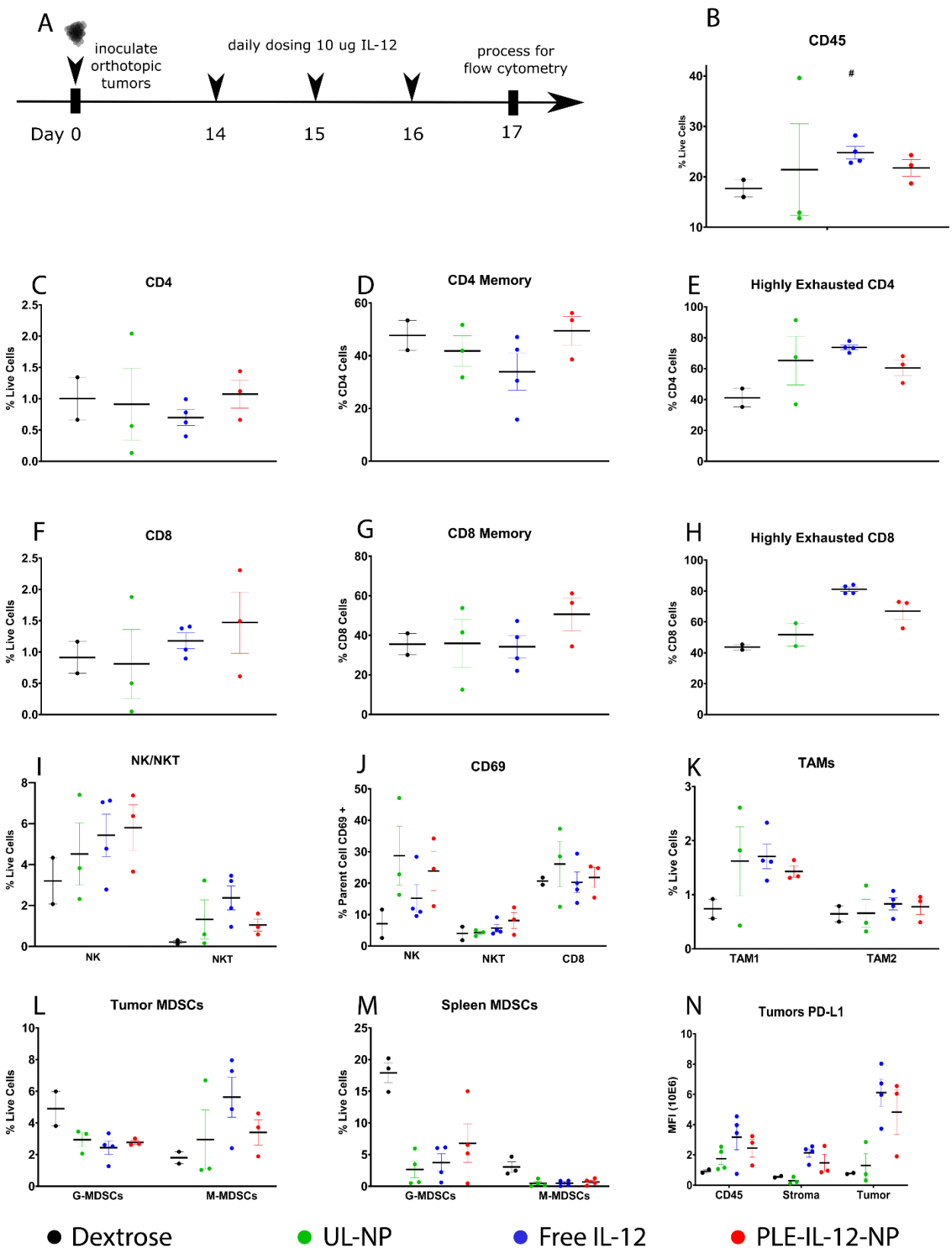
A
inoculate orthotopic tumors
daily dosing 10 ug IL-12
process for flow cytometry
Day 0
14
15
16
17
B
CD45
% Live Cells
C
CD4
% Live Cells
D
CD4 Memory
% CD4 Cells
E
Highly Exhausted CD4
% CD4 Cells
F
CD8
% Live Cells
G
CD8 Memory
% CD8 Cells
H
Highly Exhausted CD8
% CD8 Cells
I
NK/NKT
% Live Cells
NK
NKT
J
CD69
% Parent Cell CD69 +
NK
NKT
CD8
K
TAMs
% Live Cells
TAM1
TAM2
L
Tumor MDSCs
% Live Cells
G-MDSCs
M-MDSCs
M
Spleen MDSCs
% Live Cells
G-MDSCs
M-MDSCs
N
Tumors PD-L1
MFI (10E6)
CD45
Stroma
Tumor
Dextrose
UL-NP
Free IL-12
PLE-IL-12-NP

Figure 4-6 | PLE-IL-12-NPs show an equivalent immune response to carrier-free IL-12. **A,** Experimental design for immune profiling. Mice were inoculated with orthotopic HM-1 tumors and dosed with 10 μg IL-12 IP in PLE-IL-12-NPs, UL-NPs, or carrier-free and compared to vehicle control for 3 daily doses 14 days after inoculation. **B-K,** Immune population statistics found within the tumor environment as measured by flow cytometry following gating in Fig C-7. **L-N**, Immune suppressive markers found in indicated organs (tumor, spleen) as measured by flow cytometry following gating in Fig C-7.

Analysis of T cell responses to IL-12 delivery by various techniques demonstrates a shift towards a more active Th1 type immune response as is expected from IL-12 therapy, with a greater response from PLE-IL-12-NPs and carrier-free IL-12 than UL-NPs. This is most evident from the shifts in CD4+ and CD8+ populations in tumors (Fig 4-6 C-H)). Upon systemic IL-12 delivery there is a reduction in CD4+ T cell populations coupled with an increase in CD8+ T cells in the TME. Interestingly, this shift is not present when IL-12 is delivered in UL-NPs. Further, there is a substantial increase in memory CD8 T cells (Fig. 4-6 G) in the tumors upon IL-12 delivery from PLE-IL-12-NPs and carrier-free IL-12. This phenomenon is again absent when IL-12 is delivered from UL-NPs. A panel of exhaustion markers was probed including PD-1, LAG3, TIM3, TIGIT, and CTLA4. All three modes of IL-12 delivery also lead to the majority of T-cells showing a highly exhausted (PD-1, TIM3, TIGIT double or triple positive) phenotype – though free IL-12 and PLE-IL-12-NP had the largest effects. Interestingly, TIM3 expression (in terms of MFI) was increased approximately 100-fold in tumors upon IL-12 delivery from PLE-IL-12-NPs and carrier-free IL-12 as compared to vehicle controls in both CD4+ and CD8+ populations (Fig 4-7). Other exhaustion makers increased up to only 5-fold, suggesting that TIM3 blockade could be a good candidate for future combination therapy in this tumor model.

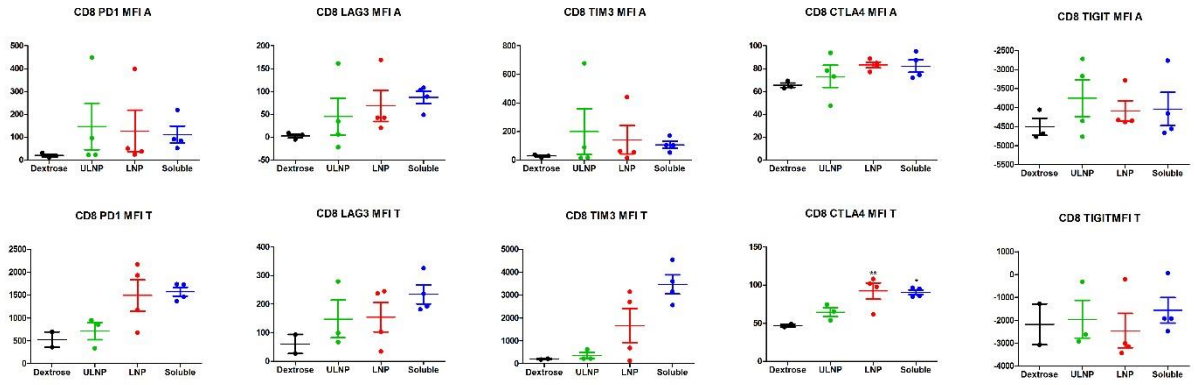

Figure 4-7| T cell exhaustion in response to IL-12 therapy. MFI of various exhaustion markers in CD8+ T cells in either the ascites (A) or tumor (T). * indicates $p<0.05$, ** indicates $p<0.01$ as measured by one way ANOVA with Dunnett's multiple comparison post hoc test comparing all groups to dextrose control.

NK and NKT cells were also increased upon IL-12 administration, though PLE-IL-12-NP elicited the greatest infiltration of NK-cells as well as a high degree of NK-cell activation indicated by CD69 expression. TAM1 infiltration was double that of vehicle control for all of the IL-12 treatment groups while MDSC infiltration was reduced. Interestingly, the MDSCs populations within the spleen were also drastically reduced (3 fold reduction) for all of the IL-12 treatments, indicating the systemic impacts of the therapies (Fig 4-6 M). Finally, PD-L1 expression was upregulated in the tumor, stroma, and immune cells (Fig 4-6 N) for PLE-IL-12-NP and carrier free IL-12 but not UL-NPs. Taken together, these data suggest PLE-IL-12-NPs show an equivalent immune activation to carrier-free cytokine, while UL-NP delivery of IL-12 failed to achieve similar results, again showing the critical role of the LbL coating in these therapies.

4.4 Conclusions

In this work we build on previous studies of PLE-IL-12-NPs in previous chapters, further demonstrating that the rational engineering of a NP delivery vehicle using the LbL technique makes significant improvements to IL-12 therapy, not only compared to carrier-free cytokine delivery but also in comparison with a simpler NP design that does not incorporate any rational engineering of NP properties to meet the delivery challenges of cytokine therapy. Importantly, in this work we demonstrate that IL-12 delivery from PLE-IL-12-NPs is both safe and efficacious via systemic delivery routes to a greater degree than previously shown with local delivery. Another

critical finding in this work is the pronounced efficacy in ovarian tumors, which have been refractory to many other forms of immunological treatments as well as the pronounced immune activation within ovarian tumors, opening the door to combination treatments and additional improvements in immunotherapy to this previously unresponsive malignancy.

Perhaps the most critical finding in this study is the demonstration of not only reduced toxicity but also increased efficacy of IL-12 therapy through a systemic delivery route. IL-12 has shown significant promise in the past with potent anti-tumor responses but was limited by off-target activity issues leading to high toxicities and even two deaths in clinical trials. To this end, it is critical for any future IL-12 studies to demonstrate reduction in systemic exposure while maintaining activity at the tumor sights. Many recent delivery techniques such as microparticles and chitosan co-formulations achieve this result through limiting systemic leakage from tumors. However, these strategies are limited to local injection of tumors directly, which is not possible in many epithelial tumors, including ovarian cancers, which do not have a singular main tumor mass to inject or easily accessible tumors for multiple injections. The described PLE-IL-12-NPs are not limited to local treatments and indeed show an even greater enhancement of IL-12 therapy via systemic delivery than previously demonstrated in local treatments in previous chapters.

Another key finding in the reported work is the enhancement of IL-12 therapy from PLE-IL-12-NPs over UL-NPs. We demonstrate throughout that the engineered LbL NP structure is critical to the reduction of toxicity as well as the enhancement of efficacy in these experiments, as a simpler liposomal particle does not show the same results in both toxicity and efficacy tests. The LbL particles were designed with thorough consideration into the design challenges required for successful cytokine therapy including efficient protein encapsulation, proficient maintenance of cytokine activity from particles, maintenance of cytokine access to surface receptors within the tumor environment, and selective interaction with tumor cells to concentrate both NP and payload in the tumor to achieve active levels of signaling in the tumor, a critical consideration for IL-12 success[55], while preventing off target activity which leads to toxicity. Previously we demonstrated *in vitro* that the described PLE-IL-12-NPs achieve all of these goals. Herein we further show that the PLE-IL-12-NPs, engineered to meet each of these challenges, do indeed enhance cytokine therapy not only in reduction of off-target toxicity but also in enhanced efficacy within tumors,

compared to a simpler delivery vehicle that does not spatio-temporally control the delivery of IL-12 in this carefully engineered way, as predicted.

In this work we demonstrate that PLE-IL-12-NPs are capable of pronounced single agent efficacy in ovarian tumors. This is a critical finding in ovarian tumors as they have been refractory to most immunotherapy strategies to date, such as checkpoint inhibition. A key concern in ovarian tumor responses has been a lack of tumor infiltrating lymphocytes, or so-called "cold" TMEs, limiting checkpoint inhibition responses in this class of malignancies. Herein we demonstrate that PLE-IL-12-NPs are capable of increasing pro-inflammatory immune activity in ovarian cancer (Fig 4-6). Indeed we show that this increased pro-inflammatory immune response within the tumor is capable of a pronounced single-agent response in these previously refractory tumors. However, there is potential for further success in these difficult to treat tumors through combination with checkpoint inhibition or other immunotherapies, which has been deemed a promising path forward for improving immune outcomes[87-89]. As IL-12 delivery drives the pro-inflammatory immune response within the tumor so too rises the exhaustion of T cells, as demonstrated herein (Fig 4-6). By adding a checkpoint inhibitor such as an antibody against PD-L1[82] or TIM3, both of which showed marked increases after IL-12 therapy, a further improvement in anti-tumor response is conceivable. Beyond combination with checkpoint inhibitors, combination therapy with additional cytokines is also likely to improve this therapy further[89]. In this study we focus on IL-12 delivery from the described LbL-NPs; however, the particle manufacture is not specific to IL-12 and thus additional NPs containing other synergistic cytokines can be made in a similar fashion. Indeed, future work will focus on delivering multiple synergistic cytokines from the same NP. This is a particularly attractive approach using the LbL-NP technique, as LbL NPs offer the opportunity for precise control over payload ratios and staged delivery of payloads from particles[90]. It is hypothesized that such careful control over ratio and timing of immune combination treatments is critical to achieve the greatest success of these therapeutic strategies[84], which is possible from the described LbL NP vehicle.

Chapter 5. Altering IL-12 linkage adjusts release and method of action in LbL-IL-12-NPs

Partially adapted from

Barberio, A.E., Smith, S.G., Correa, S., Nguyen, C., Nhan, B.T., Melo, M., Tokatlian, T., Suh, H., Irvine, D.J., Hammond, P.T., 2020. Cancer Cell Coating Nanoparticles for Optimal Tumor-Specific Cytokine Delivery. ACS Nano, *Under Revision*.

5.1 Introduction

Previous work has thoroughly demonstrated the activity of PLE-IL-12-NPs both *in vitro* and *in vivo*. PLE-IL-12-NPs have demonstrated evident activity in triggering an immune response in the form of IFN-γ production *in vitro* (chapter 2) and lymphocyte activity consistent with the expected cascade of IL-12 immunity[17,19] (chapter 3 and 4). This activity leads to pronounced anti tumoral activity in many tumor models at safer toxicity levels than experienced from carrier-free IL-12 delivery or indeed UL-NP delivery (chapter 4). This chapter focuses on developing a further understanding of the method of action of IL-12 from the previously described PLE-IL-12-NPs in order to further optimize the efficacy and reduction of toxicity from these NPs.

From the NP design, it is feasible that IL-12 can show activity in multiple ways including 1) dissociation from the liposomal surface and diffusion through the layers of an intact particle, 2) erosion of the polymer layers *in vivo* leading to exposure of IL-12 on the liposomal surface which then releases from the surface to activate nearby T cells, or 3) erosion of the polymer layers *in vivo* leading to exposure and activity of IL-12 that remains bound to the liposomal surface. It is critical to understand this method of action as we move forward in adding additional cytokines and further optimizing kinetic release of cytokines from the NP design. For example, a NP design that keeps IL-12 bound to the surface is potentially more ideal than releasing IL-12 as such a design is more likely to keep IL-12 activity restricted to the tumor and prevent systemic toxicity, a critical phenomenon for optimal IL-12 therapy[32,34,55]. To this end in this chapter we probe the method of activity for the PLE-IL-12-NPs and adjust the linker chemistry of IL-12 to the NP surface in order to adjust kinetic release and method of action from the NP.

5.2 Materials and Methods

Materials

1,2-dioleoyl-sn-glycero-3-[(N-(5-amino-1-carboxypentyl)iminodiacetic acid)succinyl] (nickel salt) (DGS-NTA (Ni)), 1,2-distearoyl-sn-glycero-3-phosphocholine (DSPC), Cholesterol, and 1-palmitoyl-2-oleoyl-sn-glycero-3-phospho-(1'-rac-glycerol) (sodium salt) (POPG) 1,2-dioleoyl-sn-glycero-3-phosphoethanolamine (DOPE) 1,2-dioleoyl-sn-glycero-3-phosphoethanolamine-N-[4-(p-maleimidophenyl)butyramide] (sodium salt) (MPB) were purchased from Avanti Polar Lipids and used without modification. PLR and PLE were purchased from Alamanda Polymers and used without modification. Single chain IL-12 was produced in house from HEK-293 cells.

PLE-IL-12-NP Formulations

PLE-IL-12-NP assembly was performed as described previously[63] with minor modifications, similar to previous chapters. Briefly, liposomes were prepared by the rehydration/extrusion method. A lipid solution containing 5% DGS-NTA (Ni), 65% DSPC, 23.9% Cholesterol, and 6.1% POPG by mole in chloroform was dried at 20 mbar for 1 hr by rotovap and desiccated under vacuum overnight. The lipid film was then reconstituted in PBS to a concentration of 1 mg/mL under sonication at 65^{o}C for 30 minutes. Rehydrated liposomes were extruded through 50 nm filters (Whatman) using Avestin Liposofast-50 pressure driven extruder at 65^{o}C until they reached a size of appx 60 nm as measured by number average diameter by DLS (Malvern ZS90). Single chain IL-12[72] with c-terminal histidine tag was added to liposomes in a 28:1 Ni:His ratio by mole overnight at 4C under agitation. Particle buffer was switched to water by tangential flow filtration (TFF) by 5x washing through a 100 kDa membrane (Spectrum Labs). Particles were added to a bath of PLR solution in glass vial under sonication at 0.1 weight equivalent of polymer compared to lipid and allowed to equilibrate on ice for 1-2 hours. Excess polymer was purified by TFF through a 100 kDa membrane (Spectrum Labs) and characterized for size and charge by DLS. Similarly, for terminal layer polyanion, particles were then added to a bath of polymer in glass vial under sonication at 1 weight equivalent of polymer compared to lipid and allowed to equilibrate on ice for 1-2 hours. Particles were purified by TFF and characterized for size and charge by DLS.

c.mPLE-IL-12-NP formulation

Similar to above formulation of PLE-IL-12-NPs with minor modifications. Briefly, liposomes were prepared by the rehydration/extrusion method. A lipid solution containing 5% or 15% MPB, 65% or 55% DSPC, 23.9% Cholesterol, and 6.1% POPG by mole in chloroform was dried at 20 mbar for 1 hr by rotovap and desiccated under vacuum overnight. The lipid film was then reconstituted in water to a concentration of 1 mg/mL under sonication at 65^{o}C for 30 minutes. Note water was used as the rehydration solvent to reduce charge screening and prevent aggregation of liposomes. Rehydrated liposomes were extruded through 50 nm filters (Whatman) using Avestin Liposofast-50 pressure driven extruder at 65^{o}C until they reached a size of appx 60 nm as measured by number average diameter by DLS (Malvern ZS90). Liposomes were diluted to a concentration of 0.1 mg/mL. Single chain IL-12 with c terminal histidine tag and added cysteine residue was added to liposomes in a 25:1 maleimide:cysteine ratio by mole overnight at 4C with aggitation. Particles were added to a bath of PLR solution in glass vial under sonication at 0.1 weight equivalent of polymer compared to lipid and allowed to equilibrate on ice for 1-2 hours. Excess polymer was purified by TFF through a 100 kDa membrane (Spectrum Labs) and characterized for size and charge by DLS. Similarly, for terminal layer polyanion, particles were then added to a bath of polymer in glass vial under sonication at 1 weight equivalent of polymer compared to lipid and allowed to equilibrate on ice for 1-2 hours. Particles were purified by TFF and characterized for size and charge by DLS.

Encapsulation characterization

Encapsulation of IL-12 in particles at various stages of the particle manufacture process was characterized by breaking up particles in 1% triton-100 (Sigma), 0.1% BSA (Sigma) under vortex for 1 min. IL-12 content was then measured by ELISA (Peprotech) and compared to initial amount of IL-12 added to the NPs (measured by nanodrop at time of addition) for encapsulation efficiency. Final particle lipid concentration was measured by Stewart assay[73] using chloroform dissolved lipid mixture from liposome formulation to produce a standard curve and weight percent encapsulation was calculated using IL-12 and lipid concentrations (mg IL-12/(mg lipid+mg IL-12)).

FRET studies

FRET pairing analysis was adapted from previous descriptions of the technique[91-93]. NPs were formulated similar to the above description. For these studies liposomes were made following the same protocol as described previously with the exception that 5% DOPE was added and DSPC mol% was reduced to accommodate. Once liposomes were extruded and buffer exchanged to water, Sulfo-Cy3 NHS-ester (Lumiprobe 11320) was added to the liposome surface following manufacture protocol for NHS-ester amine reaction with DOPE head groups. Briefly, 8 fold molar excess of dye was added to NP solution titrated to pH 8.5 and allowed to react at 4C overnight under agitation. Excess dye was purified off the NPs using TFF. NP solution was washed until the permeate from TFF showed <5% fluorescence as compared to the start of purification. IL-12 was then added to the liposome surface as described previously. For IL-12 release studies Sulfo-Cy5 NHS ester was added to the IL-12 similar to Sulfo-Cy3 NHS ester addition to DOPE described above. NPs were then layered with polymer layers similar to previous experiments. For NP erosion FRET particles Sulfo-Cy5 NHS ester was added to PLR similar to addition to IL-12. NPs were made in two groups, IL-12 tagged and PLR tagged. Each group contained NPs with only Sulfo-Cy3 on the liposome surface, NPs with only Sulfo-Cy5 either on the IL-12 or PLR respectively, and FRET pairing NPs with both dyes present. NPs were then added at 10% by volume to different media conditions. Media conditions tested included water (storage condition) and cell media that had been incubated with active cultures of MC38 cells for no less than 48 hours (spent media) as a mimic of an *in vivo* environment. Samples were taken at 1, 2, 4, 8, 24, 48 and 72 hour timepoints and measured for fluorescence. Two measurements were taken, 1) 540 excitation and 570 emission reflecting excitation and emission of Cy3 and 2) 540 excitation and 680 emission reflecting excitation of Cy3 and emission of Cy5. FRET efficiency was then calculated based on equation 1.

$$FRET\ efficiency = \frac{D_D - Fret_D}{D_D}\ ; \qquad (1)$$

D_D=fluorescence intensity of NP with donor fluorophore only in the donor channel

$Fret_D$= fluorescence intensity of NP with both fret fluorophores in the donor channel

FRET efficiency was normalized to 100%=FRET efficiency at t=0 and 0%=FRET efficiency of NPs degraded with triton x-100 similar to encapsulation experiments described above.

In vitro activity experiments

Constructed IL-12 LbL NPs were tested for bioactivity by ability to stimulate an IFN-γ response. Briefly, splenocytes were isolated from B6C3F1 by pushing spleens through 70 μm strainers, lysing red blood cells via ACK lysis buffer and resuspending splenocytes in RPMI containing 10% FBS, 1% penicillin/streptomycin, 1% sodium pyruvate, and 0.0005% β-mercaptoethanol. Splenocytes were cultured for 24 hours or less to prevent changes in populations from culture. Splenocytes were dosed with varying doses of IL-12 in particles or soluble form. Supernatants were then tested for IFN-γ content by ELISA (peprotech). Data were analyzed in Graph Pad PRISM 5 to find EC50 values based on dose response curves.

5.3 Results and Discussion

Cysteine:Maleimide linker chemistry NP formulation and IL-12 loading

Having demonstrated activity from the previously described PLE-IL-12-NPs, we hypothesized that the release and activity of IL-12 could be adjusted by altering the linker chemistry attaching the IL-12 to the liposomal surface. Nickel Histidine linkages, as used in the PLE-IL-12-NPs are fast reacting and well established for binding proteins; however, they have shown weaker binding under physiological conditions (demonstrated in Fig 5-3). As mentioned previously, an ideal NP design for IL-12 delivery would keep active IL-12 bound to the NP *in vivo* to reduce off-target activity. In order to achieve this we adjusted the NP design to bind IL-12 via cysteine-maleimide (c.m) linkage (Fig 5-1A), which has shown to be much more resilient to degradation under physiological conditions and indeed has been used in many approved therapies such as antibody drug conjugates. For these NPs we replace the DOGS-NTA (Ni) lipids with a maleimide containing lipid; 1,2-dioleoyl-sn-glycero-3-phosphoethanolamine-N-[4-(p-maleimidophenyl) butyramide] (MPB) and an IL-12 formulation with an added C-terminal cysteine residue was used. Different mole fractions of 5% and 15% MPB were tested to optimize loading of IL-12 for this change in linker chemistry (Fig 5-1B). Loading IL-12 on liposomes with 5% MPB head groups showed highly efficient encapsulation efficiency at 84% IL-12 yield; however, the loading efficiency of 7% IL-12 by weight was greatly decreased compared to the Ni:His NPs which show ~15% IL-12 by weight. Loading IL-12 on liposomes with 15% MPB head groups was less efficient, at an IL-12 yield of only 55%, but had a comparable IL-12 valency of 15% IL-12 by weight. Moving forward, we focused on the 15% MPB constructs as maintaining equivalent IL-

12 valency per NP is critical for drawing comparisons in activity between formulations. Of note, the reaction conditions (time and concentration of reactants) for the c.mPLE-IL-12-NPs were found to be critical to prevent aggregation, in contrast to the PLE-IL-12-NPs. This is likely due to the fact that IL-12 contains many cysteine residues and MPB is present in large excess. This likely leads to crosslinking of liposomes by IL-12 in high concentration or over reacted conditions. The c.mPLE-IL-12-NPs were layered in a similar manner to PLE-IL-12-NPs. Namely, an initial layer of PLR followed by an external layer of PLE were added at similar weight equivalents as found in the Ni:His NP design, leading to a final c.mPLE-IL-12-NPs construct nearly identical to the previously tested PLE-IL-12-NPs other than the altered IL-12 linker chemistry.

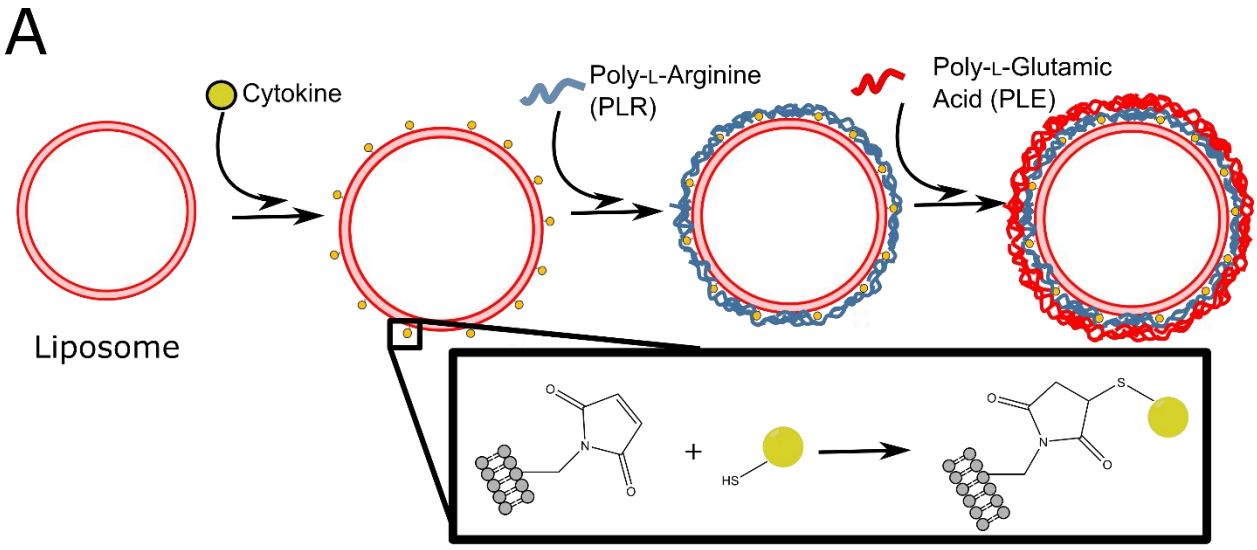

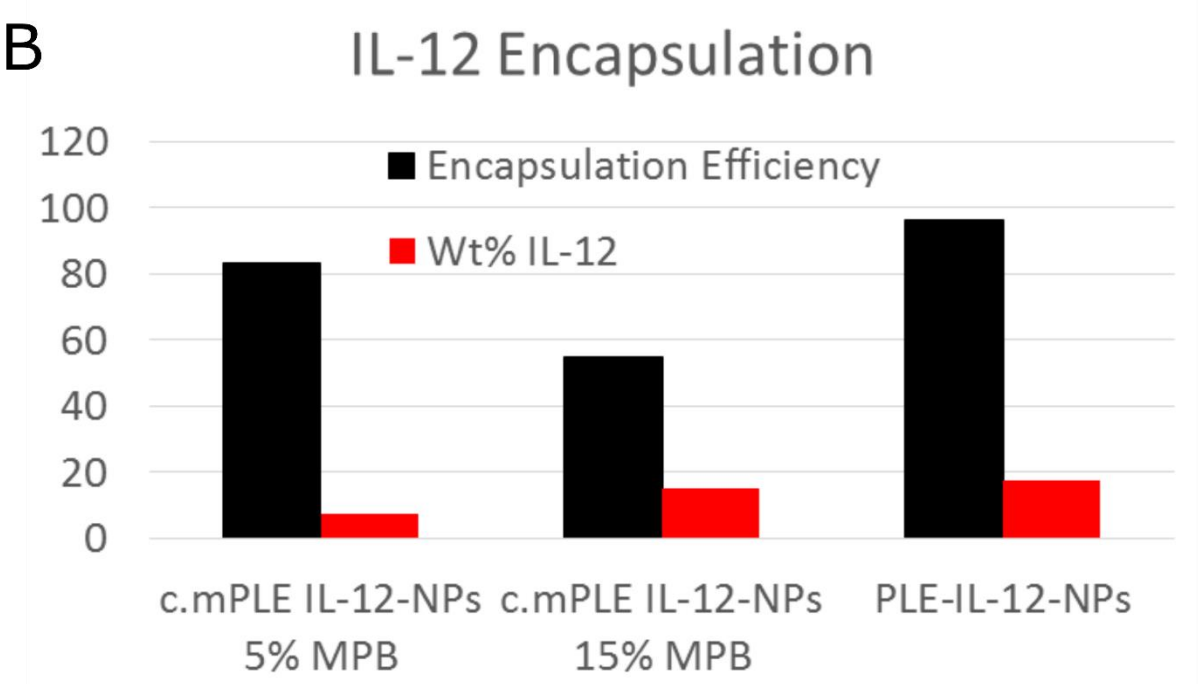

Figure 5-1. Formulation of c.mPLE-IL-12-NPs. **A,** Schematic of particle formulation. Similar formulation details to PLE-IL-12-NPs with the exception of a change in linker chemistry. **B,** Encapsulation efficiency (% recovered IL-12 in NPs from IL-12 added) and loading efficiency (mg IL-12/(mg lipid + mg IL-12)) of different NP formulations.

Particle erosion and IL-12 release in PLE-IL-12-NPs

Having demonstrated that the designed PLE-IL-12-NPs maintain pronounced activity *in vitro* and *in vivo*, the mechanism of activity from the original PLE-IL-12-NPs and c.mPLE-IL-12-NPs was probed. For these studies PLE-IL-12-NPs were created with FRET pairing fluorophores (Fig 5-2). The donor fluorophore (Cy3) of the FRET pair was bound to amines on 1,2-dioleoyl-sn-glycero-3-phosphoethanolamine (DOPE) on the liposome surface through NHS-ester chemistry. The acceptor fluorophore (Cy5) was bound to either free amines on IL-12 or the N terminal amine on PLR by NHS-ester chemistry. These NPs were then incubated at different solution conditions and samples were measured for FRET efficiency over a 72 hour period. These FRET efficiencies were then normalized to a fully intact particle as defined by FRET efficiency at t=0 and to a fully degraded (using Triton X-100) NP. FRET efficiency showed that the polymer layers undergo erosion of approximately 50% over an initial period of 8 hours followed by a slower erosion for the remainder of the study. IL-12 release showed a lag during the initial time while the polymer layers were still intact, with a matching burst between 8 and 24 hours, followed by a prolonged release over the remainder of the study (Fig 5-3A). These data demonstrate that the maintained IL-12 activity from PLE-IL-12-NPs is achieved via surface erosion, in which the polymer layers first erode over an 8 hour period, subsequently revealing and releasing the underlying IL-12 layer (Fig 5-3B). Importantly, these data show that a majority of IL-12 is released in the first 24 hours, while the NPs are still localized to tumor surfaces (Fig 2-2), allowing for maintained IL-12 activity from the PLE-IL-12-NPs.

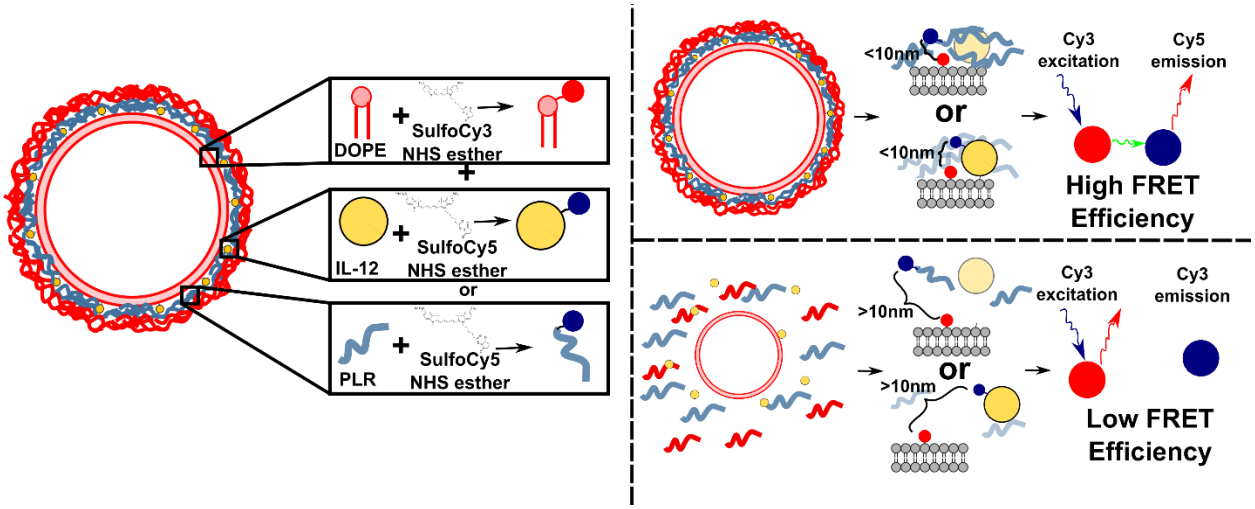

Figure 5-2. FRET experiments demonstrate mechanism and kinetics of deconstruction of PLE-IL-12-NPs. Schematic of NP structure for FRET kinetic release studies (left). FRET readouts for intact NPs (right, top) and degraded NPs (right, bottom). A mix of these states is also possible, ie IL-12 remains on the surface (high efficiency) while polymers erode (low efficiency).

We next probed if the altered linker c.mPLE-IL-12-NPs were able to adjust the kinetics of release of IL-12. Following a similar protocol to the experiments involving PLE-IL-12-NPs above (Fig 5-2) we used FRET pairing to probe the breakdown of the c.mPLE-IL-12-NP design and the release profile of IL-12. As expected, the c.m linker remained intact over the study period of 72 hours, with approximately 10% of the attached IL-12 dissociating from the c.mPLE-IL-12-NP design, even after significant amounts of the polymer layers eroded from the surface (Fig 5-3A). This represents a critical difference in NP deconstruction between the c.mPLE-IL-12-NPs, which reveal attached IL-12 on the liposomal surface overtime (Fig 5-3C) and the previously studied PLE-IL-12-NPs, which release IL-12 into their surroundings (Fig 5-3B).

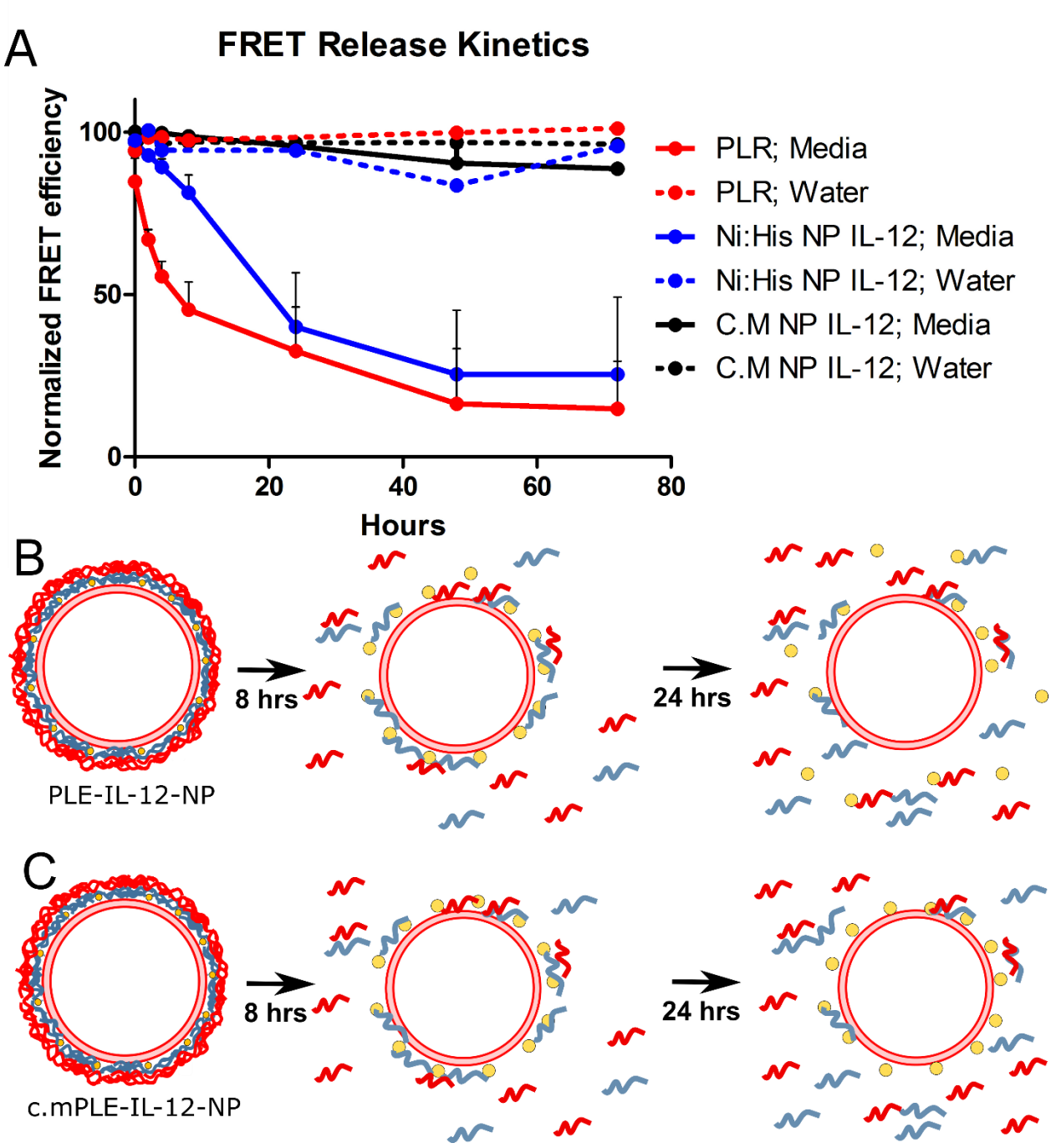

Figure 5-3 FRET efficiency shows different kinetics and mechanism of action with changing linker chemistry. **A,** Normalized FRET efficiency overtime for NPs. NPs were tested under two media conditions: water (storage media, dashed curves) and spent media (MC38 media cultured on cells for at least 48 hours as an *in vivo* mimic, solid curves). FRET efficiencies were measured for the erosion of the polymer layers as measured by FRET pairing with the acceptor fluorophore on PLR (red) and release of IL-12 as measured by FRET pairing with the acceptor fluorophore on

IL-12 for both PLE-IL-12-NPs (blue) and c.mPLE-IL-12-NPs (black). **B,** schematic of PLE-IL-12-NP break down as indicated by release data from B, shows that polymer layers erode from the NP surface initially, revealing IL-12 beneath that is subsequently released. **C,** schematic of c.mPLE-IL-12-NP break down as indicated by release data from B, shows that polymer layers erode from the NP surface initially, revealing IL-12 beneath that remains bound to the liposomal surface.

Activity of IL-12 from alternate linker chemistry

Having demonstrated an adjusted kinetic deconstruction and IL-12 release by altering linker chemistry in LbL NPs it is critical to find whether the altered kinetics have an effect on IL-12 activity. As a first test of the activity of IL-12 from c.mPLE-IL-12-NPs their ability to stimulate IFN-γ production from splenocytes was probed (Fig 5-4). In these tests the surface bound IL-12 from c.mPLE-IL-12-NPs showed no difference in activity as compared to the released IL-12 from PLE-IL-12-NPs, as evidenced by similar EC50s of maximal IFN-γ production. This suggests that the surface bound IL-12 is approximately equivalent in activity level as the released IL-12. This is critical in moving forward with the c.mPLE-IL-12-NPs as a potential improvement for cancer therapy. Interestingly, the c.mPLE-IL-12-NPs showed a trend for higher activity at lower concentrations *in vitro* as compared to the PLE-IL-12-NPs. This could be due to their remaining linked to the liposomal surface prevents ligand receptor recycle and IL-12 degradation after activation, while released IL-12 is more readily degraded. This phenomenon requires further testing to confirm and elucidate a mechanism.

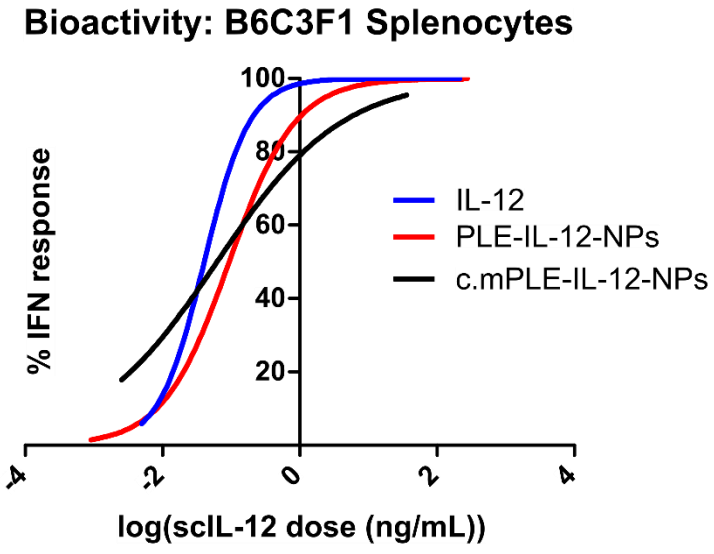

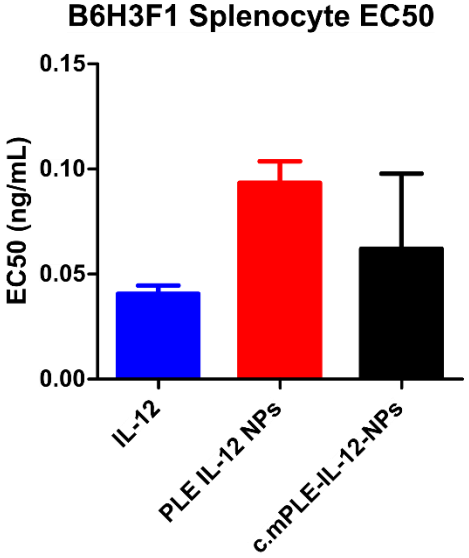

Figure 5-4 *in vitro* activity of c.mPLE-IL-12-NPs compares with that of PLE-IL-12-NPs. Dose response curves of IL-12 (left) demonstrate approximately equivalent efficacy in triggering IFN-γ production from B6C3F1 splenocytes in both c.mPLE-IL-12-NPs and PLE-IL-12-NPs, with minimal change in EC50 value for half maximal IFN-γ response (right).

5.4 Conclusions and future directions

In this chapter we demonstrated that altering the linker chemistry for IL-12 encapsulation can have a profound effect on the release (or lack thereof) of IL-12 from the NP. Furthermore, we show that IL-12 remaining bound to the surface of the NP for extended periods is as active as IL-12 that is rapidly released from the NP surface, with the potential for greater activity at lower dosing concentrations. These results are critical for the further development of the PLE-IL-12-NP platform. These changes suggest further optimization of the NP platform with potentially even greater improvements in cytokine therapy.

One important finding of these studies is the demonstration that the mechanism of action for the original PLE-IL-12-NP design is release of exposed IL-12 once polymer layers erode. Importantly, the kinetics of this release currently align with the concentration of PLE-IL-12-NPs in ovarian tumors upon systemic administration (Fig 4-5), likely leading to the reduction in toxicity and enhanced efficacy demonstrated from PLE-IL-12-NPs as compared to carrier-free IL-12, as systemic activity of IL-12 is prevented in the intact particle and released in concentration at the tumor site, a critical component to successful IL-12 therapy[55] that is not achieved by carrier-free IL-12 treatment or treatment from an UL-NP.

Another critical finding in this work is that the kinetic release and deconstruction of the NP can be readily adjusted through altered linker chemistry with minimal effect on the activity of the attached cytokine. This finding is critical in moving this cytokine delivery platform forward, not only for further optimization of IL-12 delivery but also for optimizing delivery of additional cytokines and combinations. While the current NP design shows demonstrable reduction in toxicity and enhanced efficacy, this phenomenon is likely due to the kinetic matching of NP deconstruction and IL-12 release to the concentration of NPs in the tumors. These improvements in IL-12 therapy can likely be further enhanced by careful engineering of the other NP components; for example, the reduced release of IL-12 from c.mPLE-IL-12-NPs can likely further reduce

toxicity through prevention of IL-12 leaking into systemic circulation, a critical parameter in toxicity control[35]. Future work will continue to work with c.mPLE-IL-12-NPs *in vivo* to further test these effects. In addition, other linker chemistries and layering strategies including tumor microenvironment responsive chemistries will be used to further optimize the delivery of IL-12 from these engineered LbL NPs.

The elucidation of the method of action from the described PLE-IL-12-NPs is also a critical step forward as we look towards future work in establishing delivery of a combination of cytokines. Indeed, it is critical for the greatest potential success of immunotherapy to deliver effective combinations of immunotherapeutic agents[87-89]. Moreover, it is hypothesized that fine control of ratios and timing of these therapies is critical to treatment success[84]. To this end, the ability to control the kinetic release and activity of cytokines is a critical finding in this work. Future work will focus on leveraging these findings to optimize spatio-temporally controlled cytokine combinations from the described LbL-NP constructs to provide optimal immunotherapy against aggressive cancers.

Chapter 6. Conclusions and Future Directions

This thesis has presented the construction, characterization, and testing of a NP delivery vehicle for cytokine therapy against cancer. Focusing on IL-12 as a model cytokine for its potency and clinical limitation of toxicity this thesis demonstrates significant improvement in IL-12 therapy using an LbL NP construct. IL-12 delivery presents many engineering challenges for optimal NP delivery including efficient protein encapsulation, maintaining biologic activity of protein from the NP carrier including targeting to cell surfaces, and targeting tumor tissue to concentrate payload in lesions while reducing systemic exposure upon systemic delivery. The LbL approach allows for the adjustment of the material properties of a NP delivery vehicle to meet each of these challenges. The developed LbL NP was demonstrated to meet the design criteria and ultimately demonstrated reduction of toxicity at enhanced efficacy of IL-12 therapy delivered systemically to treat ovarian cancer, which has been refractory to many immunotherapy strategies to date.

In chapter 2, the design of the PLE-IL-12-NPs is established. It is characterized extensively using *in vitro* techniques to demonstrate the design criteria for a successful IL-12 NP delivery vehicle. The NPs are shown to be monodisperse LbL constructs with >90% IL-12 loading. Importantly, chapter 2 tests the cellular and subcellular trafficking of the PLE-IL-12-NPs and shows that the particles selectively associate with tumor cells (>90% in tumor immune co-cultures) and remain on cell surfaces for >24 hours. These criteria are key for concentrating NPs in tumors and maintaining efficacy of IL-12 on nearby immune cells once in the tumor environment respectively. Indeed, chapter 2 also demonstrates that the PLE-IL-12-NP design maintains greater IL-12 activity *in vitro* than carrier-free IL-12 or a particle that is internalized.

In chapter 3 the verification of PLE-IL-12-NPs is further demonstrated with *in vivo* characterization. Particularly, the PLE-IL-12-NPs are shown to demonstrate reduced toxicity when delivered locally. Moreover, the PLE-IL-12-NPs are tolerated at higher doses *in vivo* compared to carrier-free IL-12. Importantly, this reduction in toxicity is matched with equivalent antitumor efficacy when compared to carrier-free IL-12. Indeed, in a pivotal study, PLE-IL-12-NPs are tolerated at a significantly higher dose than carrier-free IL-12, at which the antitumor response is shown to be significantly greater than that achieved in the highest tolerated dose of carrier-free IL-12. In addition, the length and intensity of the antitumoral immune response was probed,

confirming that PLE-IL-12-NPs produced an equally potent immune response compared to carrier-free IL-12.

In chapter 4 the testing of the PLE-IL-12-NPs is shown to improve IL-12 therapy in ovarian cancer upon systemic delivery. In these tests, PLE-IL-12-NPs were delivered either IP or IV and showed significant improvements in IL-12 therapy not only when compared to carrier-free delivery but also when compared to a simpler, unlayered nanoparticle design. PLE-IL-12-NPs showed greater tumor accumulation while avoiding clearance in other organs. In these tests PLE-IL-12-NPs not only showed reduction of toxicity over controls but also enhanced antitumor efficacy at equivalent doses. Finally, the intensity of the antitumor immune response was again assayed in these models and PLE-IL-12-NPs showed an equivalent immune response compared to carrier-free IL-12 and a greater immunological effect than UL-NPs.

Chapter 5 probes the mechanism of action of IL-12 delivery from LbL NPs. It is demonstrated that IL-12 is exposed on the liposomal surface of PLE-IL-12-NPs following erosion of the particle surface over an 8 hour period, followed by rapid release of IL-12 to the surrounding environment. This information is then leveraged to redesign the NPs with a different linker chemistry for IL-12. These c.mPLE-IL-12-NPs demonstrate significantly reduced release of IL-12 when exposed on the liposomal surface. Importantly, these c.mPLE-IL-12-NPs showed the same activity *in vitro*.

Future Directions

This work lays the ground work for the optimal delivery of cytokine therapies from NPs but there is still potential for improvements on the studies laid out here.

First, this work focuses on the delivery of IL-12 as a model cytokine for its potency and established limitation in the clinic due to toxicity. However, there are no IL-12 specific techniques used in the particle design. Therefore it is feasible that the described NP system could not only be expanded to deliver other cytokines but other therapeutic proteins as well such as antibodies. Future work could demonstrate the described NP design as a platform technology for delivery of any protein with a proper affinity tag that requires extracellular delivery.

In this work, the LbL technique is used to adjust material properties for the delivery of the single agent payload. However, another advantage of the LbL technique that is as yet untouched in this NP design is the ability to deliver multiple therapeutic agents from the same particle. The LbL

technique offers many drug loading compartments including the NP core, layers, and surface. Future iterations based on the current study can take advantage of these compartments to deliver combination therapies with small molecules, siRNAs or even combinations of cytokines. This is particularly critical to advance in the immunotherapy space. It is hypothesized that combination therapy is required to get the best immune response, particularly in immune refractory tumors[87-89]. Indeed, future studies can expand on this work not only by including multiple immunotherapeutic agents in a single particle but also by combining the described proinflammatory particles with additional immunotherapy strategies to elicit a further benefit to patient survival. As demonstrated in chapter 4, PLE-IL-12-NPs, as expected for many proinflammatory treatments, trigger an increase in T cell exhaustion markers. This suggests that the results shown in chapter 4 can be further improved by coupling PLE-IL-12-NPs with appropriate checkpoint inhibitors to counter T cell exhaustion.

Another key aspect of the LbL technique that has not been fully utilized in this work is the ability to adjust kinetic deconstruction NPs and sequential release of therapeutics[62]. In this work, the PLE-IL-12-NPs are demonstrated to have a kinetic release of IL-12 that matches well with the concentration of NPs in tumors, leading to the improved response demonstrated. However, this response could potentially be further improved through continued engineering of the layers. For example, incorporation of a tumor responsive layer could improve these NPs by keeping polymer layers intact until being rapidly degraded by a trigger only in the tumor environment. Moreover, the linker of cytokine to NP can be tailored to achieve differential release of payload as well, as demonstrated in chapter 5. These altered release mechanism particles can be further tested *in vivo* to elucidate optimal cytokine delivery mechanisms. As these adjustments to release kinetics and responsive release are furthered, they can also be used to introduce more than one therapeutic payload sequentially from the same particle. Recent research has indicated that proper timing of combination immunotherapies may be critical to the ultimate success of the therapy[84]. The discussed adjustments to the LbL NP design offer the opportunity to finely spatio-temporally control the delivery of immune combinations in the future at the cellular level. All of these future designs can be further built upon the foundation of LbL NPs for cytokine delivery laid out herein.

Concluding Remarks

The work presented in this thesis expands the armamentarium of immunotherapy strategies for fighting cancer. An optimized NP delivery vehicle is developed for IL-12 therapy using the LbL technique. This work demonstrates a strong foundation upon which future work in the field of NP delivery for immunotherapy can be built. In particular, the modular LbL technique offers many future opportunities to adjust the described PLE-IL-12-NPs to fit the ever expanding world of immuno-oncology. Moreover, this work stands as another example of the diverse applicability of the LbL NP technique. As laid out in chapter 1, cytokines present a very difficult engineering challenge to be delivered from a nano-scale carrier. The diversity and ease of use of the LbL technique allowed for that challenge to be met, demonstrating the diverse functionality of this NP technique.

Appendix A

Calculation A-1| Calculations for #IL-12/NP:

$$N_{lip} = \frac{\left[4\pi\left(\frac{d}{2}\right)^2 + 4\pi\left(\frac{d}{2} - h\right)^2\right]}{a}$$

Where N_{lip}=number of lipid molecules per liposome with diameter=d, monolayer thickness=h, and lipid head group area=a

For phosphotidylcholine, the majority of the described liposomes, a=0.71 nm^2

Bilayer thickness is estimated at 5 nm

Using the liposome diameter calculated from Fig 1 of 65 nm we find N_{lip}=32063

Using our liposome formula of 65% DSPC, 6% POPG, 5% DOGS-NTA(Ni), and 24% cholesterol we find our average lipid molecular weight to be 705.5 g/mol

$$N_{IL12} = \frac{\frac{N_{lip}}{N_A} * MW_{lip} * 0.15\frac{g_{IL12}}{g_{lip}}}{MW_{IL12}} * N_A \sim 50\frac{IL12}{NP}$$

Calculations based on (ref 54)

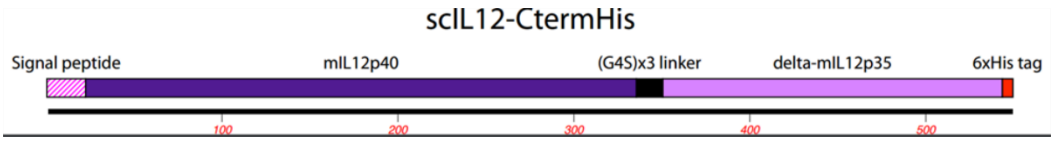

Figure A-1|scIL-12 protein construct. The described single chain IL-12 from Lieschke *et al* contains the murine IL-12p40 subunit with signal peptide attached to the murine IL-12p35 subunit without the leader (signified as delta-mIL12p35) by a (G4S)x3 linker. Attached at the c-terminus is a His tag for purification and chemical handle purposes.

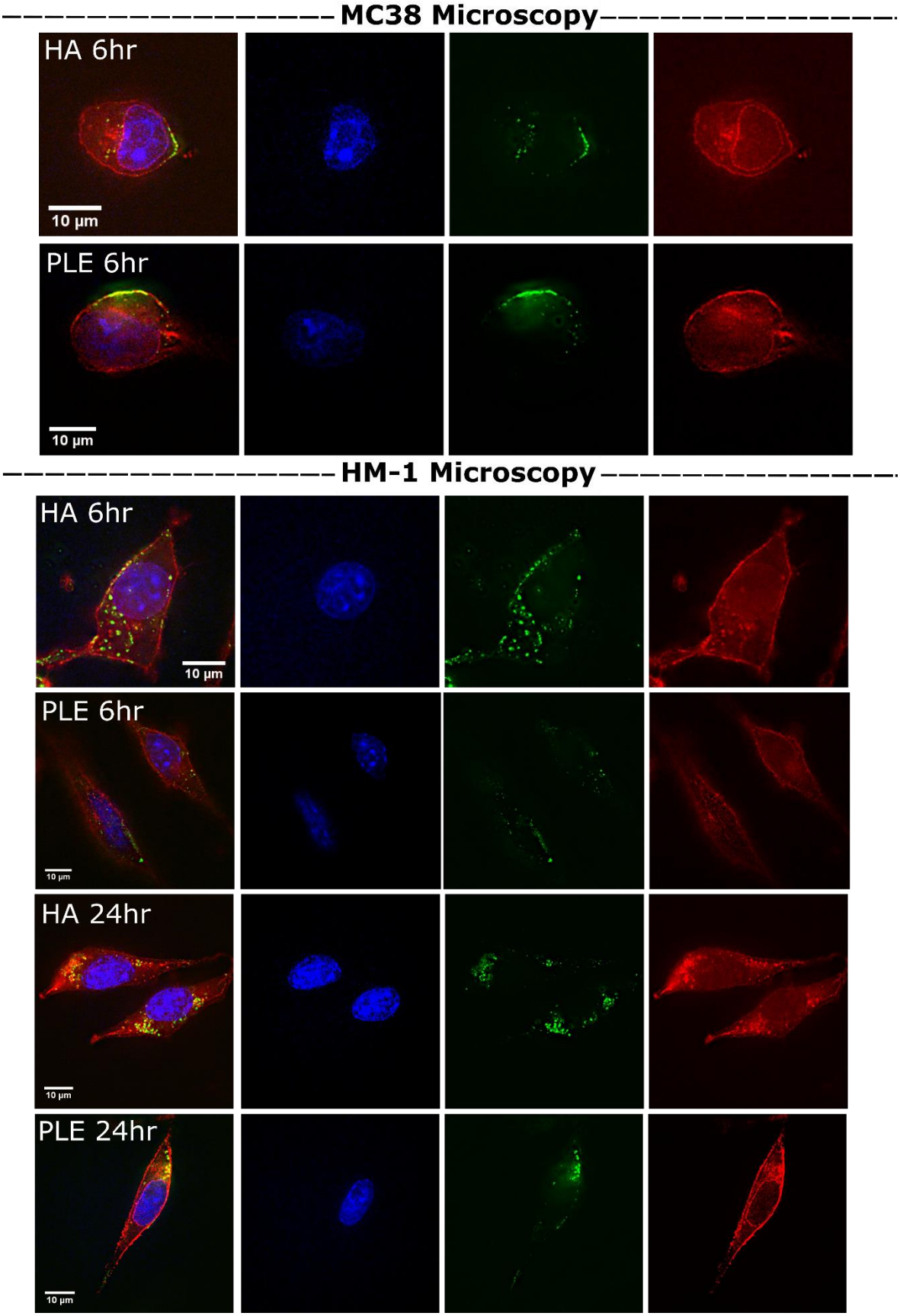
MC38 Microscopy
HA 6hr
10 µm
PLE 6hr
10 µm
HM-1 Microscopy
HA 6hr
10 µm
PLE 6hr
10 µm
HA 24hr
10 µm
PLE 24hr
10 µm

Figure A-2|Subcellular localization of LbL-CML-NPs fluorescence microscopy was done at 6 hr time periods for both MC38 and HM-1 cell lines and 24 hr time period for HM-1 cells. While both PLE and HA NPs are external at 6 hours, by 24 hours the HA NPs show a greater degree of internalization.

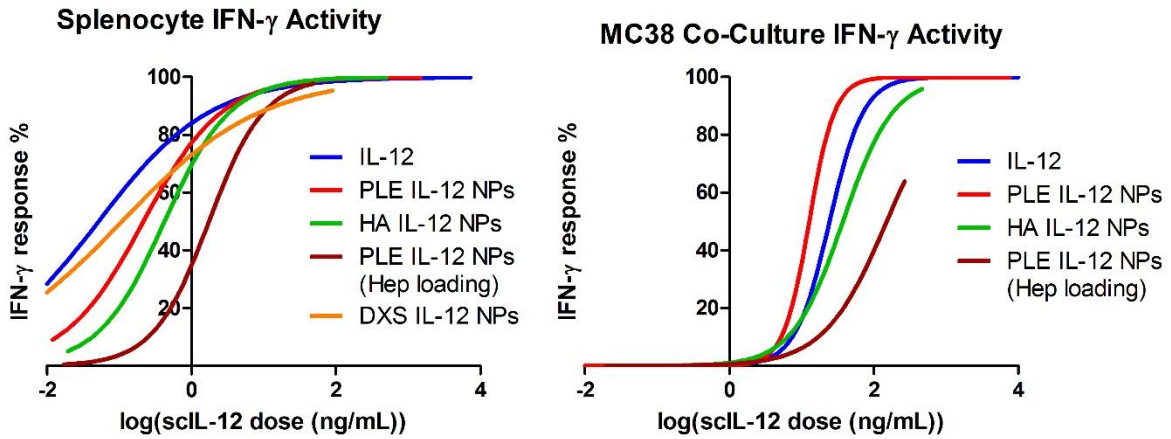

Figure A-3| Dose response curves of *in vitro* activity of IL-12 NPs IFN-γ responses. IFN-γ levels in response to various IL-12 therapies both in splenocyte only assays and co-cultured with MC38 cells. Used to calculated EC50 values.

Appendix B

Figure B-1|Flowcytometry gating strategy

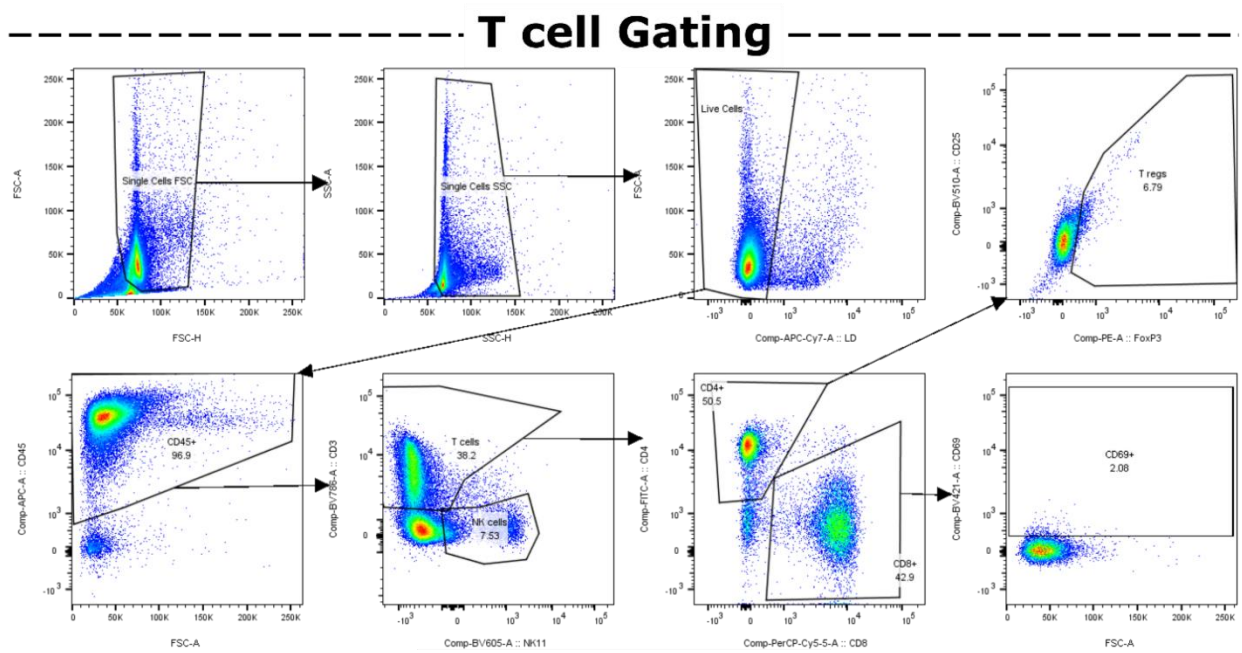

Monocyte Gating

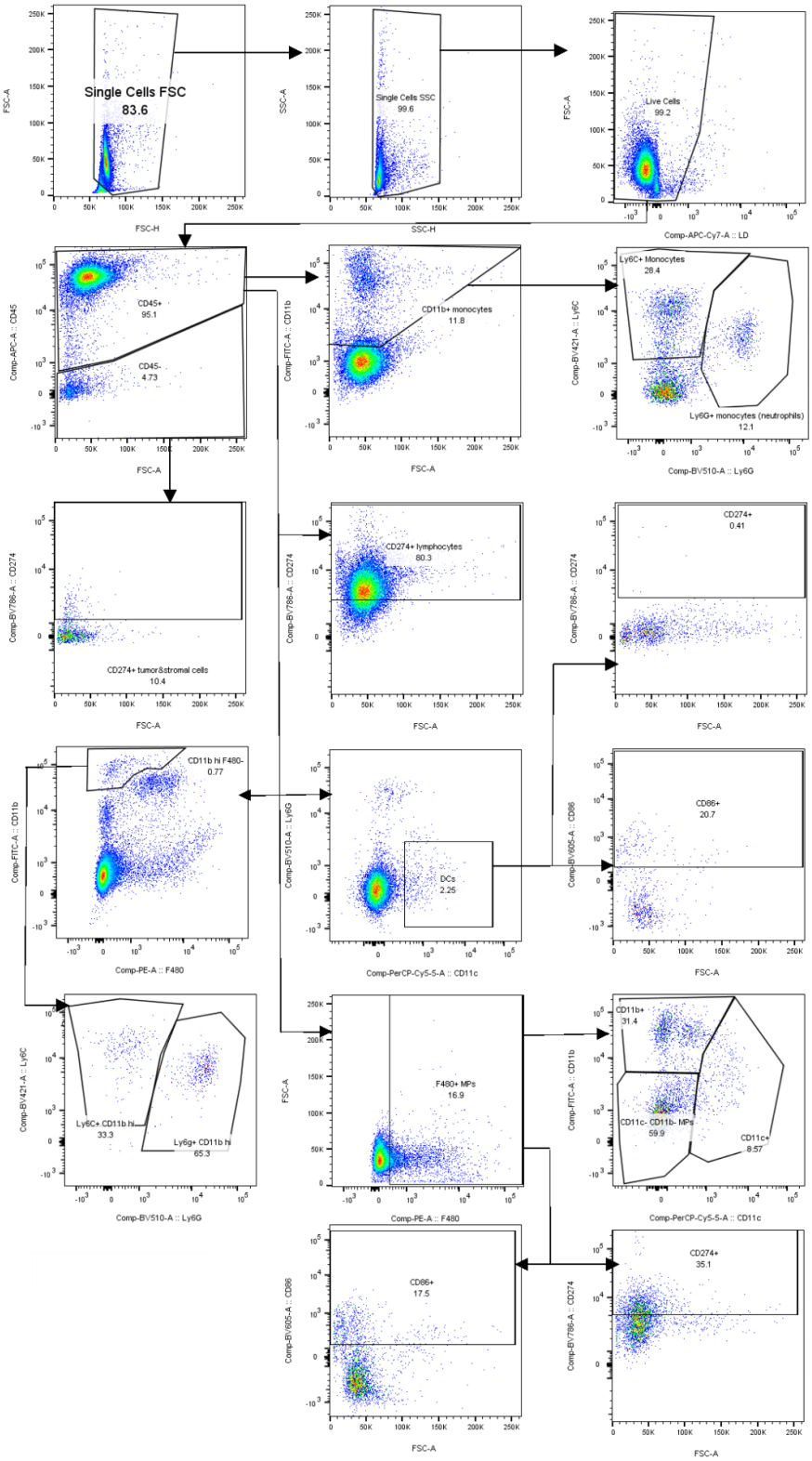

Figure B-2|Immune population changes upon IL-12 treatment

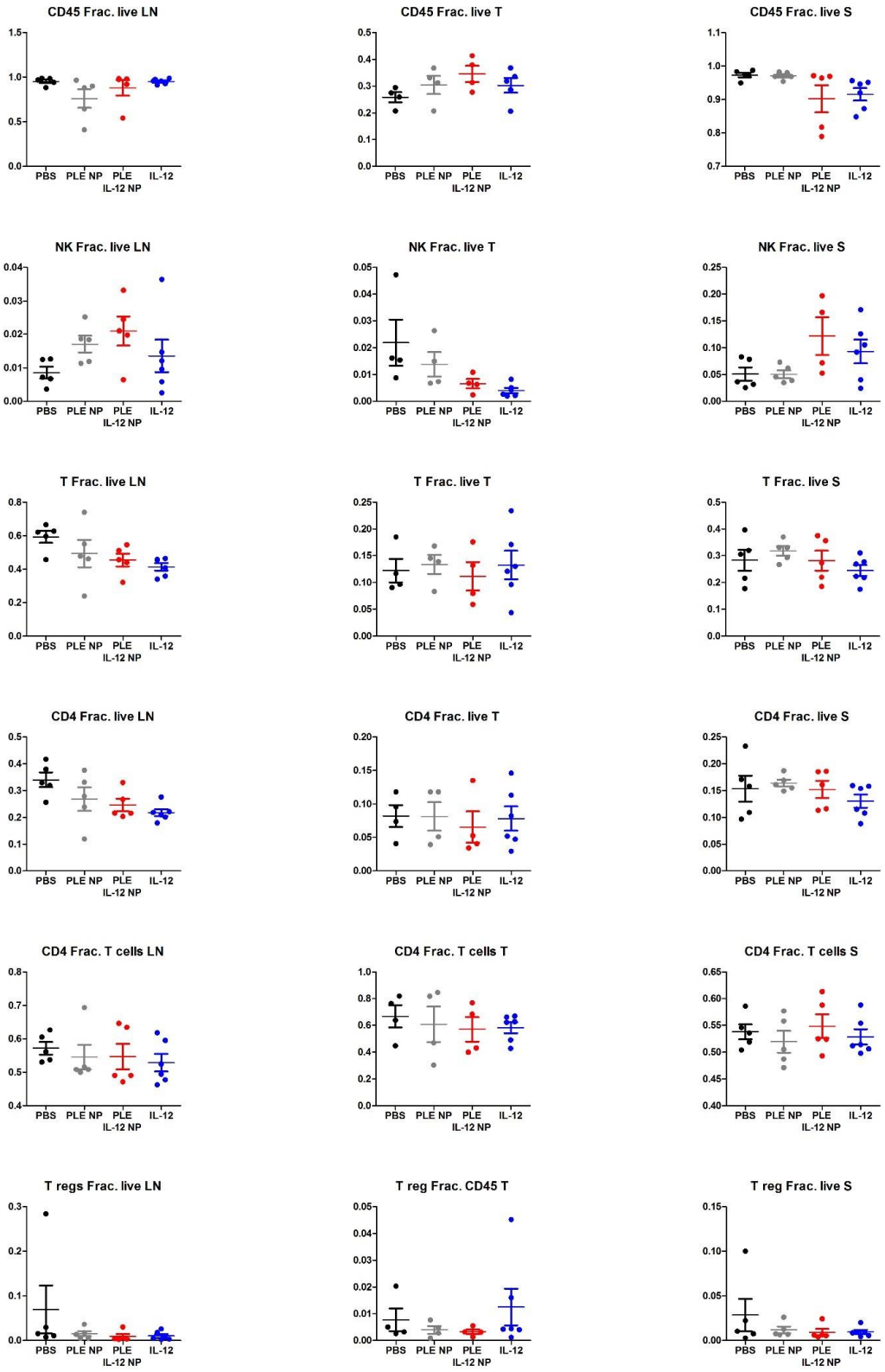

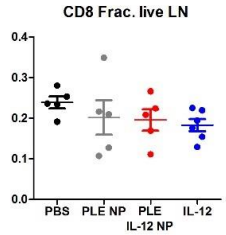
CD8 Frac. live LN
0.4
0.3
0.2
0.1
0.0
PBS
PLE NP
PLE IL-12 NP
IL-12

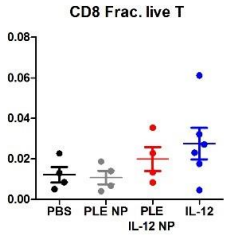
CD8 Frac. live T
0.08
0.06
0.04
0.02
0.00
PBS
PLE NP
PLE IL-12 NP
IL-12

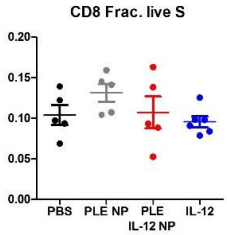
CD8 Frac. live S
0.20
0.15
0.10
0.05
0.00
PBS
PLE NP
PLE IL-12 NP
IL-12

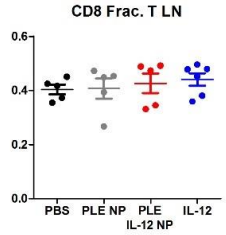
CD8 Frac. T LN
0.6
0.4
0.2
0.0
PBS
PLE NP
PLE IL-12 NP
IL-12

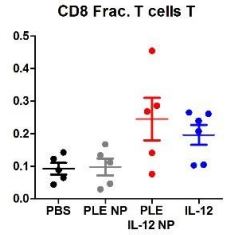
CD8 Frac. T cells T
0.5
0.4
0.3
0.2
0.1
0.0
PBS
PLE NP
PLE IL-12 NP
IL-12

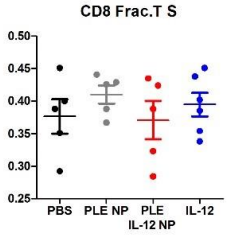
CD8 Frac.T S
0.50
0.45
0.40
0.35
0.30
0.25
PBS
PLE NP
PLE IL-12 NP
IL-12

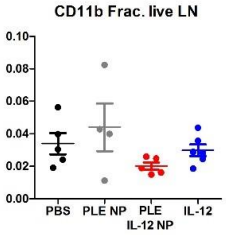
CD11b Frac. live LN
0.10
0.08
0.06
0.04
0.02
0.00
PBS
PLE NP
PLE IL-12 NP
IL-12

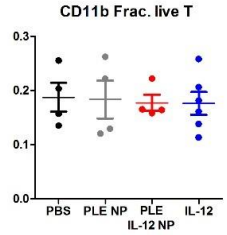
CD11b Frac. live T
0.3
0.2
0.1
0.0
PBS
PLE NP
PLE IL-12 NP
IL-12

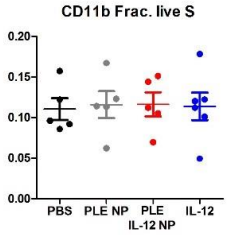
CD11b Frac. live S
0.20
0.15
0.10
0.05
0.00
PBS
PLE NP
PLE IL-12 NP
IL-12

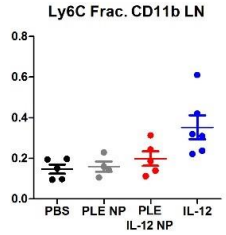
Ly6C Frac. CD11b LN
0.8
0.6
0.4
0.2
0.0
PBS
PLE NP
PLE IL-12 NP
IL-12

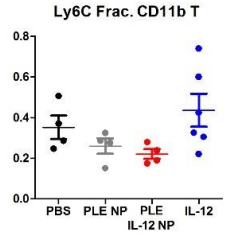
Ly6C Frac. CD11b T
0.8
0.6
0.4
0.2
0.0
PBS
PLE NP
PLE IL-12 NP
IL-12

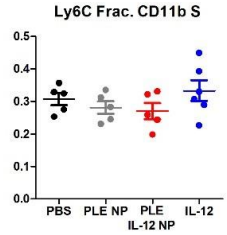
Ly6C Frac. CD11b S
0.5
0.4
0.3
0.2
0.1
0.0
PBS
PLE NP
PLE IL-12 NP
IL-12

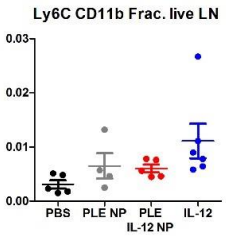
Ly6C CD11b Frac. live LN
0.03
0.02
0.01
0.00
PBS
PLE NP
PLE IL-12 NP
IL-12

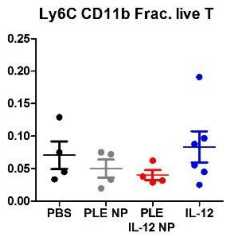
Ly6C CD11b Frac. live T
0.25
0.20
0.15
0.10
0.05
0.00
PBS
PLE NP
PLE IL-12 NP
IL-12

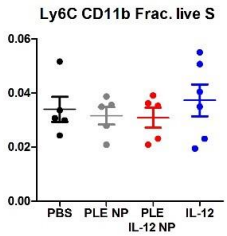
Ly6C CD11b Frac. live S
0.06
0.04
0.02
0.00
PBS
PLE NP
PLE IL-12 NP
IL-12

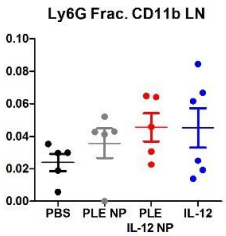
Ly6G Frac. CD11b LN
0.10
0.08
0.06
0.04
0.02
0.00
PBS
PLE NP
PLE IL-12 NP
IL-12

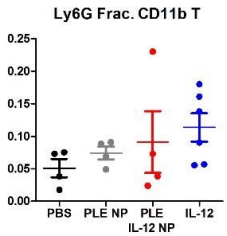
Ly6G Frac. CD11b T
0.25
0.20
0.15
0.10
0.05
0.00
PBS
PLE NP
PLE IL-12 NP
IL-12

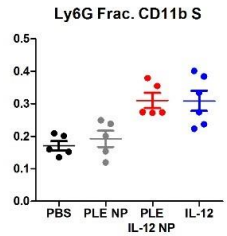
Ly6G Frac. CD11b S
0.5
0.4
0.3
0.2
0.1
0.0
PBS
PLE NP
PLE IL-12 NP
IL-12

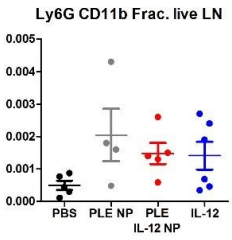
Ly6G CD11b Frac. live LN
0.005
0.004
0.003
0.002
0.001
0.000
PBS
PLE NP
PLE IL-12 NP
IL-12

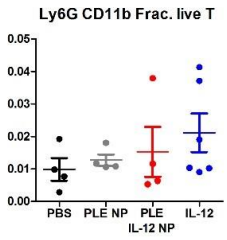
Ly6G CD11b Frac. live T
0.05
0.04
0.03
0.02
0.01
0.00
PBS
PLE NP
PLE IL-12 NP
IL-12

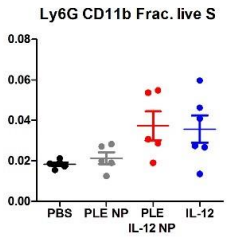
Ly6G CD11b Frac. live S
0.08
0.06
0.04
0.02
0.00
PBS
PLE NP
PLE IL-12 NP
IL-12

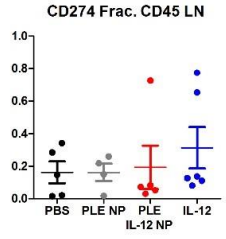
CD274 Frac. CD45 LN
1.0
0.8
0.6
0.4
0.2
0.0
PBS
PLE NP
PLE IL-12 NP
IL-12

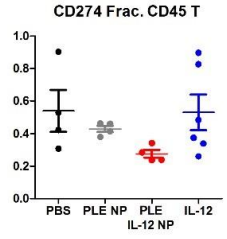
CD274 Frac. CD45 T
1.0
0.8
0.6
0.4
0.2
0.0
PBS
PLE NP
PLE IL-12 NP
IL-12

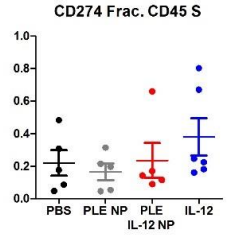
CD274 Frac. CD45 S
1.0
0.8
0.6
0.4
0.2
0.0
PBS
PLE NP
PLE IL-12 NP
IL-12

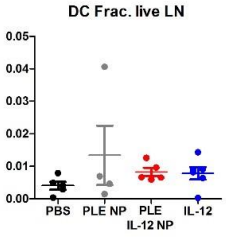
DC Frac. live LN
0.05
0.04
0.03
0.02
0.01
0.00
PBS
PLE NP
PLE IL-12 NP
IL-12

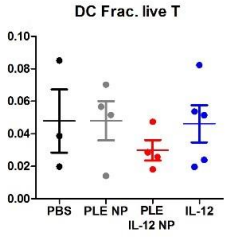
DC Frac. live T
0.10
0.08
0.06
0.04
0.02
0.00
PBS
PLE NP
PLE IL-12 NP
IL-12

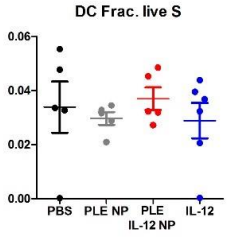
DC Frac. live S
0.06
0.04
0.02
0.00
PBS
PLE NP
PLE IL-12 NP
IL-12

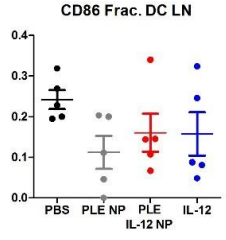
CD86 Frac. DC LN
0.4
0.3
0.2
0.1
0.0
PBS
PLE NP
PLE IL-12 NP
IL-12

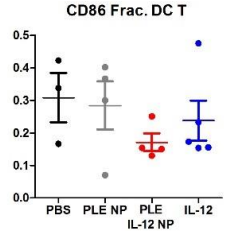
CD86 Frac. DC T
0.5
0.4
0.3
0.2
0.1
0.0
PBS
PLE NP
PLE IL-12 NP
IL-12

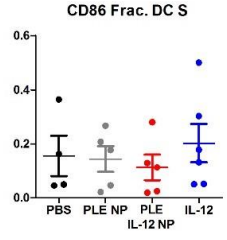
CD86 Frac. DC S
0.6
0.4
0.2
0.0
PBS
PLE NP
PLE IL-12 NP
IL-12

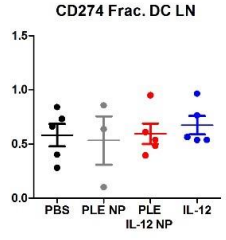
CD274 Frac. DC LN
1.5
1.0
0.5
0.0
PBS
PLE NP
PLE IL-12 NP
IL-12

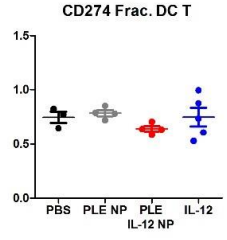
CD274 Frac. DC T
1.5
1.0
0.5
0.0
PBS
PLE NP
PLE IL-12 NP
IL-12

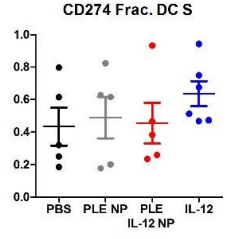
CD274 Frac. DC S
1.0
0.8
0.6
0.4
0.2
0.0
PBS
PLE NP
PLE IL-12 NP
IL-12

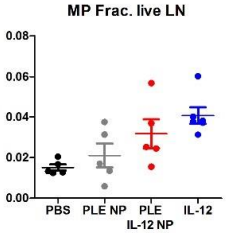
MP Frac. live LN
0.08
0.06
0.04
0.02
0.00
PBS
PLE NP
PLE IL-12 NP
IL-12

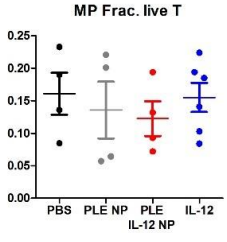
MP Frac. live T
0.25
0.20
0.15
0.10
0.05
0.00
PBS
PLE NP
PLE IL-12 NP
IL-12

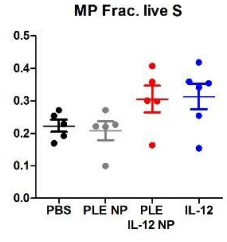
MP Frac. live S
0.5
0.4
0.3
0.2
0.1
0.0
PBS
PLE NP
PLE IL-12 NP
IL-12

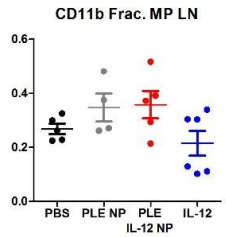
CD11b Frac. MP LN
0.6
0.4
0.2
0.0
PBS
PLE NP
PLE IL-12 NP
IL-12

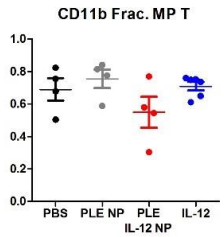
CD11b Frac. MP T
1.0
0.8
0.6
0.4
0.2
0.0
PBS
PLE NP
PLE IL-12 NP
IL-12

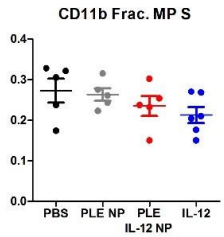
CD11b Frac. MP S
0.4
0.3
0.2
0.1
0.0
PBS
PLE NP
PLE IL-12 NP
IL-12

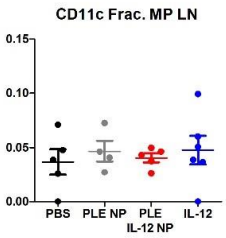
CD11c Frac. MP LN
0.15
0.10
0.05
0.00
PBS
PLE NP
PLE IL-12 NP
IL-12

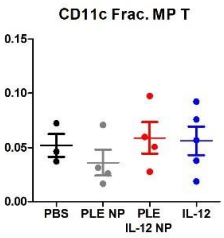
CD11c Frac. MP T
0.15
0.10
0.05
0.00
PBS
PLE NP
PLE IL-12 NP
IL-12

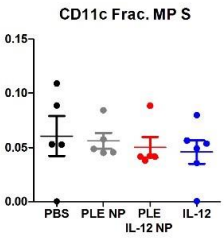
CD11c Frac. MP S
0.15
0.10
0.05
0.00
PBS
PLE NP
PLE IL-12 NP
IL-12

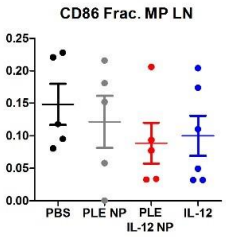
CD86 Frac. MP LN
0.25
0.20
0.15
0.10
0.05
0.00
PBS
PLE NP
PLE IL-12 NP
IL-12

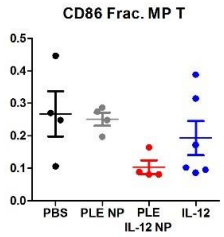
CD86 Frac. MP T
0.5
0.4
0.3
0.2
0.1
0.0
PBS
PLE NP
PLE IL-12 NP
IL-12

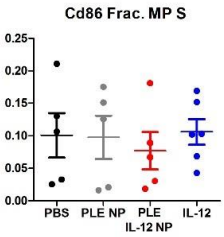
Cd86 Frac. MP S
0.25
0.20
0.15
0.10
0.05
0.00
PBS
PLE NP
PLE IL-12 NP
IL-12

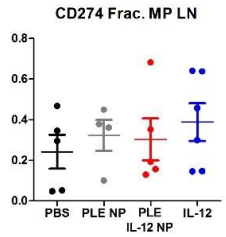
CD274 Frac. MP LN
0.8
0.6
0.4
0.2
0.0
PBS
PLE NP
PLE IL-12 NP
IL-12

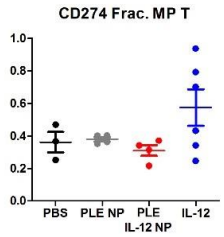
CD274 Frac. MP T
1.0
0.8
0.6
0.4
0.2
0.0
PBS
PLE NP
PLE IL-12 NP
IL-12

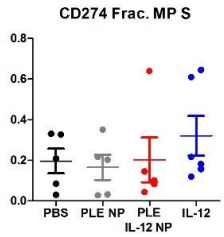
CD274 Frac. MP S
0.8
0.6
0.4
0.2
0.0
PBS
PLE NP
PLE IL-12 NP
IL-12

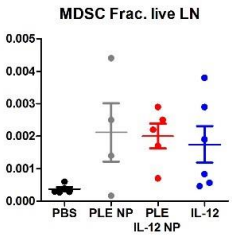
MDSC Frac. live LN
0.005
0.004
0.003
0.002
0.001
0.000
PBS
PLE NP
PLE IL-12 NP
IL-12

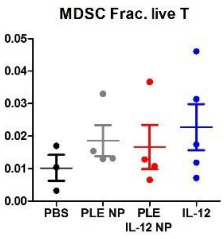
MDSC Frac. live T
0.05
0.04
0.03
0.02
0.01
0.00
PBS
PLE NP
PLE IL-12 NP
IL-12

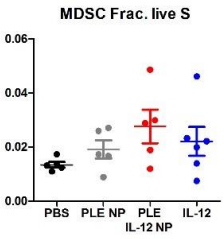
MDSC Frac. live S
0.06
0.04
0.02
0.00
PBS
PLE NP
PLE IL-12 NP
IL-12

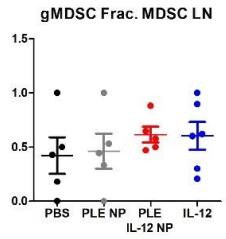
gMDSC Frac. MDSC LN
1.5
1.0
0.5
0.0
PBS
PLE NP
PLE IL-12 NP
IL-12

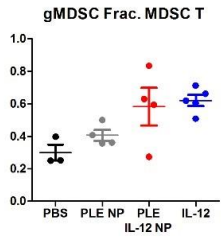
gMDSC Frac. MDSC T
1.0
0.8
0.6
0.4
0.2
0.0
PBS
PLE NP
PLE IL-12 NP
IL-12

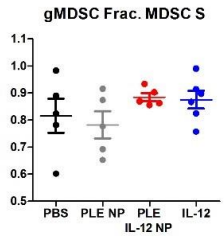
gMDSC Frac. MDSC S
1.1
1.0
0.9
0.8
0.7
0.6
0.5
PBS
PLE NP
PLE IL-12 NP
IL-12

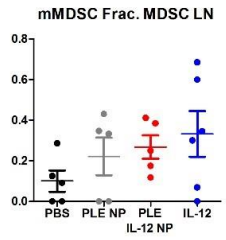
mMDSC Frac. MDSC LN
PBS
PLE NP
PLE
IL-12
IL-12 NP

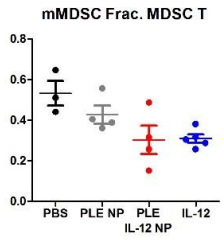
mMDSC Frac. MDSC T
PBS
PLE NP
PLE
IL-12
IL-12 NP

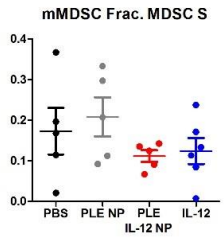
mMDSC Frac. MDSC S
PBS
PLE NP
PLE
IL-12
IL-12 NP

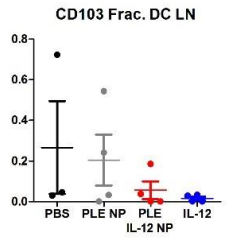
CD103 Frac. DC LN
PBS
PLE NP
PLE
IL-12
IL-12 NP

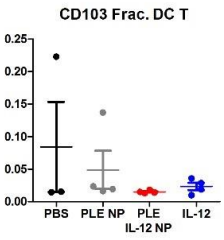
CD103 Frac. DC T
PBS
PLE NP
PLE
IL-12
IL-12 NP

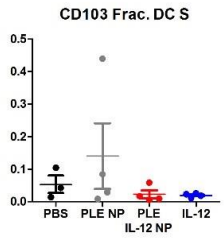
CD103 Frac. DC S
PBS
PLE NP
PLE
IL-12
IL-12 NP

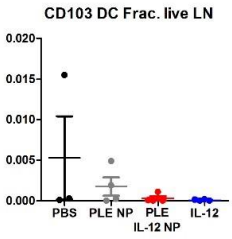
CD103 DC Frac. live LN
PBS
PLE NP
PLE
IL-12
IL-12 NP

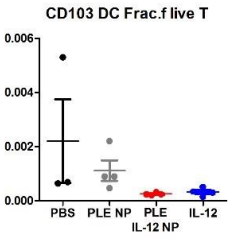
CD103 DC Frac.f live T
PBS
PLE NP
PLE
IL-12
IL-12 NP

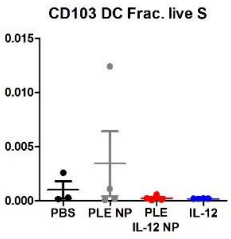
CD103 DC Frac. live S
PBS
PLE NP
PLE
IL-12
IL-12 NP

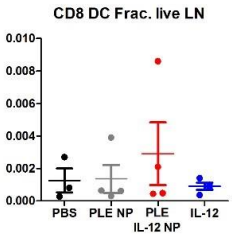
CD8 DC Frac. live LN
PBS
PLE NP
PLE
IL-12
IL-12 NP

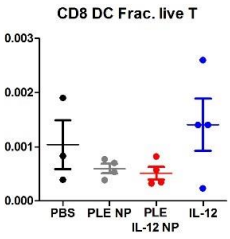
CD8 DC Frac. live T
PBS
PLE NP
PLE
IL-12
IL-12 NP

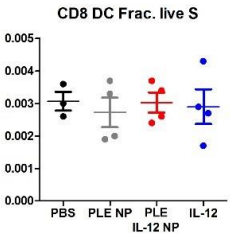
CD8 DC Frac. live S
PBS
PLE NP
PLE
IL-12
IL-12 NP

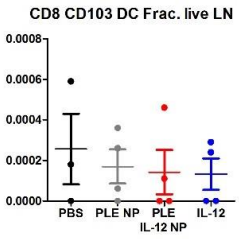
CD8 CD103 DC Frac. live LN
PBS
PLE NP
PLE
IL-12
IL-12 NP

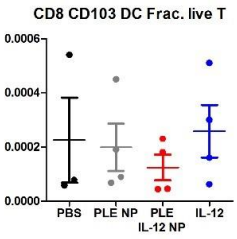
CD8 CD103 DC Frac. live T
PBS
PLE NP
PLE
IL-12
IL-12 NP

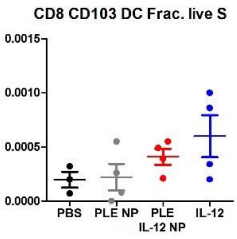
CD8 CD103 DC Frac. live S
PBS
PLE NP
PLE
IL-12
IL-12 NP

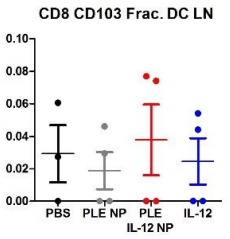
CD8 CD103 Frac. DC LN
PBS
PLE NP
PLE
IL-12
IL-12 NP

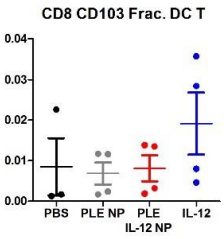
CD8 CD103 Frac. DC T
PBS
PLE NP
PLE
IL-12
IL-12 NP

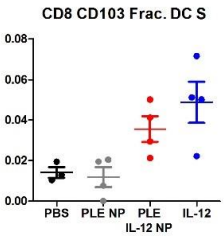
CD8 CD103 Frac. DC S
PBS
PLE NP
PLE
IL-12
IL-12 NP

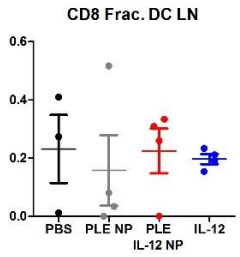
CD8 Frac. DC LN
0.6
0.4
0.2
0.0
PBS
PLE NP
PLE IL-12 NP
IL-12

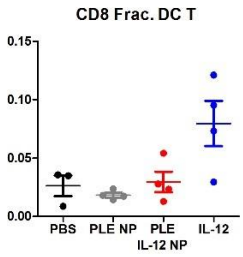
CD8 Frac. DC T
0.15
0.10
0.05
0.00
PBS
PLE NP
PLE IL-12 NP
IL-12

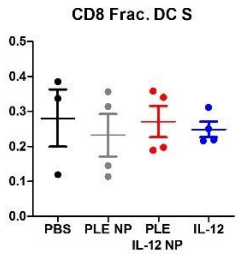
CD8 Frac. DC S
0.5
0.4
0.3
0.2
0.1
0.0
PBS
PLE NP
PLE IL-12 NP
IL-12

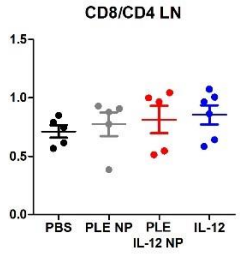
CD8/CD4 LN
1.5
1.0
0.5
0.0
PBS
PLE NP
PLE IL-12 NP
IL-12

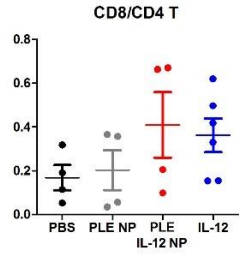
CD8/CD4 T
0.8
0.6
0.4
0.2
0.0
PBS
PLE NP
PLE IL-12 NP
IL-12

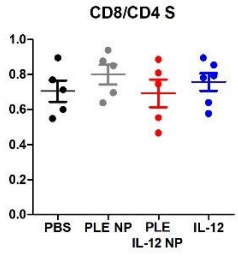
CD8/CD4 S
1.0
0.8
0.6
0.4
0.2
0.0
PBS
PLE NP
PLE IL-12 NP
IL-12

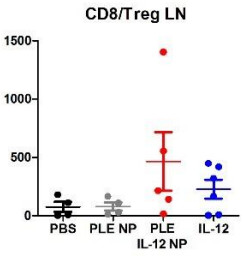
CD8/Treg LN
1500
1000
500
0
PBS
PLE NP
PLE IL-12 NP
IL-12

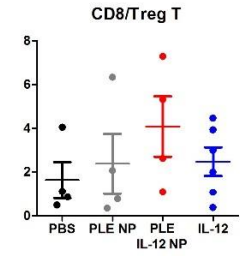
CD8/Treg T
8
6
4
2
0
PBS
PLE NP
PLE IL-12 NP
IL-12

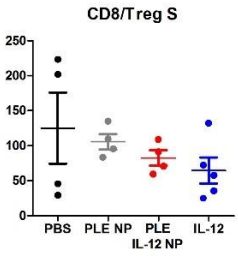
CD8/Treg S
250
200
150
100
50
0
PBS
PLE NP
PLE IL-12 NP
IL-12

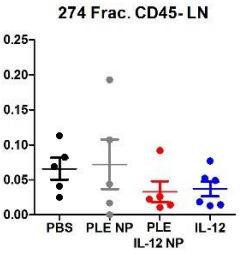
274 Frac. CD45- LN
0.25
0.20
0.15
0.10
0.05
0.00
PBS
PLE NP
PLE IL-12 NP
IL-12

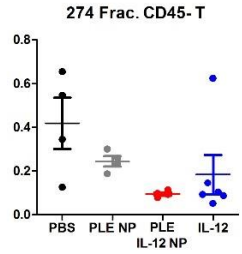
274 Frac. CD45- T
0.8
0.6
0.4
0.2
0.0
PBS
PLE NP
PLE IL-12 NP
IL-12

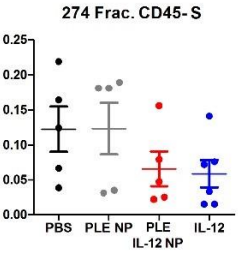
274 Frac. CD45- S
0.25
0.20
0.15
0.10
0.05
0.00
PBS
PLE NP
PLE IL-12 NP
IL-12

Appendix C

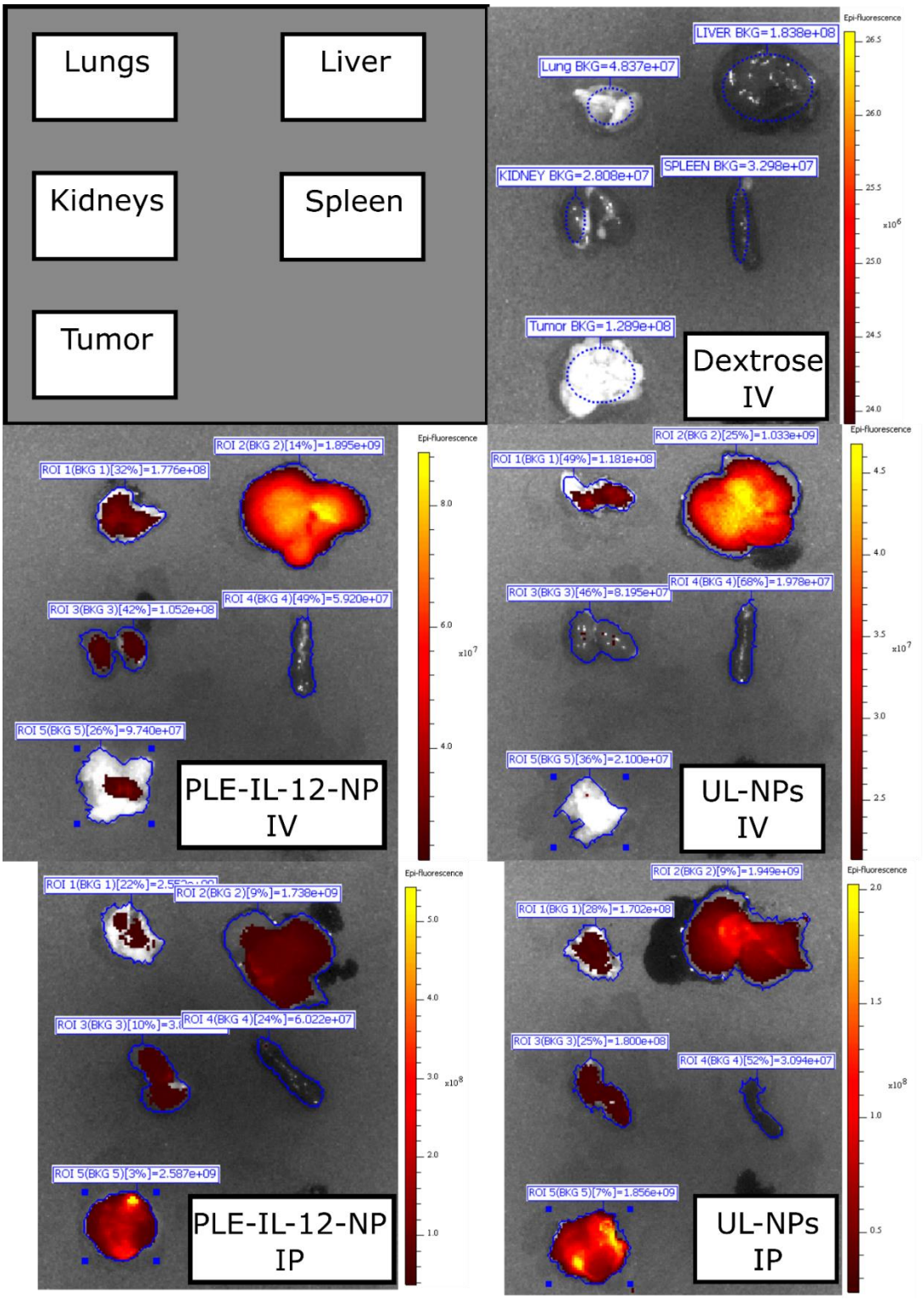

Figure C-1. Sample Images from IVIS BioD studies of all collected organs.

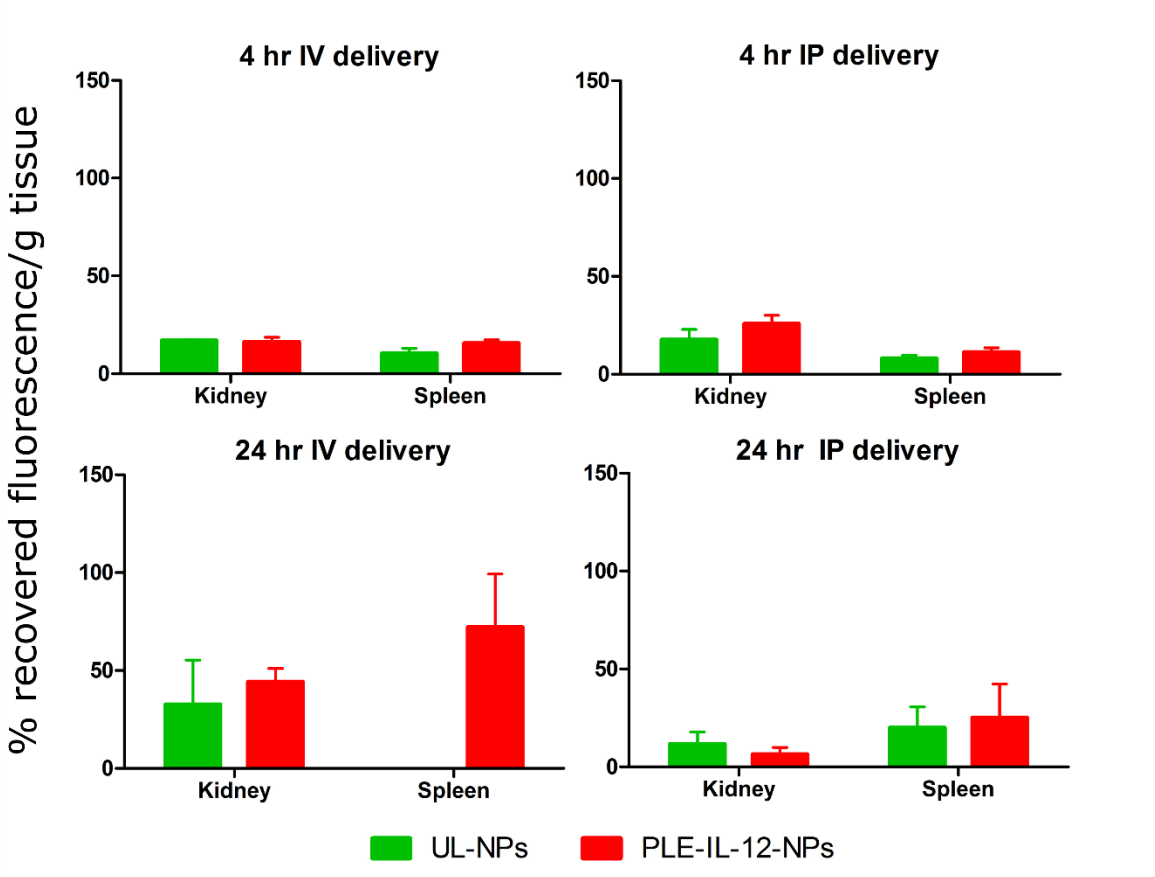

Figure C-2. Biodistribution in the kidney and spleen as measured by fluorescence

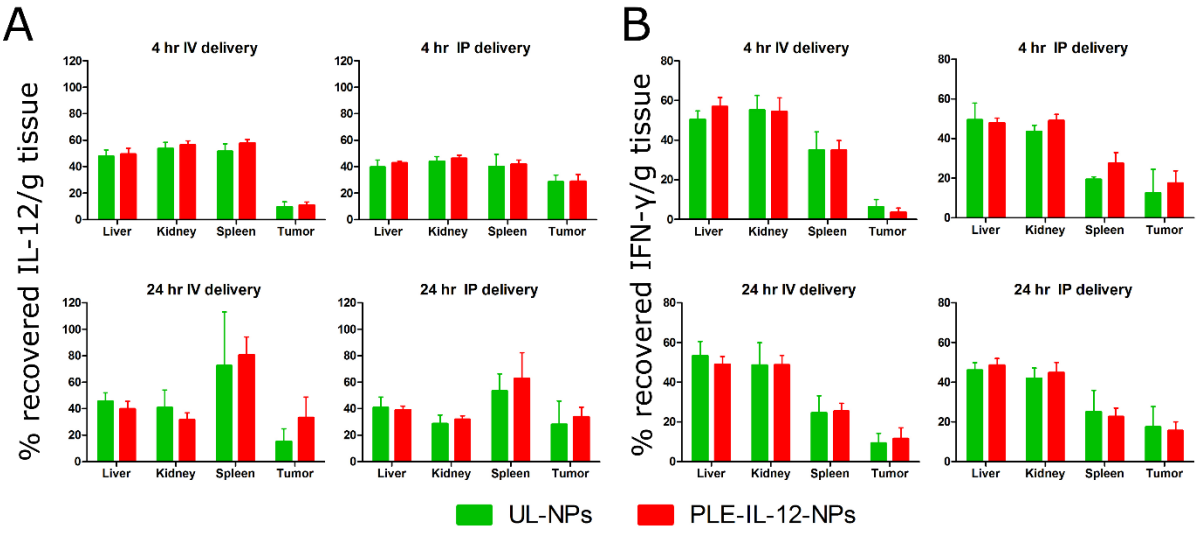

Figure C-3. IL-12 and IFN-γ recovery upon systemic IL-12 delivery

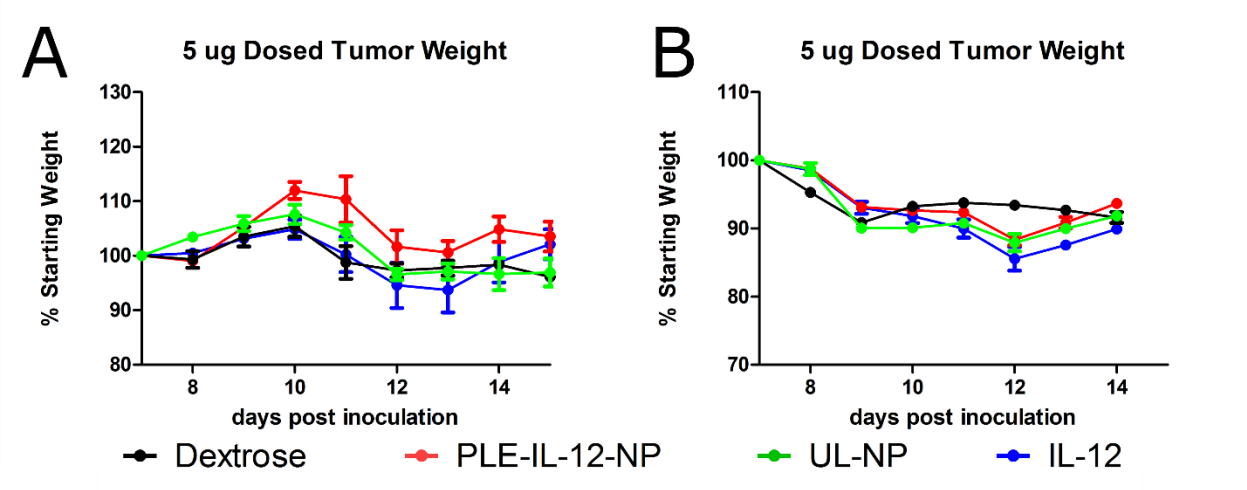

Figure C-4. 5 µg dosed IL-12 tumor bearing mice toxicity

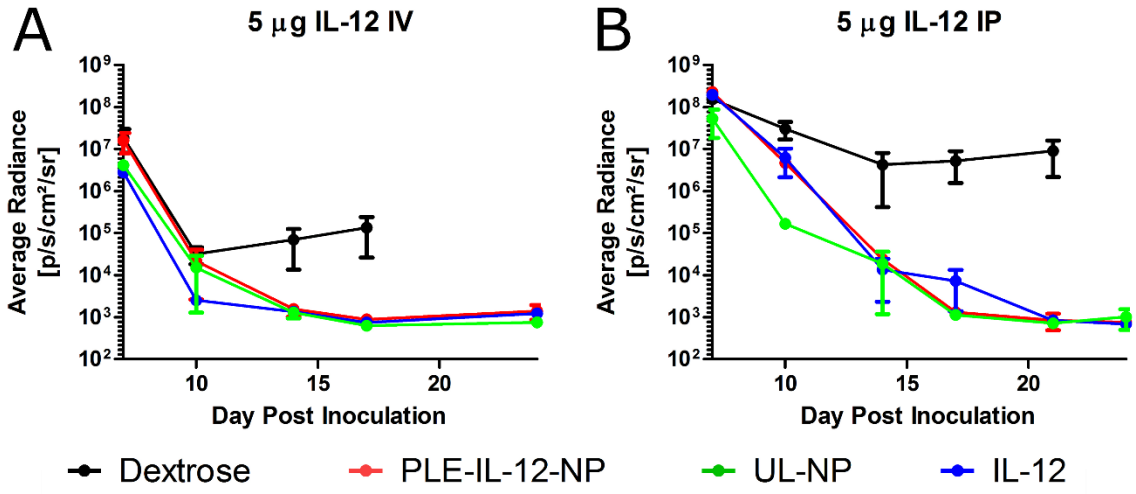

Figure C-5. 5 µg dosed IL-12 tumor burden

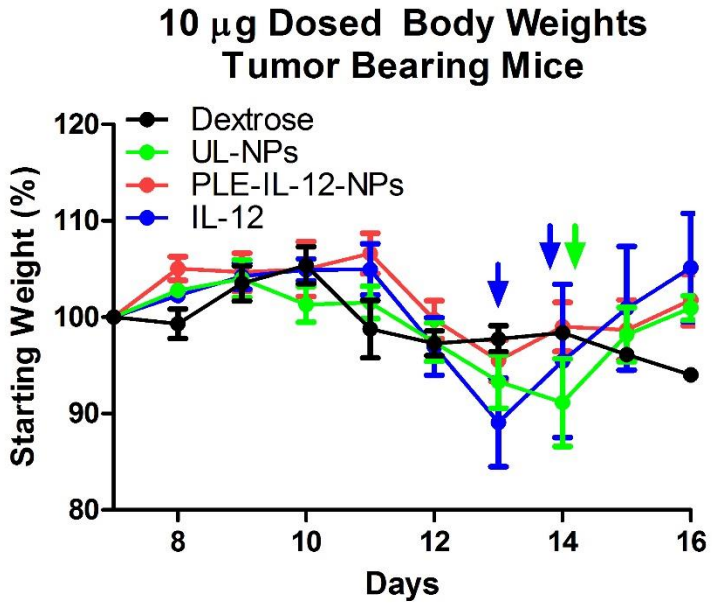

Figure C-6. 10 μg dosed IL-12 tumor bearing mice toxicity. Arrows indicate toxicity induced deaths.

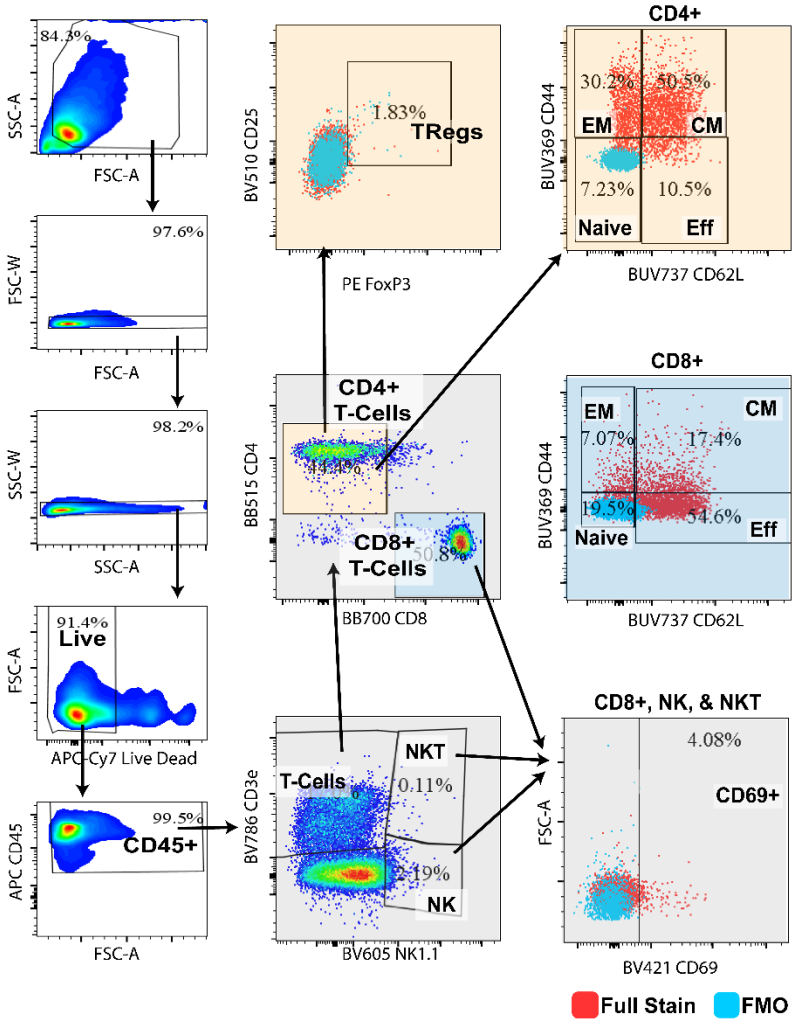
84.3%
SSC-A
FSC-A
97.6%
FSC-W
FSC-A
98.2%
SSC-W
SSC-A
91.4%
Live
FSC-A
APC-Cy7 Live Dead
99.5%
CD45+
APC CD45
FSC-A
BV510 CD25
1.83%
TRegs
PE FoxP3
CD4+
T-Cells
44.4%
BB515 CD4
CD8+
T-Cells
50.8%
BB700 CD8
T-Cells
NKT
0.11%
2.19%
NK
BV786 CD3e
BV605 NK1.1
CD4+
30.2%
50.5%
EM
CM
7.23%
10.5%
Naive
Eff
BUV369 CD44
BUV737 CD62L
CD8+
EM
7.07%
CM
17.4%
19.5%
54.6%
Naive
Eff
BUV369 CD44
BUV737 CD62L
CD8+, NK, & NKT
4.08%
CD69+
FSC-A
BV421 CD69
Full Stain
FMO

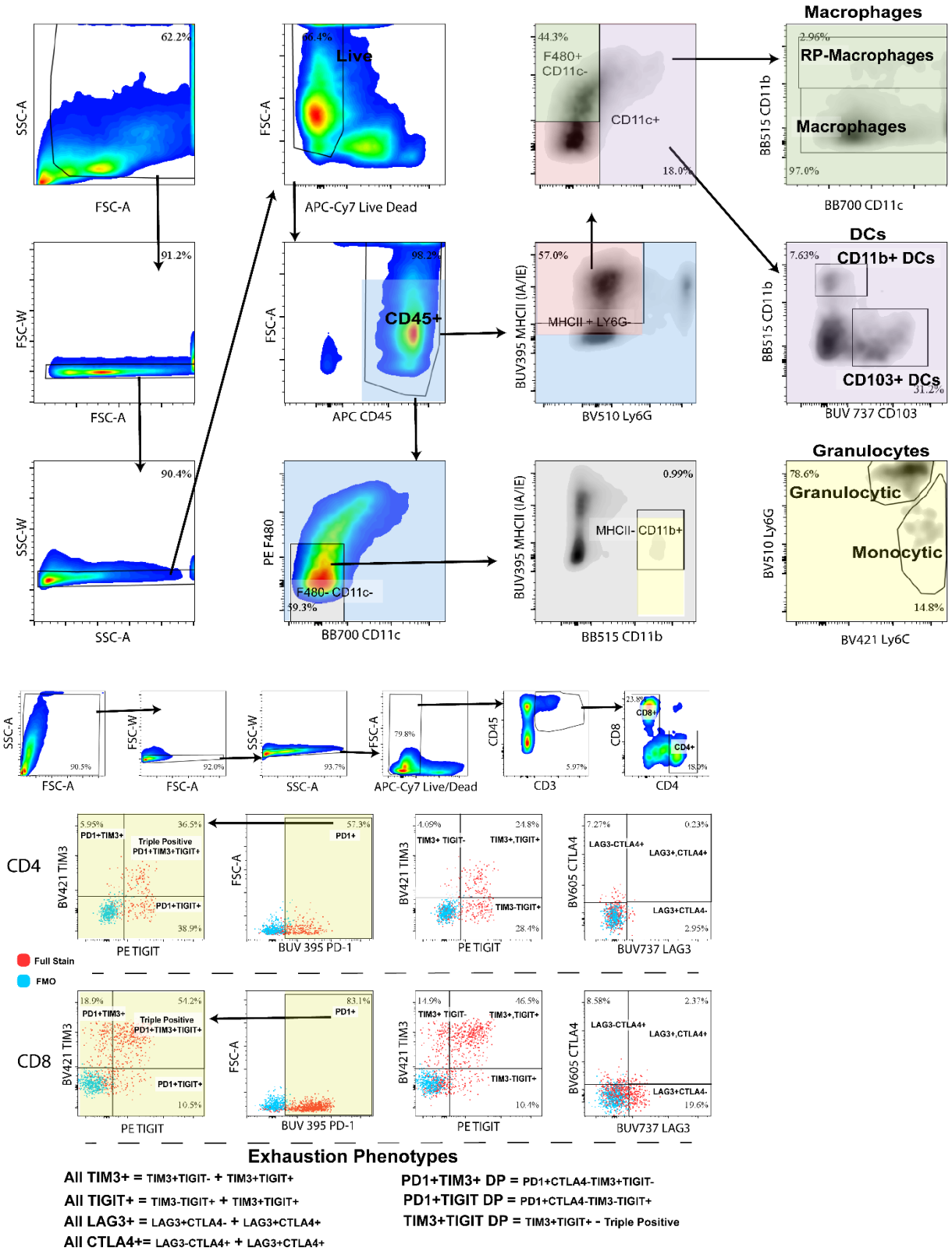

Figure C-7. Gating strategy for immune profiling

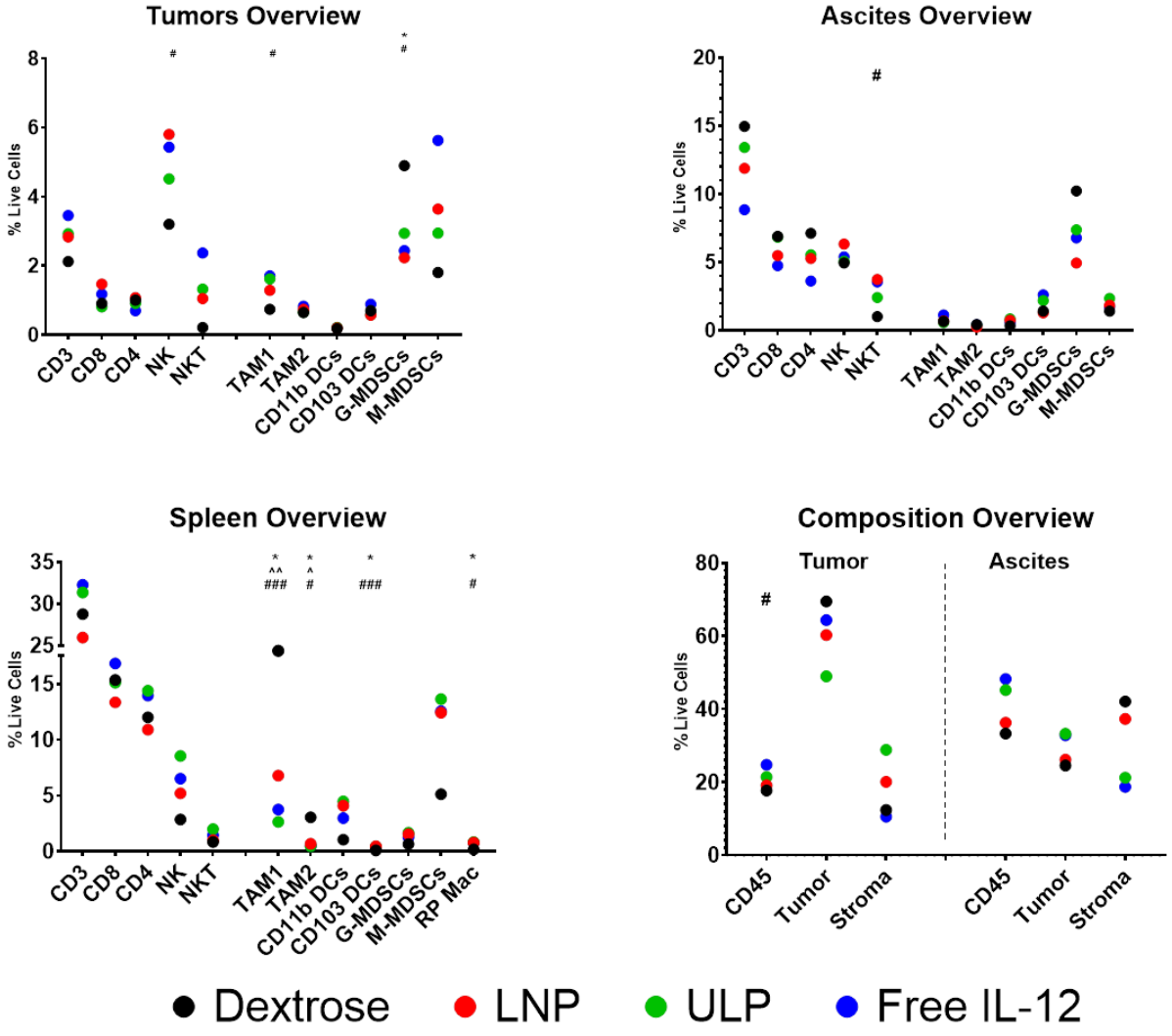
Tumors Overview
% Live Cells
CD3
CD8
CD4
NK
NKT
TAM1
TAM2
CD11b DCs
CD103 DCs
G-MDSCs
M-MDSCs
Ascites Overview
Spleen Overview
RP Mac
Composition Overview
Tumor
Ascites
CD45
Stroma
Dextrose
LNP
ULP
Free IL-12

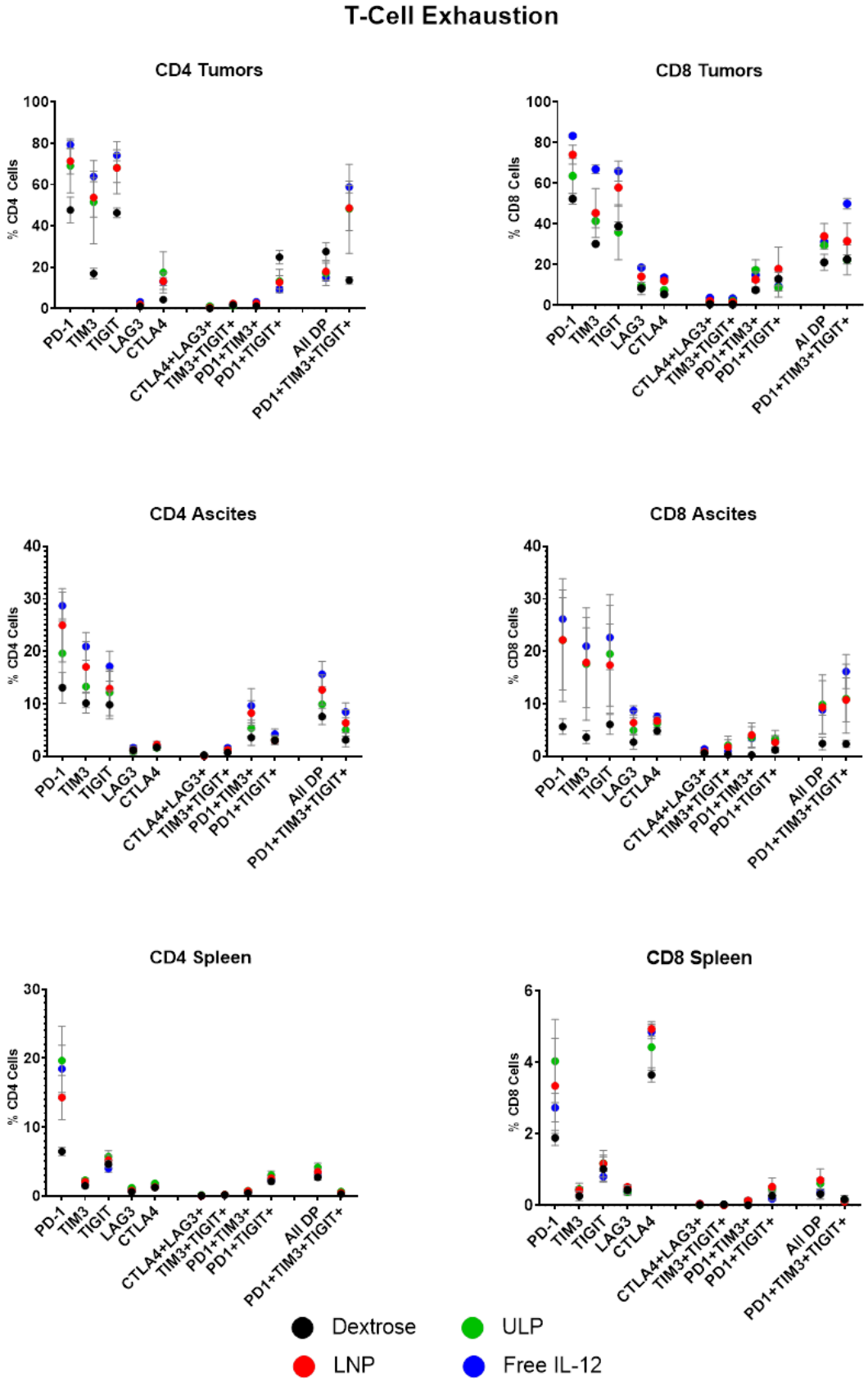
T-Cell Exhaustion
CD4 Tumors
% CD4 Cells
CD8 Tumors
% CD8 Cells
CD4 Ascites
% CD4 Cells
CD8 Ascites
% CD8 Cells
CD4 Spleen
% CD4 Cells
CD8 Spleen
% CD8 Cells
PD-1
TIM3
TIGIT
LAG3
CTLA4
CTLA4+LAG3+
TIM3+TIGIT+
PD1+TIM3+
PD1+TIGIT+
All DP
PD1+TIM3+TIGIT+
Dextrose
ULP
LNP
Free IL-12

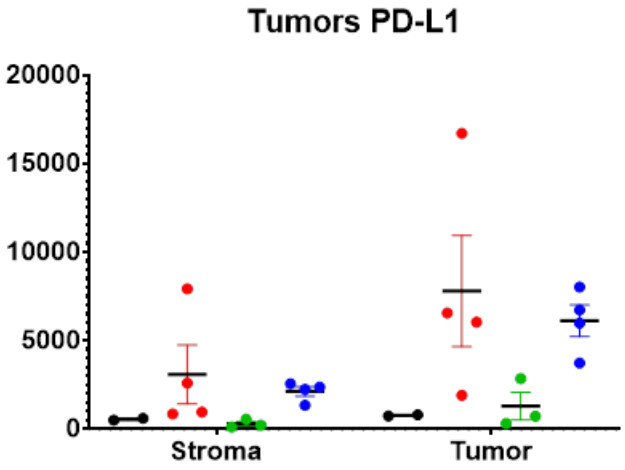
Tumors PD-L1
20000
15000
10000
5000
0
Stroma
Tumor

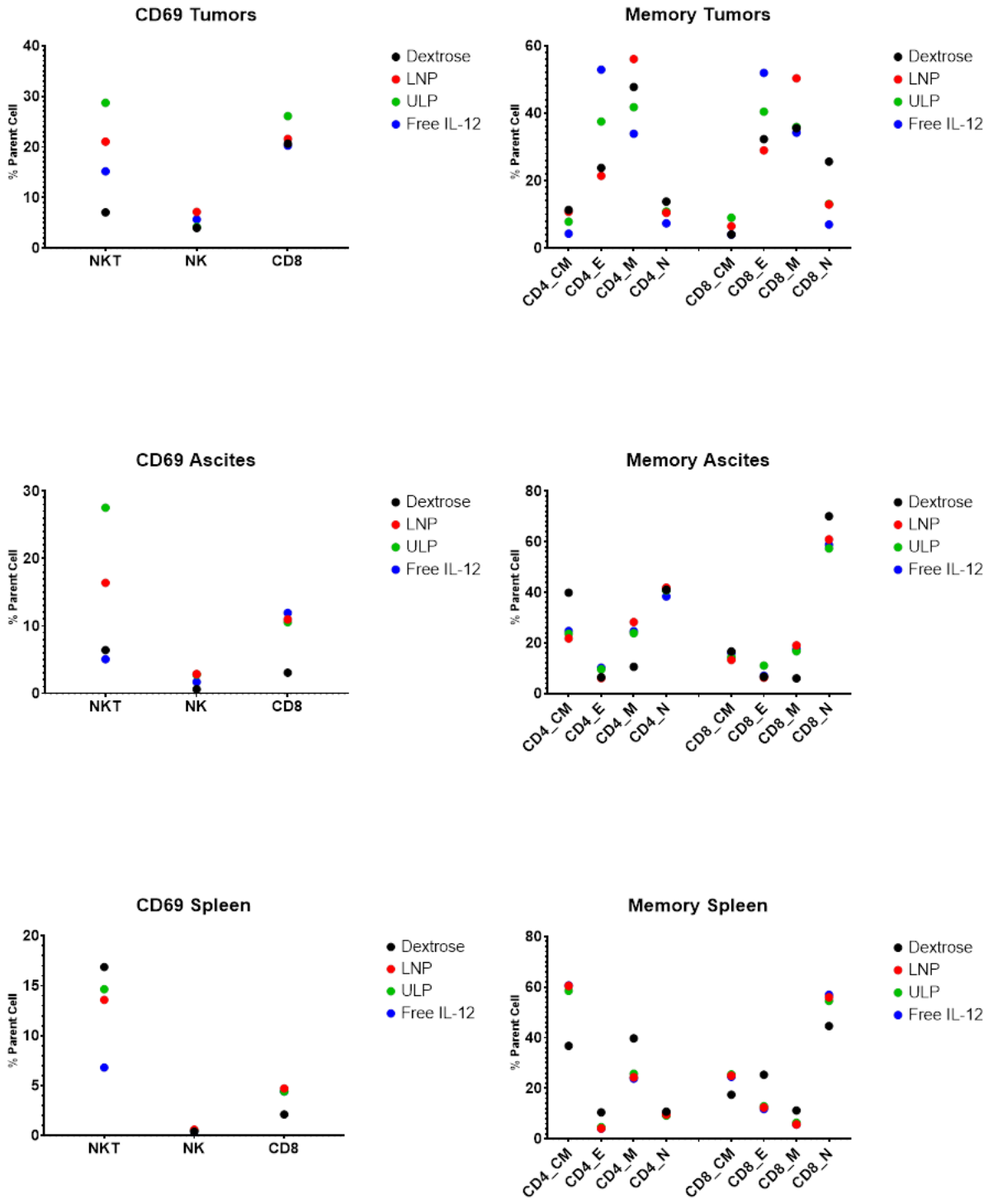

Figure C-8. Summary of immune profiling data.

Chapter 7. References.

References Cited

1. Immunotherapy Timeline of Progress. (Accessed 1/15/19, 2019, at https://www.cancerresearch.org/immunotherapy/timeline-of-progress.)
2. Mellman I, Coukos G, Dranoff G. Cancer immunotherapy comes of age. Nature 2011;480:480-9.
3. Immunotherapy Timeline of Progress. Cancer Research Institute. (Accessed May 26, 2020, at http://www.cancerresearch.org/immunotherapy/timeline-of-progress.)
4. Chen DS, Mellman I. Oncology meets immunology: the cancer-immunity cycle. Immunity 2013;39:1-10.
5. Chen DS, Mellman I. Elements of cancer immunity and the cancer-immune set point. Nature 2017;541:321-30.
6. Gabrilovich DI, Ostrand-Rosenberg S, Bronte V. Coordinated regulation of myeloid cells by tumours. Nature Reviews Immunology 2012;12:253.
7. Ostrand-Rosenberg S, Sinha P. Myeloid-derived suppressor cells: linking inflammation and cancer. The Journal of Immunology 2009;182:4499-506.
8. Noy R, Pollard JW. Tumor-associated macrophages: from mechanisms to therapy. Immunity 2014;41:49-61.
9. Zhang M, He Y, Sun X, et al. A high M1/M2 ratio of tumor-associated macrophages is associated with extended survival in ovarian cancer patients. Journal of ovarian research 2014;7:19.
10. What is Cancer Immunotherapy. American Cancer Spciety. (Accessed Oct. 05, 2016,
11. Lawrence MS, Stojanov P, Polak P, et al. Mutational heterogeneity in cancer and the search for new cancer-associated genes. Nature 2013;499:214-8.
12. Galon J, Pages F, Marincola FM, et al. Cancer classification using the Immunoscore: a worldwide task force. J Transl Med 2012;10:205.
13. Pages F, Mlecnik B, Marliot F, et al. International validation of the consensus Immunoscore for the classification of colon cancer: a prognostic and accuracy study. Lancet 2018;391:2128-39.
14. Bindea G, Mlecnik B, Angell HK, Galon J. The immune landscape of human tumors: Implications for cancer immunotherapy. Oncoimmunology 2014;3:e27456.
15. Kobayashi M, Fitz L, Ryan M, et al. Identification and purification of natural killer cell stimulatory factor (NKSF), a cytokine with multiple biologic effects on human lymphocytes. The Journal of experimental medicine 1989;170:827-45.
16. Wolf SF, Sieburth D, Sypek J. Interleukin 12: a key modulator of immune function. Stem Cells 1994;12:154-68.
17. Trinchieri G. Interleukin-12: a proinflammatory cytokine with immunoregulatory functions that bridge innate resistance and antigen-specific adaptive immunity. Annual review of immunology 1995;13:251-76.
18. Robertson MJ, Ritz J. Interleukin 12: basic biology and potential applications in cancer treatment. The Oncologist 1996;1:88-97.
19. Trinchieri G, Scott P. Interleukin-12: basic principles and clinical applications. Redirection of Th1 and Th2 Responses: Springer; 1999:57-78.

20. Colombo MP, Trinchieri G. Interleukin-12 in anti-tumor immunity and immunotherapy. Cytokine & growth factor reviews 2002;13:155-68.
21. Brunda MJ, Luistro L, Warrier RR, et al. Antitumor and antimetastatic activity of interleukin 12 against murine tumors. Journal of Experimental Medicine 1993;178:1223-30.
22. Andrews J, Schoof D, Bertagnolli M, Peoples G, Goedegebuure P, Eberlein T. Immunomodulatory effects of interleukin-12 on human tumor-infiltrating lymphocytes. Journal of immunotherapy with emphasis on tumor immunology: official journal of the Society for Biological Therapy 1993;14:1-10.
23. Atkins MB, Robertson MJ, Gordon M, et al. Phase I evaluation of intravenous recombinant human interleukin 12 in patients with advanced malignancies. Clinical Cancer Research 1997;3:409-17.
24. Portielje JE, Kruit WH, Schuler M, et al. Phase I study of subcutaneously administered recombinant human interleukin 12 in patients with advanced renal cell cancer. Clinical cancer research 1999;5:3983-9.
25. van Herpen CM, Huijbens R, Looman M, et al. Pharmacokinetics and immunological aspects of a phase Ib study with intratumoral administration of recombinant human interleukin-12 in patients with head and neck squamous cell carcinoma: a decrease of T-bet in peripheral blood mononuclear cells. Clinical cancer research 2003;9:2950-6.
26. Bael TE, Gollob JA. Interleukin-12 and Cancer Therapy. Cytokines in the Genesis and Treatment of Cancer: Springer; 2007:317-38.
27. Lasek W, Zagożdżon R, Jakobisiak M. Interleukin 12: still a promising candidate for tumor immunotherapy? Cancer Immunology, Immunotherapy 2014;63:419-35.
28. Lasek W, Zagozdzon R. Clinical trials with IL-12 in cancer immunotherapy. Interleukin 12: Antitumor Activity and Immunotherapeutic Potential in Oncology: Springer; 2016:43-75.
29. Lai I, Swaminathan S, Baylot V, et al. Lipid nanoparticles that deliver IL-12 messenger RNA suppress tumorigenesis in MYC oncogene-driven hepatocellular carcinoma. Journal for immunotherapy of cancer 2018;6:125.
30. Thaker PH, Bradley WH, Leath CA, et al. Phase I study of the safety and activity of formulated IL-12 plasmid administered intraperitoneally in combination with neoadjuvant chemotherapy in patients with newly diagnosed advanced-stage ovarian cancer. American Society of Clinical Oncology; 2019.
31. Smith SG, Baltz JL, Koppolu BP, Ravindranathan S, Nguyen K, Zaharoff DA. Immunological mechanisms of intravesical chitosan/interleukin-12 immunotherapy against murine bladder cancer. Oncoimmunology 2017;6:e1259050.
32. Smith SG, prasanth Koppolu B, Ravindranathan S, et al. Intravesical chitosan/interleukin-12 immunotherapy induces tumor-specific systemic immunity against murine bladder cancer. Cancer immunology, immunotherapy 2015;64:689-96.
33. Vo JL, Yang L, Kurtz SL, et al. Neoadjuvant immunotherapy with chitosan and interleukin-12 to control breast cancer metastasis. Oncoimmunology 2014;3:e968001.
34. Yang L, Zaharoff DA. Role of chitosan co-formulation in enhancing interleukin-12 delivery and antitumor activity. Biomaterials 2013;34:3828-36.
35. Momin N, Mehta NK, Bennett NR, et al. Anchoring of intratumorally administered cytokines to collagen safely potentiates systemic cancer immunotherapy. Science translational medicine 2019;11.

36. Mansurov A, Ishihara J, Hosseinchi P, et al. Collagen-binding IL-12 enhances tumour inflammation and drives the complete remission of established immunologically cold mouse tumours. Nature biomedical engineering 2020;4:531-43.
37. Boulikas T. Clinical overview on Lipoplatin (TM): a successful liposomal formulation of cisplatin. Expert Opinion on Investigational Drugs 2009;18:1197-218.
38. Stathopoulos GP, Antoniou D, Dimitroulis J, et al. Liposomal cisplatin combined with paclitaxel versus cisplatin and paclitaxel in non-small-cell lung cancer: a randomized phase III multicenter trial. Annals of Oncology 2010;21:2227-32.
39. Safra T, Muggia F, Jeffers S, et al. Pegylated liposomal doxorubicin (doxil): Reduced clinical cardiotoxicity in patients reaching or exceeding cumulative doses of 500 mg/m(2). Annals of Oncology 2000;11:1029-33.
40. Bertrand N, Wu J, Xu XY, Kamaly N, Farokhzad OC. Cancer nanotechnology: The impact of passive and active targeting in the era of modern cancer biology. Advanced Drug Delivery Reviews 2014;66:2-25.
41. Shao K, Singha S, Clemente-Casares X, Tsai S, Yang Y, Santamaria P. Nanoparticle-based immunotherapy for cancer. ACS nano 2015;9:16-30.
42. Visaria RK, Griffin RJ, Williams BW, et al. Enhancement of tumor thermal therapy using gold nanoparticle-assisted tumor necrosis factor-alpha delivery. Molecular Cancer Therapeutics 2006;5:1014-20.
43. Cui W, Wang A, Zhao J, Yang X, Cai P, Li J. Layer by layer assembly of albumin nanoparticles with selective recognition of tumor necrosis factor-related apoptosis-inducing ligand (TRAIL). Journal of Colloid and Interface Science 2016;465:11--7.
44. Mejias R, Perez-Yague S, Gutierrez L, et al. Dimercaptosuccinic acid-coated magnetite nanoparticles for magnetically guided in vivo delivery of interferon gamma for cancer immunotherapy. Biomaterials 2011;32:2938-52.
45. Park J, Gao W, Whiston R, Strom TB, Metcalfe S, Fahmy TM. Modulation of CD4+ T lymphocyte lineage outcomes with targeted, nanoparticle-mediated cytokine delivery. Molecular pharmaceutics 2011;8:143-52.
46. Kwong B, Gai SA, Elkhader J, Wittrup KD, Irvine DJ. Localized Immunotherapy via Liposome-Anchored Anti-CD137+IL-2 Prevents Lethal Toxicity and Elicits Local and Systemic Antitumor Immunity. Cancer Research 2013;73:1547-58.
47. Kwong B, Liu HP, Irvine DJ. Induction of potent anti-tumor responses while eliminating systemic side effects via liposome-anchored combinatorial immunotherapy. Biomaterials 2011;32:5134-47.
48. Egilmez NK, Jong YS, Sabel MS, Jacob JS, Mathiowitz E, Bankert RB. In situ tumor vaccination with interleukin-12-encapsulated biodegradable microspheres: induction of tumor regression and potent antitumor immunity. Cancer research 2000;60:3832-7.
49. Hill HC, Conway TF, Sabel MS, et al. Cancer immunotherapy with interleukin 12 and granulocyte-macrophage colony-stimulating factor-encapsulated microspheres: coinduction of innate and adaptive antitumor immunity and cure of disseminated disease. Cancer research 2002;62:7254-63.
50. Sabel MS, Hill H, Jong YS, Mathiowitz E, Bankert RB, Egilmez NK. Neoadjuvant therapy with interleukin-12–loaded polylactic acid microspheres reduces local recurrence and distant metastases. Surgery 2001;130:470-8.

51. Meraz IM, Savage DJ, Segura-Ibarra V, et al. Adjuvant cationic liposomes presenting MPL and IL-12 induce cell death, suppress tumor growth, and alter the cellular phenotype of tumors in a murine model of breast cancer. Molecular pharmaceutics 2014;11:3484-91.
52. Xu Q, Guo L, Gu X, et al. Prevention of colorectal cancer liver metastasis by exploiting liver immunity via chitosan-TPP/nanoparticles formulated with IL-12. Biomaterials 2012;33:3909-18.
53. Shimizu T, Kishida T, Hasegawa U, et al. Nanogel DDS enables sustained release of IL-12 for tumor immunotherapy. Biochemical and biophysical research communications 2008;367:330-5.
54. Carson WE, Dierksheide JE, Jabbour S, et al. Coadministration of interleukin-18 and interleukin-12 induces a fatal inflammatory response in mice: critical role of natural killer cell interferon-γ production and STAT-mediated signal transduction. Blood 2000;96:1465-73.
55. Colombo MP, Vagliani M, Spreafico F, et al. Amount of interleukin 12 available at the tumor site is critical for tumor regression. Cancer Res 1996;56:2531-4.
56. Decher G. Fuzzy Nanoassemblies: Toward Layered Polymeric Multicomposites. Science 1997;277:1232.
57. Hammond PT. Form and function in multilayer assembly: New applications at the nanoscale. Advanced Materials 2004;16:1271-93.
58. Correa S, Dreaden EC, Gu L, Hammond PT. Engineering nanolayered particles for modular drug delivery. Journal of Controlled Release 2016;240:364-86.
59. Shaillender M, Luo RC, Venkatraman SS, Neu B. Layer-by-layer microcapsules templated on erythrocyte ghost carriers. International Journal of Pharmaceutics 2011;415:211-7.
60. Dreaden EC, Kong YW, Morton SW, et al. Tumor-Targeted Synergistic Blockade of MAPK and PI3K from a Layer-by-Layer Nanoparticle. Clinical Cancer Research 2015;21:4410-9.
61. Dreaden EC, Morton SW, Shopsowitz KE, et al. Bimodal Tumor-Targeting from Microenvironment Responsive Hyaluronan Layer-by-Layer (LbL) Nanoparticles. Acs Nano 2014;8:8374-82.
62. Hammond PT. Engineering Materials Layer-by-Layer: Challenges and Opportunities in Multilayer Assembly. AIChE Journal 2011;57:2928-40.
63. Correa S, Choi KY, Dreaden EC, et al. Highly Scalable, Closed-Loop Synthesis of Drug-Loaded, Layer-by-Layer Nanoparticles. Advanced functional materials 2016;26:991-1003.
64. Dang X, Gu L, Qi J, et al. Layer-by-layer assembled fluorescent probes in the second near-infrared window for systemic delivery and detection of ovarian cancer. Proceedings of the National Academy of Sciences of the United States of America 2016;113:5179-84.
65. Deng ZJ, Morton SW, Ben-Akiva E, Dreaden EC, Shopsowitz KE, Hammond PT. Layer-by-Layer Nanoparticles for Systemic Codelivery of an Anticancer Drug and siRNA for Potential Triple-Negative Breast Cancer Treatment. ACS Nano 2013;7:9571-84.
66. Morton SW, Lee MJ, Deng ZJ, et al. A Nanoparticle-Based Combination Chemotherapy Delivery System for Enhanced Tumor Killing by Dynamic Rewiring of Signaling Pathways. Science Signaling 2014;7.
67. Morton SW, Poon Z, Hammond PT. The architecture and biological performance of drug-loaded LbL nanoparticles. Biomaterials 2013;34:5328-35.
68. Statistics. Ovarian Cancer Research Alliance. (Accessed May 26, 2020, at https://ocrahope.org/patients/about-ovarian-cancer/statistics/.)

69. Yarchoan M, Hopkins A, Jaffee EM. Tumor mutational burden and response rate to PD-1 inhibition. The New England journal of medicine 2017;377:2500.
70. Sabel MS, Arora A, Su G, Mathiowitz E, Reineke JJ, Chang AE. Synergistic effect of intratumoral IL-12 and TNF-α microspheres: systemic anti-tumor immunity is mediated by both CD8+ CTL and NK cells. Surgery 2007;142:749-60.
71. Morton SW, Shah NJ, Quadir MA, Deng ZJ, Poon Z, Hammond PT. Osteotropic Therapy via Targeted Layer-by-Layer Nanoparticles. Advanced Healthcare Materials 2014;3:867-75.
72. Lieschke GJ, Mulligan RC. Bioactive fusion proteins comprising the p35 and p40 subunits of IL-12. Google Patents; 1999.
73. Stewart JCM. Colorimetric determination of phospholipids with ammonium ferrothiocyanate. Analytical biochemistry 1980;104:10-4.
74. Colletier J-P, Chaize B, Winterhalter M, Fournier D. Protein encapsulation in liposomes: efficiency depends on interactions between protein and phospholipid bilayer. BMC biotechnology 2002;2:9.
75. Johnston AP, Cortez C, Angelatos AS, Caruso F. Layer-by-layer engineered capsules and their applications. Current opinion in colloid & interface science 2006;11:203-9.
76. Correa SB, N.; Barberio, A.E.; Deiss-Yehiely, E.; Shi, A.; Oberlton, B.; Smith, S.G.; Zervantonakis, I.K.; Dreaden, E.C.; Brugge, J.S.; Hammond, P.T. Tuning nanoparticle interactions with ovarian cancer through layer by layer modification of surface chemistry.
77. Gu L, Deng ZJ, Roy S, Hammond PT. A Combination RNAi-Chemotherapy Layer-by-Layer Nanoparticle for Systemic Targeting of KRAS/P53 with Cisplatin to Treat Non-Small Cell Lung Cancer. Clin Cancer Res 2017;in press.
78. Cohen K, Emmanuel R, Kisin-Finfer E, Shabat D, Peer D. Modulation of drug resistance in ovarian adenocarcinoma using chemotherapy entrapped in hyaluronan-grafted nanoparticle clusters. ACS nano 2014;8:2183-95.
79. Ganesh S, Iyer AK, Gattacceca F, Morrissey DV, Amiji MM. In vivo biodistribution of siRNA and cisplatin administered using CD44-targeted hyaluronic acid nanoparticles. Journal of controlled release 2013;172:699-706.
80. Choi KY, Yoon HY, Kim J-H, et al. Smart nanocarrier based on PEGylated hyaluronic acid for cancer therapy. ACS nano 2011;5:8591-9.
81. Hasan M, Najjam S, Gordon MY, Gibbs RV, Rider CC. IL-12 is a heparin-binding cytokine. The Journal of Immunology 1999;162:1064-70.
82. Abiko K, ., et al. IFN-γ from lymphocytes induces PD-L1 expression and promotes progression of ovarian cancer. British journal of cancer 2015;112.
83. Peng J, Hamanishi J, Matsumura N, et al. Chemotherapy induces programmed cell death-ligand 1 overexpression via the nuclear factor-κB to foster an immunosuppressive tumor microenvironment in ovarian cancer. Cancer research 2015;75:5034-45.
84. Rothschilds AM, Wittrup KD. What, Why, Where, and When: Bringing Timing to Immuno-Oncology. Trends in immunology 2018.
85. Hargadon KM, Johnson CE, Williams CJ. Immune checkpoint blockade therapy for cancer: An overview of FDA-approved immune checkpoint inhibitors. International immunopharmacology 2018;62:29-39.
86. Correa S, Choi KY, Dreaden EC, et al. Highly Scalable, Closed-Loop Synthesis of Drug-Loaded, Layer-by-Layer Nanoparticles. Advanced Functional Materials 2016;26:991-1003.
87. Ott PA, Hodi FS, Kaufman HL, Wigginton JM, Wolchok JD. Combination immunotherapy: a road map. J Immunother Cancer 2017;5:16.

88. Schmidt C. The benefits of immunotherapy combinations. Nature 2017;552:S67-S9.
89. Weiss JM, Subleski JJ, Wigginton JM, Wiltrout RH. Immunotherapy of cancer by IL-12-based cytokine combinations. Expert opinion on biological therapy 2007;7:1705-21.
90. Liao L, Liu J, Dreaden EC, et al. A Convergent Synthetic Platform for Single-Nanoparticle Combination Cancer Therapy: Ratiometric Loading and Controlled Release of Cisplatin, Doxorubicin, and Camptothecin. Journal of the American Chemical Society 2014;136:5896--9.
91. Edidin M. Fluorescence Resonance Energy Transfer: Techniques for Measuring Molecular Conformation and Molecular Proximity. Current Protocols in Immunology 2003;57:18.0.1-.0.
92. Gravier J, Sancey L, Hirsjärvi S, et al. FRET imaging approaches for in vitro and in vivo characterization of synthetic lipid nanoparticles. Molecular pharmaceutics 2014;11:3133-44.
93. Lleres D, Swift S, Lamond AI. Detecting protein-protein interactions in vivo with FRET using multiphoton fluorescence lifetime imaging microscopy (FLIM). Current protocols in cytometry 2007;42:12.0. 1-.0. 9.